(12) INTERNATIONAL APPLICATION PUBLISHED UNDER THE PATENT COOPERATION TREATY (PCT)

(19) World Intellectual Property Organization
International Bureau

(43) International Publication Date
23 May 2019 (23.05.2019)

WIPO | PCT

(10) International Publication Number
WO 2019/099657 A1

(51) International Patent Classification:
C01G 21/16 (2006.01) *H01G 9/20* (2006.01)
C09K 11/57 (2006.01) *H01L 51/50* (2006.01)
C07F 7/24 (2006.01) *H01L 51/42* (2006.01)

(21) International Application Number:
PCT/US2018/061261

(22) International Filing Date:
15 November 2018 (15.11.2018)

(25) Filing Language: English

(26) Publication Language: English

(30) Priority Data:
62/586,846 15 November 2017 (15.11.2017) US

(71) Applicant: **PRESIDENT AND FELLOWS OF HARVARD COLLEGE** [US/US]; 17 Quincy Street, Cambridge, MA 02138 (US).

(72) Inventors: **CONGREVE, Daniel, N.**; 90 Fawcett Street, #216, Cambridge, MA 02138 (US). **GANGISHETTY, Mahesh, Kumar**; 75 Canal Street, Medford, MA 02155 (US). **QUAN, Qimin**; 20 Wilson Ave., #1, Somerville, MA 02145 (US). **HOU, Shaocong**; 2 Peabody Terrace, Apt. 504, Cambridge, MA 02138 (US).

(74) Agent: **CHEN, Tani**; Wolf, Greenfield & Sacks, P.C., 600 Atlantic Avenue, Boston, MA 02210-2206 (US).

(81) Designated States *(unless otherwise indicated, for every kind of national protection available)*: AE, AG, AL, AM, AO, AT, AU, AZ, BA, BB, BG, BH, BN, BR, BW, BY, BZ, CA, CH, CL, CN, CO, CR, CU, CZ, DE, DJ, DK, DM, DO, DZ, EC, EE, EG, ES, FI, GB, GD, GE, GH, GM, GT, HN, HR, HU, ID, IL, IN, IR, IS, JO, JP, KE, KG, KH, KN, KP, KR, KW, KZ, LA, LC, LK, LR, LS, LU, LY, MA, MD, ME, MG, MK, MN, MW, MX, MY, MZ, NA, NG, NI, NO, NZ, OM, PA, PE, PG, PH, PL, PT, QA, RO, RS, RU, RW, SA, SC, SD, SE, SG, SK, SL, SM, ST, SV, SY, TH, TJ, TM, TN, TR, TT, TZ, UA, UG, US, UZ, VC, VN, ZA, ZM, ZW.

(84) Designated States *(unless otherwise indicated, for every kind of regional protection available)*: ARIPO (BW, GH, GM, KE, LR, LS, MW, MZ, NA, RW, SD, SL, ST, SZ, TZ, UG, ZM, ZW), Eurasian (AM, AZ, BY, KG, KZ, RU, TJ,

(54) Title: DOPED PEROVSKITE STRUCTURES FOR LIGHT-EMITTING DEVICES AND OTHER APPLICATIONS

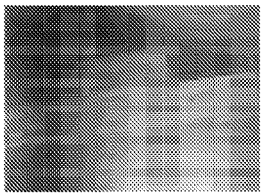

FIG. 13A

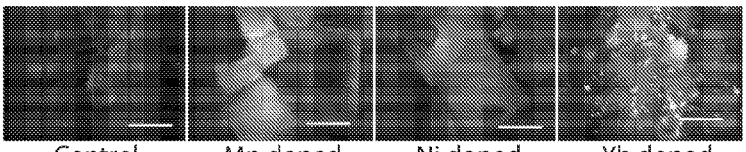

Control Mn doped Ni doped Yb doped

FIG. 13B FIG. 13C FIG. 13D FIG. 13E

(57) Abstract: The present disclosure generally relates to materials for use in applications such as light-emitting devices. For example, certain aspects are generally directed to a composition such as a composition including a perovskite structure (e.g., a perovskite nanocrystal) having a formula ABX_3, and methods of making or using such compositions. In some embodiments, A comprises one or more cations, e.g., methylammonium, formamidinium, and/or cesium. In certain cases, B comprises one or more metals and/or one or more transition metals (e.g., lead) and/or one or more dopants (e.g., manganese). In some embodiments, a dopant is incorporated into the perovskite structure. X may comprise one or more halides. Certain aspects of the disclosure are also generally directed to light-emitting diodes such as perovskite structure light-emitting diodes having high efficiency, and methods of making or using such devices.

WO 2019/099657 A1

[Continued on next page]

TM), European (AL, AT, BE, BG, CH, CY, CZ, DE, DK, EE, ES, FI, FR, GB, GR, HR, HU, IE, IS, IT, LT, LU, LV, MC, MK, MT, NL, NO, PL, PT, RO, RS, SE, SI, SK, SM, TR), OAPI (BF, BJ, CF, CG, CI, CM, GA, GN, GQ, GW, KM, ML, MR, NE, SN, TD, TG).

Published:

— *with international search report (Art. 21(3))*

DOPED PEROVSKITE STRUCTURES FOR LIGHT-EMITTING DEVICES AND OTHER APPLICATIONS

RELATED APPLICATIONS

This application claims priority under 35 U.S.C. § 119(e) to U.S. Provisional Application No. 62/586,846, filed November 15, 2017 and entitled "MANGANESE-DOPED PEROVSKITE STRUCTURES FOR LIGHT-EMITTING DEVICES AND OTHER APPLICATIONS," which is incorporated herein by reference in its entirety for all purposes.

FIELD

The present invention generally relates to materials for use in applications such as light-emitting devices, such as perovskite structures comprising manganese.

BACKGROUND

Light-emitting devices are useful for a variety of applications, including automobiles and traffic signals, aviation, cameras, home use, and personal electronics. One common example is the light-emitting diode, or LED. LEDs may include a hole transport region, an electron transport region, and a light-emitting region. Typically, extra electrons from the electron transport region and "holes" from the hole transport region combine together within the light-emitting region to produce light. (A hole is more accurately described as the lack of an electron in a position where one could exist, although those of ordinary skill in the art will often refer to a hole as if it were an actual particle, rather than the absence of a particle.) The efficiency of currently available LEDs, for example based on perovskite structures, has faced limitations. Therefore, improvements are needed.

SUMMARY

The present invention generally relates to materials for use in applications such as light-emitting devices, such as perovskite structures. The subject matter of the present invention involves, in some cases, interrelated products, alternative solutions to a particular problem, and/or a plurality of different uses of one or more systems and/or articles.

In one aspect, the present invention is generally directed to a composition. According to a first set of embodiment, the composition comprises a perovskite nanocrystal having a formula ABX_3, where A comprises methylammonium, formamidinium, and/or cesium, B comprises lead and manganese, and X comprises one or more halides. In some instances, the manganese and lead have a mole ratio of between 0.65 and 1.15. According to some embodiments, the

composition comprises a perovskite structure (e.g., nanocrystal) having a formula ABX_3, where A comprises methylammonium, formamidinium, and/or cesium, B comprises lead and a dopant (e.g., manganese), and X comprises one or more halides. In some instances, the dopant (e.g., manganese) and lead have a mole ratio of between 0.65 and 1.15. In some instances, the dopant (e.g., manganese) and lead have a precursor mole ratio of between 0.65 and 1.15. In some instances, B has a percentage of dopant of between 0.1% and 10%.

In another set of embodiments, the composition comprises a perovskite nanocrystal having a formula ABX_3, where A comprises methylammonium, formamidinium, and/or cesium, B comprises lead and manganese, and X comprises one or more halides. In some embodiments, the perovskite nanocrystal is formed from a source of A, a lead halide, and a manganese halide. In some cases, the manganese halide and the lead halide have a mole ratio of between 0.65 and 1.15. In some instances, B has a percentage of dopant of between 0.1% and 10%. In some embodiments, the composition comprises a perovskite structure (e.g., nanocrystal) having a formula ABX_3, where A comprises methylammonium, formamidinium, and/or cesium, B comprises lead and a dopant (e.g., manganese), and X comprises one or more halides. In some embodiments, the perovskite structure is formed from a source of A, a lead halide, and a dopant halide. In some cases, the dopant halide and the lead halide have a mole ratio of between 0.65 and 1.15. In some instances, B has a percentage of dopant of between 0.1% and 10%.

The composition, in yet another set of embodiments, comprises a composition comprising a perovskite nanocrystal having a formula $Cs(Pb_xMn_{1-x})X_3$, where X comprises one or more halides, and x is at least 0.4. In some embodiments, x is at least 0.9. The composition, in some embodiments, comprises a composition comprising a perovskite structure having a formula $Cs(Pb_xY_{1-x})X_3$, where X comprises one or more halides, Y comprises a dopant, and x is at least 0.4. In some embodiments, x is at least 0.9.

According to still another set of embodiments, the composition comprises a perovskite nanocrystal having a formula $Cs(Pb_xBi_{1-x})X_3$, where X comprises one or more halides, and x is at least 0.4. In some embodiments, x is at least 0.9.

In another aspect, the present invention is generally directed to a light-emitting device. According to one set of embodiments, the light-emitting device comprises an electron transport region, a hole transport region, and a light-emitting region in electrical contact with each of the electron transport region and the hole transport region. In some cases, the light-emitting region comprises a perovskite nanocrystal having a formula ABX_3, where A comprises

methylammonium, formamidinium, and/or cesium, B comprises lead and manganese, and X comprises one or more halides. In certain embodiments, the manganese and lead have a mole ratio of between 0.65 and 1.15. In some instances, B has a percentage of dopant of between 0.1% and 10%. In some cases, the light-emitting region comprises a perovskite structure having a formula ABX_3, where A comprises methylammonium, formamidinium, and/or cesium, B comprises lead and a dopant, and X comprises one or more halides. In certain embodiments, the dopant and lead have a precursor mole ratio of between 0.65 and 1.15. In some instances, B has a percentage of dopant of between 0.1% and 10%.

In another set of embodiments, the light-emitting device includes an electron transport region, a hole transport region, and a light-emitting region in electrical contact with each of the electron transport region and the hole transport region. In certain embodiments, the light-emitting region comprises a perovskite nanocrystal having a formula ABX_3, where A comprises methylammonium, formamidinium, and/or cesium, B comprises lead and manganese, and X comprises one or more halides. In some cases, the perovskite nanocrystal is formed from a source of A, a lead halide, and a manganese halide. The manganese halide and the lead halide, in some embodiments, have a mole ratio of between 0.65 and 1.15. In certain embodiments, the light-emitting region comprises a perovskite structure having a formula ABX_3, where A comprises methylammonium, formamidinium, and/or cesium, B comprises lead and a dopant, and X comprises one or more halides. In some cases, the perovskite structure is formed from a source of A, a lead halide, and a dopant halide. The dopant halide and the lead halide, in some embodiments, have a mole ratio of between 0.65 and 1.15. In some instances, B has a percentage of dopant of between 0.1% and 10%.

The light-emitting device, in yet another set of embodiments, may comprise an electron transport region, a hole transport region, and a light-emitting region in electrical contact with each of the electron transport region and the hole transport region. In certain embodiments, the light-emitting region comprises a perovskite nanocrystal having a formula $Cs(Pb_xMn_{1-x})X_3$, where X comprises one or more halides, and x is at least 0.4. In certain embodiments, the light-emitting region comprises a perovskite structure having a formula $Cs(Pb_xY_{1-x})X_3$, where X comprises one or more halides, Y comprises a dopant, and x is at least 0.9.

In still another set of embodiments, the light-emitting device comprises an electron transport region, a hole transport region, and a light-emitting region in electrical contact with each of the electron transport region and the hole transport region, where the light-emitting

region comprises a perovskite nanocrystal having a formula ABX_3. In certain instances, A comprises a perovskite nanocrystal having a formula $Cs(Pb_xBi_{1-x})X_3$, where X comprises one or more halides, and x is at least 0.4.

In one set of embodiments, the light-emitting device, comprises a blue light-emitting region comprising a first perovskite having a formula ABX_3, where A comprises methylammonium, formamidinium, and/or cesium, B comprises lead and manganese, and X comprises one or more halides. In one set of embodiments, the light-emitting device, comprises a blue light-emitting region comprising a first perovskite having a formula ABX_3, where A comprises methylammonium, formamidinium, and/or cesium, B comprises lead and a dopant, and X comprises one or more halides. The light-emitting device may also comprise a red light-emitting region positioned to downconvert blue light from the blue light-emitting region and emit red light, the red light-emitting region comprising a second perovskite, and/or a green light-emitting region positioned to downconvert blue light from the blue light-emitting region and emit green light, the green light-emitting region comprising a third perovskite.

The light-emitting device, in another set of embodiments, may comprise a blue light-emitting region comprising a first perovskite having a formula $Cs(Pb_xMn_{1-x})X_3$, where X comprises one or more halides, and x is at least 0.4. The light-emitting device, in some embodiments, may comprise a blue light-emitting region comprising a first perovskite having a formula $Cs(Pb_xY_{1-x})X_3$, where X comprises one or more halides, Y comprises a dopant, and x is at least 0.9. In certain cases, the light-emitting device may also comprise a red light-emitting region positioned to downconvert blue light from the blue light-emitting region and emit red light, the red light-emitting region comprising a second perovskite, and/or a green light-emitting region positioned to downconvert blue light from the blue light-emitting region and emit green light, the green light-emitting region comprising a third perovskite.

Yet another aspect of the present invention is generally directed to a method, such as a method of fabricating a light-emitting device. In one set of embodiments, the method includes depositing a first layer on a substrate, depositing a second layer on the first layer, and depositing a third layer on the second layer. The second layer may comprise a perovskite nanocrystal having a formula ABX_3, where A comprises methylammonium, formamidinium, and/or cesium, B comprises lead and manganese, and X comprises one or more halides. In some cases, the manganese and lead have a mole ratio of between 0.65 and 1.15. The second layer may comprise a perovskite structure having a formula ABX_3, where A comprises methylammonium,

formamidinium, and/or cesium, B comprises lead and a dopant, and X comprises one or more halides. In some cases, the dopant and lead have a precursor mole ratio of between 0.65 and 1.15. In some instances, B has a percentage of dopant of between 0.1% and 10%.

In another set of embodiments, the method includes depositing a first layer on a substrate, depositing a second layer on the first layer, and depositing a third layer on the second layer. The second layer may comprise a perovskite nanocrystal having a formula $Cs(Pb_xMn_{1-x})X_3$, where X comprises one or more halides, and x is at least 0.4. The second layer may comprise a perovskite structure having a formula $Cs(Pb_xY_{1-x})X_3$, where X comprises one or more halides, Y comprises a dopant, and x is at least 0.9.

The method, in yet another set of embodiments, includes depositing a first layer on a substrate, depositing a second layer on the first layer, and depositing a third layer on the second layer. The second layer may comprise a perovskite nanocrystal having a formula $Cs(Pb_xBi_{1-x})X_3$, wherein X comprises one or more halides, and x is at least 0.4. The second layer may comprise a perovskite structure having a formula $Cs(Pb_xY_{1-x})X_3$, wherein X comprises one or more halides, Y comprises a dopant, and x is at least 0.9.

Still another aspect of the present invention is generally directed to a method of operating a light-emitting device. In one set of embodiments, the method comprises applying a voltage between an electron transport region and a hole transport region of a light-emitting device, where the light-emitting device comprises a light-emitting region in electrical contact with each of the electron transport region and the hole transport region. In some embodiments, the light-emitting region may comprise a perovskite nanocrystal having a formula ABX_3, where A comprises methylammonium, formamidinium, and/or cesium, B comprises lead and manganese, and X comprises one or more halides. In some cases, the manganese and lead have a mole ratio of between 0.65 and 1.15. In some embodiments, the light-emitting region may comprise a perovskite structure having a formula ABX_3, where A comprises methylammonium, formamidinium, and/or cesium, B comprises lead and a dopant, and X comprises one or more halides. In some cases, the dopant and lead have a precursor mole ratio of between 0.65 and 1.15. In some instances, B has a percentage of dopant of between 0.1% and 10%.

The method, in another set of embodiments, includes applying a voltage between an electron transport region and a hole transport region of a light-emitting device, where the light-emitting device comprises a light-emitting region in electrical contact with each of the electron transport region and the hole transport region. In certain cases, the light-emitting region

comprises a perovskite nanocrystal having a formula ABX_3, where A comprises methylammonium, formamidinium, and/or cesium, B comprises lead and manganese, and X comprises one or more halides. In some embodiments, the perovskite nanocrystal is formed from a source of A, a lead halide, and a manganese halide. In certain cases, the manganese halide and the lead halide have a mole ratio of between 0.65 and 1.15. In certain cases, the light-emitting region comprises a perovskite structure having a formula ABX_3, where A comprises methylammonium, formamidinium, and/or cesium, B comprises lead and a dopant, and X comprises one or more halides. In some embodiments, the perovskite structure is formed from a source of A, a lead halide, and a dopant halide. In certain cases, the dopant halide and the lead halide have a mole ratio of between 0.65 and 1.15. In some instances, B has a percentage of dopant of between 0.1% and 10%.

In still another set of embodiments, the method includes applying a voltage between an electron transport region and a hole transport region of a light-emitting device, where the light-emitting device comprises a light-emitting region in electrical contact with each of the electron transport region and the hole transport region. In some cases, the light-emitting region comprises a perovskite nanocrystal having a formula ABX_3. In certain embodiments, A comprises a perovskite nanocrystal having a formula $Cs(Pb_xBi_{1-x})X_3$, where X comprises one or more halides, and x is at least 0.4. In some cases, the light-emitting region comprises a perovskite structure having a formula ABX_3. In certain embodiments, A comprises a perovskite structure having a formula $Cs(Pb_xY_{1-x})X_3$, where X comprises one or more halides, Y comprises a dopant, and x is at least 0.9.

In another aspect, the present invention encompasses methods of making one or more of the embodiments described herein. In still another aspect, the present invention encompasses methods of using one or more of the embodiments described herein.

Other advantages and novel features of the present invention will become apparent from the following detailed description of various non-limiting embodiments of the invention when considered in conjunction with the accompanying figures.

BRIEF DESCRIPTION OF DRAWINGS

Non-limiting embodiments of the present invention will be described by way of example with reference to the accompanying figures, which are schematic and are not intended to be drawn to scale. In the figures, each identical or nearly identical component illustrated is typically represented by a single numeral. For purposes of clarity, not every component is

labeled in every figure, nor is every component of each embodiment of the invention shown where illustration is not necessary to allow those of ordinary skill in the art to understand the invention. In the figures:

FIG. 1 illustrates a perovskite nanocrystal structure comprising an organic cation A or inorganic cation A, a metal cation B or a transition metal cation B, and a halide X, in accordance with some embodiments of the invention;

FIG. 2A illustrates a plot of photoluminescence spectra of perovskite nanocrystals in solution with different amounts of Mn doping, as expressed as Manganese to Lead (Mn:Pb) precursor mole ratios, in accordance with some embodiments of the invention;

FIG. 2B illustrates a plot of photoluminescence quantum yield (PLQY) and 1/e lifetime of thin films of perovskite nanocrystals with each thin film having nanocrystals with a respective amount of Mn doping, as expressed as a Mn:Pb precursor mole ratio, in accordance with some embodiments of the invention;

FIG. 2C illustrates a plot of time-resolved photoluminescence (PL) of perovskite nanocrystal species with different amounts of Mn doping, in accordance with some embodiments of the invention;

FIG. 2D illustrates a plot of Urbach energy measurements on absorption spectra for perovskite nanocrystal species with different amounts of Mn doping, in accordance with some embodiments of the invention;

FIG. 3A illustrates a schematic diagram of a device structure of a light-emitting diode (LED), in accordance with some embodiments of the invention;

FIG. 3B illustrates a plot of electroluminescence of fabricated LEDs with nanocrystals of different respective Mn amount, in accordance with some embodiments of the invention;

FIG. 3C illustrates a plot of current density-voltage-luminance (J-V-L) characteristics for LEDs (of which a device containing nanocrystals having an Mn:Pb precursor mole ratio of 0.972 is inset) containing nanocrystals of different respective Mn amount, in accordance with some embodiments of the invention;

FIG. 3D illustrates a plot of external quantum efficiency (EQE) of fabricated light-emitting devices comprising perovskite nanocrystals of different respective Mn amount, showing up to a four-fold (4x) enhancement over LEDs comprising control (undoped) perovskite nanocrystals, in accordance with some embodiments of the invention;

FIG. 4A illustrates a schematic diagram of a white LED design, in accordance with some embodiments of the invention;

FIG. 4B illustrates a plot of photoluminescence from a red downconverter layer and a green downconverter layer (dashed red and green; downconverter layers under room lights and UV illumination are inset) and electroluminescence from a blue LED and a white LED (solid lines), in accordance with some embodiments of the invention;

FIG. 4C delineates International Commission on Illumination (CIE) 1931 color space coordinates of light-emitting devices containing perovskite nanocrystals, in accordance with some embodiments of the invention;

FIG. 4D-FIG. 4E illustrate current density-voltage-luminance (J-V-L) and EQE curves respectively of a white LED, in accordance with some embodiments of the invention;

FIG. 5A illustrates photoluminescence spectra for perovskite nanocrystals, having an Mn:Pb precursor mole ratio of zero (0), as a function of time, in accordance with some embodiments of the invention;

FIG. 5B illustrates photoluminescence spectra for perovskite nanocrystals, having an Mn:Pb precursor mole ratio of 0.694, as a function of time, in accordance with some embodiments of the invention;

FIG. 5C illustrates photoluminescence spectra for perovskite nanocrystals, having an Mn:Pb precursor mole ratio of 0.972, as a function of time, in accordance with some embodiments of the invention;

FIG. 5D illustrates photoluminescence spectra for perovskite nanocrystals, having an Mn:Pb precursor mole ratio of 1.111, as a function of time, in accordance with some embodiments of the invention;

FIG. 5E illustrates photoluminescence spectra for perovskite nanocrystals, having an Mn:Pb precursor mole ratio of 1.250, as a function of time, in accordance with some embodiments of the invention;

FIG. 6 illustrates a transmission electron microscopy (TEM) image of perovskite nanocrystals having an Mn:Pb precursor mole ratio of 0.972, in accordance with some embodiments of the invention;

FIG. 7A illustrates a schematic diagram of a perovskite crystal structure, in accordance with some embodiments of the invention;

FIG. 7B illustrates photographic images of perovskite films with (y = 0.15, 0.3) and without (y = 0) a manganese dopant, in accordance with some embodiments of the invention;

FIG. 7C illustrates a series of x-ray diffraction (XRD) spectra of green perovskite films with (y = 0.15, 0.3) and without (y = 0) a manganese dopant, in accordance with some embodiments of the invention;

FIGs. 8A-C illustrate scanning electron microscopy (SEM) images of small undoped perovskite crystallites, in accordance with some embodiments of the invention;

FIGs. 8D-F illustrate scanning electron microscopy (SEM) images of doped perovskite thin films, in accordance with some embodiments of the invention;

FIG. 9 illustrates a plot of photoluminescence quantum yield (PLQY) for green, red, and blue perovskite films with (y = 0.15, 0.3) and without (y = 0) a manganese (Mn) dopant, in accordance with some embodiments of the invention;

FIG. 10A illustrates a plot of electroluminescence spectra for green perovskite light emitting diodes (LEDs) with varying amounts of Mn, in accordance with some embodiments of the invention;

FIGs. 10B, 10D, and 10F illustrate current density-voltage-luminance (J-V-L) plots for LEDs with perovskites with (y = 0.15, 0.3) and without (y = 0) a manganese (Mn) dopant, in accordance with some embodiments of the invention;

FIGs. 10C, 10E, and 10G illustrate external quantum efficiency-current density (EQE-J) plots for LEDs with perovskites with (y = 0.15, 0.3) and without (y = 0) a manganese (Mn) dopant as in FIGs. 10B, D, and F, in accordance with some embodiments of the invention;

FIGs. 11A-C illustrate plots of luminance over time for perovskite LEDs with (y = 0.15, 0.3) and without (y = 0) a manganese (Mn) dopant as in FIGs. 10B, 10D, and 10F, in accordance with some embodiments of the invention;

FIG. 12 illustrates a perovskite crystal growth apparatus, in accordance with some embodiments of the invention; and

FIGs. 13A-E illustrate microscopic images of perovskite crystals, including Figure 13A illustrating a bright field image of control crystals, and FIGs. 13B-13E illustrating images under ultraviolet (UV)-illumination of control perovskite crystals, Mn-doped perovskite crystals, Ni-doped perovskite crystals, and Yb-doped perovskite crystals respectively, in accordance with some embodiments of the invention.

DETAILED DESCRIPTION

The present disclosure generally relates to materials for use in applications such as light-emitting devices. For example, certain aspects are generally directed to a composition such as a composition including a perovskite structure (e.g., a perovskite nanocrystal) having a formula ABX_3, and methods of making or using such compositions. In some embodiments, a perovskite structure comprises a nanocrystal, a film, a bulk structure, or a combination thereof. In some embodiments, A comprises one or more cations, e.g., methylammonium, formamidinium, and/or cesium. In certain cases, B comprises one or more metals and/or one or more transition metals (e.g., lead) and/or one or more dopants (e.g., manganese). In some cases, the dopant comprises manganese, ytterbium, or nickel, or a combination thereof. In some embodiments, the dopant is manganese, ytterbium, or nickel. In some embodiments, a dopant is incorporated into the perovskite structure. In some embodiments, the dopant is incorporated into a perovskite nanocrystal, perovskite film, or perovskite bulk structure. X may comprise one or more halides. Certain aspects of the disclosure are also generally directed to light-emitting diodes such as perovskite structure light-emitting diodes having high efficiency, and methods of making or using such devices.

Certain aspects of the invention are generally directed to blue perovskite nanocrystal light emitting diodes (LEDs). In some embodiments, manganese doping of perovskite nanocrystals may increase the photoluminescence quantum yield (PLQY) and/or the lifetime of excitons to an unexpectedly large extent while preventing significant manganese emission and reducing the emission bandwidth. For example, the perovskite nanocrystals may be formed as thin films. In some embodiments, manganese doping may allow for a blue perovskite light-emitting device. In some cases, the blue emissions may be sufficient to meet the National Television System Committee (NTSC) standard. In some embodiments, green- and red-emitting perovskite nanocrystal downconverters can be utilized with the blue perovskite nanocrystals to form a "white" all-perovskite LED. For example, the white LED may be able to meet the International Commission on Illumination (CIE) 1931 color space coordinates for white light, e.g., as discussed below.

The embodiments described above are examples of the present disclosure. However, the light-emitting device need not have any and/or all of the above-described features in all embodiments. More generally, other embodiments of light-emitting devices are described below.

In some embodiments, for example, a composition is provided. The composition in some embodiments comprises a perovskite structure (e.g., a perovskite material, such as a perovskite nanocrystal). In some embodiments, the perovskite structure comprises a nanocrystal, a film, a bulk structure, or a combination thereof. A perovskite structure may have a chemical formula ABX_3, where A comprises one or more cations, e.g. an organic cation (e.g., methylammonium or formamidinium) and/or an inorganic cation (e.g., cesium). B may comprise one or more metals and/or one or more transition metals (e.g., lead). X may comprise one or more halides (e.g., fluoride, chloride, bromide, or iodide, or a combination thereof). For example, a perovskite may contain F_3, Cl_3, Br_3, I_3, or combination thereof, e.g., Br_xCl_{3-x}, Br_xI_{3-x}, Cl_xI_{3-x}, F_xCl_{3-x}, F_xBr_{3-x}, $Br_xCl_yI_{3-x-y}$, etc., where x may be any suitable number between 0 and 3, e.g., 0 or more, 0.1 or more, 0.2 or more, 0.3 or more, 0.4 or more, 0.5 or more, 0.6 or more, 0.7 or more, 0.8 or more, 0.9 or more, 1.0 or more, 1.1 or more, 1.2 or more, 1.3 or more, 1.4 or more, 1.5 or more, 1.6 or more, 1.7 or more, 1.8 or more, 1.9 or more, 2.0 or more, 2.1 or more, 2.2 or more, 2.3 or more, 2.4 or more, 2.5. or more, 2.6 or more, 2.7 or more, 2.8, or more, 2.9 or more, and/or 3.0 or less, 2.9 or less, 2.8 or less, 2.7 or less, 2.6 or less, 2.5 or less, 2.4 or less, 2.3 or less, 2.2 or less, 2.1 or less, 2.0 or less, 1.9 or less, 1.8 or less, 1.7 or less, 1.6 or less, 1.5 or less, 1.4 or less, 1.3 or less, 1.2 or less, 1.1 or less, 1.0 or less, 0.9 or less, 0.8 or less, 0.7 or less, 0.6 or less, 0.5 or less, 0.4 or less, 0.3 or less, 0.2 or less, or 0.1 or less. In addition combinations of any of these are also possible in certain embodiments, e.g., x may be between 1.5 and 2.5, between 0.5 and 1.5, etc.

In addition, in one set of embodiments, the perovskite structure is doped with one or more dopants. For example, the perovskite structure may be doped with a transition metal, e.g., manganese, or a post-transition metal, e.g. bismuth, or a metal, etc. In some embodiments, the perovskite structure may be doped with manganese, ytterbium, or nickel, or a combination thereof.

For instance, in one embodiment, the perovskite structure has a formula $CsPbX_3$, wherein the perovskite structure is doped with manganese, e.g., in concentrations such as those described herein. In another embodiment, the perovskite structure may be doped with bismuth.

In some embodiments, the perovskite structure is synthesized at least from one or more metal and/or transition metal precursors (e.g., a lead precursor, such as a lead halide) and one or more dopant precursors (e.g., a manganese precursor, such as a manganese halide). In certain cases, a dopant precursor comprises: a manganese precursor, such as a manganese halide; a

ytterbium precursor, such as a ytterbium halide; a nickel precursor, such as a nickel halide; or a combination thereof. In some embodiments, the final manganese:lead mole ratio in the synthesized perovskite structure is the same as an initial manganese:lead mole ratio in a precursor substance (e.g., a precursor solution, a precursor suspension, a precursor mixture, etc.). However, in other embodiments, the final ratio can be different than the initial ratio. Non-limiting examples of lead halides include $PbBr_2$ and $PbCl_2$. Non-limiting examples of manganese halides include $MnCl_2$ and $MnBr_2$. In addition other salts or other compounds, other than halides, may also be used, e.g., oxides.

The dopant may be present in the perovskite structure at a variety of suitable compositions. In some embodiments, the dopant may be present in the perovskite structure such that an emission (e.g., photoluminescence) peak height corresponding to a dopant is, as a percentage of an emission peak height corresponding to the perovskite structure, at least 0.01%, at least 1%, at least 2%, at least 3%, at least 4%, at least 5%, at least 6%, at least 7%, at least 8%, at least 9%, at least 10%, at least 11%, at least 12%, at least 13%, at least 14%, at least 15%, at least 16%, at least 17%, at least 18%, at least 19%, at least 20%, at least 22%, at least 24%, at least 26%, at least 28%, or at least 30%. In some embodiments, the dopant may be present in the perovskite structure such that an emission (e.g., photoluminescence) peak height corresponding to a dopant is, as a percentage of an emission peak height corresponding to the perovskite structure, at most 30%, most 28%, at most 26%, most 24%, at most 22%, most 20%, at most 19%, at most 18%, at most 17%, at most 16%, at most 15%, at most 14%, at most 13%, at most 12%, at most 11%, at most 10%, at most 9%, at most 8%, at most 7%, at most 6%, at most 5%, at most 4%, at most 3%, at most 2%, or at most 1%. Combinations of the above-referenced ranges are also possible (e.g., by weight of the perovskite nanocrystal, from 0.01% to 30%, from 2% to 30%, from 2% to 12%, from 4% to 6%).

The dopant may be present in the perovskite structure at a variety of suitable compositions. In some embodiments, the dopant may be present in the perovskite structure at a mole ratio of dopant:(one or more metals and/or one or more transition metals) of at least 0.01, at least 0.05, at least 0.1, at least 0.15, at least 0.2, at least 0.25, at least 0.3, at least 0.35, at least 0.4, at least 0.45, at least 0.5, at least 0.55, at least 0.6, at least 0.65, at least 0.69, at least 0.7, at least 0.75, at least 0.8, at least 0.85, at least 0.9, at least 0.95, at least 0.97, at least 1, at least 1.05, at least 1.1, at least 1.11, at least 1.15, at least 1.2, at least 1.24, at least 1.25, or at least 1.30. In some embodiments, the dopant may be present in the perovskite structure at a mole

ratio of dopant:(one or more metals and/or one or more transition metals) of at most 1.30, at most 1.25, at most 1.24, at most at most 1.2, at most 1.15, at most 1.11, at most 1.1, at most 1.05, at most 1, at most 0.97, at most 0.95, at most 0.9, at most 0.85, at most 0.8, at most 0.75, at most 0.7, at most 0.69, at most 0.65, at most 0.6, at most 0.55, at most 0.5, at most 0.45, at most 0.4, at most 0.35, at most 0.3, at most 0.25, at most 0.2, at most 0.15, at most 0.1, at most 0.05, or at most 0.01. Combinations of the above-referenced ranges are also possible (e.g., from 0.01 to 1.30, from 0.694 to 1.25, from 0.694 to 1.111, from 0.65 to 1.15, etc.). For example, in one embodiment, the perovskite may have a ratio of manganese to lead of 0.65 to 1.15, or any of the other ratios described herein.

The dopant may be present in the perovskite structure at a variety of suitable compositions. In some embodiments, the dopant may be present in the perovskite structure at a percent of B site, in the ABX_3 perovskite structure, of at least 0.1%, at least 0.15%, at least 0.2%, at least 0.25%, at least 0.3%, at least 0.35%, at least 0.4%, at least 0.45%, at least 0.5%, at least 0.55%, at least 0.6, at least 0.65%, at least 0.69%, at least 0.7%, at least 0.75%, at least 0.8%, at least 0.85%, at least 0.9, at least 0.95%, at least 0.97%, at least 1%, at least 1.05%, at least 1.1%, at least 1.11%, at least 1.15%, at least 1.2%, at least 1.24%, at least 1.25%, or at least 1.30%. In some embodiments, the dopant may be present in the perovskite structure at a percent of B site, in the ABX_3 perovskite structure, of at most 10%, at most 8%, at most 6%, at most 5%, at most 4%, at most 3%, at most 2%, at most 1.8%, or at most 1.5%. For example, 1.5% of the B sites having dopant corresponds to 15 dopant atoms and 985 Pb atoms out of every 1000 B sites, i.e., a mole ratio. Combinations of the above-referenced ranges are also possible (e.g., from 0.1% to 10%, from 0.1% to 5%, from 0.1% to 1.5%, etc.). For example, in some embodiments, a perovskite structure has from 0.1% to 10% of the B site as dopant, or any of the other percentages described herein.

In some embodiments, the dopant is present in the B position of the perovskite structure. As a non-limiting example, in a $CsPbX_3$ perovskite, a dopant such as manganese may replace some of the Pb in the B position. As a non-limiting example, in a $CsPbX_3$ perovskite, a dopant such as manganese, ytterbium, or nickel, or a combination thereof may replace some of the Pb in the B position. For instance, the manganese may be present at a Mn:Pb mole ratio of from 0.65 to 1.15 in the perovskite structure, or in any of the other amounts discussed herein. Thus, as an example, certain embodiments of the invention are generally directed to compositions having a formula $Cs(Pb_xMn_{1-x})X_3$, x being between 0 and 1. For instance, x may be chosen such that

manganese may be present at a Mn:Pb mole ratio of from 0.65 to 1.15 in the perovskite structure. In some cases, x may be at least 0.05, at least 0.1, at least 0.15, at least 0.2, at least 0.25, at least 0.3, at least 0.35, at least 0.4, at least 0.45, at least 0.47, at least 0.5, at least 0.55, at least 0.6, at least 0.65, at least 0.7, at least 0.75, at least 0.8, at least 0.85, at least 0.9, at least 0.92, at least 0.94, at least 0.95, at least 0.96, at least 0.98, or at least 0.99. In some cases x may be at most 0.99, at most 0.98, at most 0.96, at most 0.95, at most 0.94, at most 0.92, at most 0.9, at most 0.85, at most 0.8, at most 0.75, at most 0.7, at most 0.65, at most 0.6, at most 0.55, at most 0.5, at most 0.47, at most 0.45, at most 0.4, at most 0.35, at most 0.3, at most 0.25, at most 0.2, at most 0.15, at most 0.1, or at most 0.05. Combinations of any of the above-referenced ranges are also possible (e.g., from 0.01 to 0.99, from 0.45 to 0.6, from 0.47 to 0.6).

Certain embodiments of the invention are generally directed to perovskite structures having a formula $A(Pb_zY_{1-z})X_3$, z being between 0 and 1. In some cases, z may be at least 0.9, at least 0.95, at least 0.98, at least 0.99. In some cases z may be at most 0.999 or at most 0.995. Combinations of any of the above-referenced ranges are also possible (e.g., from 0.9 to 0.999, from 0.95 to 0.999, from 0.985 to 0.999).

In some embodiments, the dopant comprises manganese, ytterbium, or nickel, or a combination thereof. In some embodiments, the dopant is manganese, ytterbium, or nickel.

In some embodiments, a perovskite structure comprises a perovskite nanocrystal, which may be a nanocrystalline grain of the perovskite material surrounded by an organic ligand. In some embodiments, the composition comprises a plurality of perovskite nanocrystals.

In some embodiments, perovskite structure materials have advantageous features for electronic devices including but not limited to low cost, solution processability, and high quality electronic properties. Perovskite nanocrystals may demonstrate high photoluminescence quantum yields (PLQY).

A perovskite nanocrystal comprising a dopant may have an Urbach energy of a suitably low value. In some embodiments, the perovskite nanocrystal has an Urbach energy of at most 17.4 meV, at most 17.2 meV, at most 17.0 meV, at most 16.9 meV,at most 16.8 meV, at most 16.7 meV, at most 16.6 meV, at most 16.5 meV, at most 16.4 meV, at most 16.3 meV, at most 16.2 meV, at most 16.1 meV, at most 16.0 meV, at most 15.8 meV, at most 15.6 meV, at most 15.4 meV, at most 15.2 meV, at most 15.0 meV, at most 14.9 meV, at most 14.8 meV, or at most 14.7 meV. In some embodiments, the perovskite nanocrystal has an Uhrbach energy of at least 14.7 meV, at least 14.8 meV, at least 14.9 meV, at least 15.0 meV, at least 15.2 meV, at

least 15.4 meV, at least 15.6 meV, at least 15.8 meV, at least 16.0 meV, at least 16.1 meV, at least 16.2 meV, at least 16.3 meV, at least 16.4 meV, at least 16.5 meV, at least 16.6 meV, at least 16.7 meV, at least 16.8 meV, at least 16.9 meV, at least 17.0 meV, at least 17.2 meV, or at least 17.4 meV. Combinations of the above-referenced ranges are also possible (e.g., from 14.7 meV to 17.4 meV, from 14.7 eV to 16.7 eV). In some embodiments, the perovskite nanocrystal has an Uhrbach energy of at most 16.7 meV.

Some embodiments of this disclosure are directed to a film, e.g., a thin film, which comprises a composition comprising a perovskite structure, for instance, as discussed herein. A thin film may have a thickness of, for example, from 0.1 nm to 100 microns, or any other thicknesses such as described herein. In some embodiments, the thin film comprises one or more layers of perovskite nanocrystals.

In some embodiments, a light-emitting region as further described herein comprises one or more thin films (e.g., two, three, four, or more thin films), and/or other regions. For example, the light-emitting region of a light-emitting device may comprise a first thin film comprising one or more perovskite nanocrystals having a first composition, a second thin film comprising one or more perovskite nanocrystals having a second composition, and/or a third thin film comprising one or more perovskite nanocrystals having a third composition. In some embodiments, perovskite nanocrystals having the first composition may emit blue light, perovskite nanocrystals having the second composition may emit red light, and perovskite nanocrystals having the third composition may emit green light. In certain cases, the light-emitting device has an International Commission on Illumination (CIE) 1931 color space coordinate within the triangular area defined by vertices: (0.661,0.318); (0.071, 0.660); and (0.127, 0.077).

As another example, the device may contain a first, blue-emitting region, e.g., comprising a perovskite as discussed herein. The device may also contain red light-emitting regions and/or green light-emitting regions. In some cases, these regions may be positioned so as to be able to downconvert blue light from the blue light-emitting region, e.g., to produce red or green light. In some cases, one or both of these regions, if present, may also comprise perovskites, e.g., known to emit in red or blue light. Several such perovskites can be readily obtained commercially. Accordingly, some embodiments of the invention are generally directed to devices able to emit white light using only perovksites.

It should be understood that light that is "white," "blue," "green," or "red," e.g., as discussed herein, is not necessarily pure (monochromatic) light, but instead, in reality, may be a

mixture of several different wavelengths, e.g., resulting in the general appearance of white light, blue light, green light, or red light, etc. In some cases, the human eye may perceive such a mixture of wavelengths as a certain color, based on the strongest intensity wavelengths that are present. Thus, as an example, "white light," in reality, may be "off-white," "light grey" or other colors or shades that closely approximates white light when viewed by the unaided human eye.

In certain embodiments, the light-emitting device comprises one or more downconverters, e.g., one or more perovskite nanocrystal downconverters. In some embodiments, the one or more perovskite nanocrystal downconverters are on the display side of the light-emitting device. The perovskite nanocrystal downconverter(s) may be, e.g., a red downconverter (e.g., a red emitting perovskite nanocrystal) and/or a green downconverter (e.g., a green emitting perovskite nanocrystal). In certain embodiments, the red downconverter has a PLQY of at least 70% and/or the green downconverter has a PLQY of at least 60%. In some embodiments, at least some of the perovskite nanocrystal downconverters are red and/or green downconverters. In some embodiments, the downconverter is suspended in a suspending medium (e.g., comprising rubber or another polymer). In some embodiments, the suspending medium comprises poly(methyl methacrylate) (PMMA), poly(9-vinylcarbazole) (PVK), or a wide bandgap small molecule (e.g., 1,3,5-tri(m-pyridin-3-ylphenyl)benzene (TmPyPB), 1,3-bis(N-carbazolyl)benzene (mCP), 4,4′-bis(N-carbazolyl)-1,1′-biphenyl (CBP)), or a combination thereof.

The film may comprise red and/or green downconverters that may have a sufficiently high photoluminescence quantum yield (PLQY) to emit light at an efficiency so as to be commercially relevant. In some embodiments, the one or more downconverters independently have a PLQY of at least 9%, at least 10, at least 11%, at least 12%, at least 13%, at least 14, at least 15%, at least 16%, at least 17%, at least 18, at least 19%, at least 20%, at least 21%, at least 22%, at least 23%, at least 24%, at least 25%, at least 26%, at least 27%, at least 30%, at least 40%, at least 50%, at least 60%, at least 67%, at least 70%, at least 77%, at least 80%, at least 85%, at least 90%, at least 95%, or 100%. In some embodiments, the one or more downconverters have a PLQY of at most 100% or at most 90%. In some embodiments, the one or more downconverters have a PLQY of at most 80%, at most 77%, at most 70%, at most 67%, at most 60%, at most 50%, at most 40%, at most 30%, at most 27%, at most 26%, at most 25%, at most 24%, at most 23%, at most 22%, at most 21%, at most 20%, at most 19%, at most 18%, at most 17%, at most 16%, at most 15%, at most 14%, at most 13%, at most 12%, at most 11%,

or at most 10%. Combinations of the above-referenced ranges are also possible (e.g., from 9% to 80%, from 9% to 77%, from 9% to 67%). Other combinations of the above-referenced ranges are also possible (e.g., from 9% to 100%, from 9% to 90%).

The thin film may comprise blue emitting perovskite nanocrystals and may have a sufficiently high photoluminescence quantum yield (PLQY) to emit light at a relatively high efficiency. In some embodiments, the thin film has a PLQY of at least 9%, at least 10, at least 11%, at least 12%, at least 13%, at least 14, at least 15%, at least 16%, at least 17%, at least 18, at least 19%, at least 20%, at least 21%, at least 22%, at least 23%, at least 24%, at least 25%, at least 26%, at least 27%, at least 28%, at least 29%, at least 30%, or at least 31%. In some embodiments, the thin film has a PLQY of at most 32%, at most 31%, at most 30%, at most 29%, at most 28%, at most 27%, at most 26%, at most 25%, at most 24%, at most 23%, at most 22%, at most 21%, at most 20%, at most 19%, at most 18%, at most 17%, at most 16%, at most 15%, at most 14%, at most 13%, at most 12%, at most 11%, or at most 10%. Combinations of the above-referenced ranges are also possible (e.g., from 9% to 32%, from 12% to 32%, from 16% to 32%).

In some embodiments, the thin film has a suitably high 1/e photoluminescence lifetime, also referred to herein as lifetime. In some embodiments, the thin film has a 1/e photoluminescence lifetime of at least 1.70 ns, at least 1.77 ns, at least 2.00 ns, at least 2.08 ns, at least 2.10 ns, at least 2.20 ns, at least 2.30 ns, at least 2.40 ns, at least 2.50 ns, at least 2.60 ns, at least 2.70 ns, at least 2.80 ns, at least 2.90 ns, at least 3.00 ns, at least 3.03 ns, at least 3.06 ns, at least 3.10 ns, at least 3.20 ns, at least 3.23 ns, at least 3.25 ns, at least 3.3 ns, at least 3.35 ns, at least 4 ns, at least 4,5 ns, at least 5 ns, at least 5.5 ns, at least 6 ns, at least 6.5 ns, at least 7 ns, at least 7.5 ns, at least 8 ns, at least 8.5 ns, at least 9 ns, at least 9.5 ns, at least 10 ns, etc. In some embodiments, the thin film has a 1/e photoluminescence lifetime of at most 10 ns, at most 8 ns, at most 6 ns, or at most 4 ns. In some embodiments, the thin film has a 1/e photoluminescence lifetime of at most 3.35 ns, at most 3.3 ns, at most 3.25 ns, at most 3.23 ns, at most 3.20 ns, at most 3.10 ns, at most 3.06 ns, at most 3.03 ns, at most 3.00 ns, at most 2.90 ns, at most 2.80 ns, at most 2.70 ns, at most 2.60 ns, at most 2.50 ns, at most 2.40 ns, at most 2.30 ns, at most 2.20 ns, at most 2.10 ns, at most 2.08 ns, at most 2.00 ns, or at most 1.77 ns. Combinations of the above-referenced ranges are also possible (e.g., from 1.70 ns to 3.23 ns, from 1.77 ns to 3.23 ns, from 2.08 ns to 3.23 ns, from 2.50 ns to 3.23 ns, from 3.03 ns to 3.23 ns). Other combinations of the above-referenced ranges are also possible (e.g., from 1.70 ns to

10 ns). In some embodiments, the thin film has a 1/e photoluminescence lifetime longer than 10 ns.

In some embodiments, the plurality of perovskite nanocrystals are monodisperse. For example, in some cases, the monodisperse nanocrystals may have a standard deviation in maximum cross-sectional dimension of the nanocrystals less than or equal to 10% or 5% of the average cross-sectional dimension of the nanocrystals.

In some embodiments, in perovskite materials, the bandgap (and therefore the peak emission wavelength) can be controlled by adjusting a halide composition of the perovskite material, from deep blue (e.g., from chloride) to the near infrared (e.g., from iodide).

In some embodiments, a perovskite structure comprises a nanocrystal, a film, a bulk structure, or a combination thereof. In some embodiments, a perovskite film has a thickness of from 5 nm to 1 microns (e.g., from 20 nm to 500 nm). For example, the thickness may be at least 5 nm, at least 10 nm, at least 20 nm, at least 30 nm, at least 50 nm, at least 100 nm, at least 200 nm, at least 300 nm, at least 500 nm, etc., and/or no more than 1000 nm, no more than 500 nm, no more than 300 nm, no more than 200 nm, no more than 100 nm, no more than 50 nm, no more than 30 nm, no more than 20 nm, no more than 10 nm, etc. In some embodiments, the film comprises crystalline grains having a size of from 20 nm and 10 microns (e.g., from 50 nm to 1 micron). For example, the size may be at least 20 nm, at least 30 nm, at least 50 nm, at least 100 nm, at least 200 nm, at least 300 nm, at least 500 nm, at least 1 micron, at least 2 microns, at least 3 microns, at least 5 microns, etc., and/or no more than 10 microns, no more than 5 microns, no more than 3 microns, no more than 2 microns, no more than 1 micron, no more than 500 nm, no more than 300 nm, no more than 200 nm, no more than 100 nm, no more than 50 nm, no more than 30 nm, etc. In some embodiments, a bulk structure has a minimum dimension of at least 50 nm, at least 100 nm, at least 300 nm, at least 1 micron, at least 10 microns, etc.

In some embodiments, a light-emitting device is provided, as further described herein. For instance, the device may be an LED. In some embodiments, red and green light-emitting diodes (LEDs) based on perovskite nanocrystals have external quantum efficiencies reaching over 5%. Without wishing to be bound by theory, when considered in the context of LEDs, multi-color systems such as white may be achieved by using a combination of different perovskite structures with different emitting bandgaps. Without wishing to be bound be theory, in order to achieve white light and accurate color renderings in real world applications, efficient blue LEDs may be incorporated along with efficient red and/or green LEDs.

In some embodiments, the light-emitting device is a blue light-emitting device that meets the National Television System Committee (NTSC) standard. In order to meet the NTSC standard, in some embodiments, blue LEDs comprising perovskite nanocrystals are provided that emit at most at 470 nm (e.g., having a peak emission wavelength from 450 nm to 470 nm, 469 nm, 468 nm). In some embodiments, blue LEDs comprising perovskite nanocrystals are provided that have a peak emission wavelength of 469 nm and CIE coordinate of (0.127, 0.077).

The light-emitting device in some embodiments has an external quantum efficiency of at least 0.2%, at least 0.4%, at least 0.6%, at least 0.8%, at least 1.0%, at least 1.2%, at least 1.4%, at least 1.6%, at least 1.8%, at least 2.0%, at least 2.1%, at least 2.13%, at least 2.15%, at least 2.2%, at least 2.25%, at least 2.3%, at least 3%, at least 4%, at least 5%, at least 7%, at least 10%, at least 12%, at least 15%, at least 20%, at least 25%, etc. The light-emitting device in some embodiments has an external quantum efficiency of at most 25%, at most 20%, at most 15%, at most 10%, at most 5%, or at most 3%. The light-emitting device in some embodiments has an external quantum efficiency of at most 2.3%, at most 2.25%, at most 2.2%, at most 2.15%, at most 2.13%, at most 2.1%, at most 2.0%, at most 1.8%, at most 1.6%, at most 1.4%, at most 1.2%, at most 1.0%, at most 0.8%, at most 0.6%, at most 0.4%, or at most 0.2%. Combinations of the above-reference ranges are also possible (e.g., from 0.2% to 2.3%, from 0.73% to 2.3%, from 0.87% to 2.3%, from 1.46% to 2.3%). Other combinations of the above-reference ranges are also possible (e.g., from 0.2% to 25%, from 0.2% to 20%). The light-emitting device in some embodiments has an external quantum efficiency of 2.2% at a peak emission wavelength of 469 nm.

The light-emitting device, according to certain embodiments, has an emission peak having a full width half maximum (FWHM) of at most 26 nm, at most 25 nm, at most 20 nm, at most 19 nm, at most 18 nm, or at most 17 nm. The light-emitting device in some embodiments has an emission peak having a full width half maximum (FWHM) of at least 17 nm, at least 18 nm, at least 19 nm, at least 20 nm, or at least 25 nm. Combinations of the above-referenced ranges are also possible (e.g., from 17 nm to 26 nm, from 17.1 nm to 25.1 nm, from 17.1 nm to 18.4 nm, from 17.1 nm to 17.9 nm).

The light-emitting device, in some embodiments, has a turn-on voltage of at most 5 V, at most 4.8 V, at most 4.6 V, at most 4.4 V, at most 4.2 V, at most 4.0 V, at most 3.9 V, at most 3.8 V, at most 3.7 V, or at most 3.6 V. The light-emitting device in some embodiments has a turn-on voltage of at least 3.6 V, at least 3.7 V, at least 3.8 V, at least 3.9 V, at least 4.0 V, at least 4.2

V, at least 4.4 V, at least 4.6 V, or at least 4.8 V. Combinations of the above-reference ranges are also possible (e.g., from 3.6 V to 5 V, from 3.6 V to 4.0 V, from 3.6 V to 3.9 V).

In some embodiments, methods of fabricating a light-emitting device are provided, as further described herein. In some embodiments, the method comprises depositing a first layer on a substrate; depositing a second layer on the first layer, the second layer comprising a perovskite structure described herein, and depositing a third layer on the second layer. In some embodiments, the first layer comprises an electron transport region and the third layer comprises a hole transport region, or vice versa.

In addition, certain aspects of the present disclosure are generally directed to light-emitting diodes such as perovskite structure light-emitting diodes having high efficiency, and methods of making or using such devices. In some embodiments, the light-emitting device includes an electron transport region and a hole transport region. The hole transport region, in some cases, includes poly((9,9-dioctylfluorenyl-2,7-diyl)-co-(4,4'-(N-(4-sec-butylphenyl)diphenylamine))) (TFB) and/or a perfluorinated ionomer (PFI), e.g., as discussed in U.S. Provisional Application Ser. No. 62/586,837 filed on November 15, 2017, entitled "Light-Emitting Device Structures for Blue Light and Other Applications," incorporated herein by reference in its entirety. The light-emitting device may also include a light-emitting region that, in some cases, is in electrical contact with the electron transport region and the hole transport region.

In accordance with some embodiments of the disclosure, a light-emitting device is provided, e.g., a light-emitting diode. The light-emitting device may include a hole transport layer that includes poly(3,4-ethylenedioxythiophene):(polystyrene sulfonate) (PEDOT:PSS), TFB, and PFI layered directly on top of one another, e.g., in the listed order. Each of the PEDOT:PSS, the TFB, and the PFI can be deposited by spin coating onto an indium tin oxide (ITO) electrode, followed by annealing before depositing the next material layer. Other techniques are discussed in more detail below. The light-emitting device can also include a light-emitting layer of perovskite nanocrystals having a composition $CsPbBr_xCl_{3-x}$, layered directly on top of the hole transport layer by spin coating. In some embodiments, the light-emitting device includes an electron transport layer that includes 2,2',2"-(1,3,5-benzinetriyl)-tris(1-phenyl-1-H-benzimidazole) (TPBi) and lithium fluoride (LiF) layered directly on top of the layer of perovskite nanocrystals and directly on top of one another in the listed order. This can be formed using deposition in an evaporation chamber. In one embodiment, the light-

emitting device includes an aluminum (Al) electrode that is deposited directly onto the LiF layer in an evaporation chamber. The light-emitting device may emit blue light, or other wavelengths, e.g., as discussed herein.

Without wishing to be bound by theory, it is believed that the combination of the TFB and the PFI results in an increase in external quantum efficiency (EQE). In some embodiments, the light-emitting device has an EQE of greater than or equal to 0.1%. In some embodiments, the light-emitting device has a brightness of at least 111 cd/m^2 at an emission wavelength of 469 nm, or other brightnesses such as those discussed herein.

In some embodiments, for example, a light-emitting device is provided. The light-emitting device may comprise a hole transport region, an electron transport region, and a light-emitting region. In some embodiments, the light-emitting region is in contact with the electron transport region and/or the hole transport region. The contact may be physical, i.e., the regions may be in direct or indirect physical contact with each other, or there may be an intervening region. Without wishing to be bound by any theory, it is believed that holes (from the hole transport region) and electrons (from the electron transport region) may be able to recombine to produce light within the light-emitting region. One of more of these regions may each independently be substantially planar, e.g., forming a layer of material within the device, and/or the regions may be nonplanar in some cases. Thus, in one embodiment, the device may comprise three layers of material, e.g., a hole transport layer, an electron transport layer, and a light-emitting layer.

The hole transport region may be formed out of any material able to transport "holes" (lack of electrons) from one location to another, e.g., to a light-emitting region. The hole transport region may have any shape and/or size, e.g., as discussed herein. In some embodiments, the hole transport region may comprise poly((9,9-dioctylfluorenyl-2,7-diyl)-co-(4,4'-(N-(4-sec-butylphenyl)diphenylamine) (TFB) and/or a perfluorinated ionomer (PFI). It is believed that the combination of TFB and PFI within the hole transport region may present surprisingly large quantum efficiencies or photoluminescence quantum yields, e.g., as discussed herein, even as compared to other materials, or to separate uses of TFB and PFI. Without wishing to be bound by any theory, it is believed that the combination of TFB and PFI within a hole transport region surprisingly prevents or limits non-radiative decay from the hole transport region, thus promoting a higher efficiency of hole transport, and accordingly, more light production due to the recombination of holes and electrons within the light-emitting region.

TFB is also known as poly((9,9-dioctylfluorenyl-2,7-diyl)-co-(4,4'-(N-(4-sec-butylphenyl)diphenylamine))). It can be readily obtained commercially. The TFB may have any distribution of sizes, molecular weights, or polydispersities. For example, the TFB, in some embodiments, has a weight-average molecular weight of at least 500 Daltons (Da), at least 1 kilodaltons (kDa), at least 2 kDa, at least 5 kDa, at least 10 kDa, at least 20 kDa, at least 30 kDa, at least 35 kDa, at least 40 kDa, at least 45 kDa, at least 50 kDa, at least 60 kDa, at least 70 kDa, at least 80 kDa, at least 90 kDa, at least 100 kDa, or at least 500 kDa. The TFB, in some embodiments, has a weight-average molecular weight of at most 1000 kDa, at most 500 kDa, at most 100 kDa, at most 90 kDa, at most 80 kDa, at most 70 kDa, at most 60 kDa, at most 50 kDa, at most 45 kDa, at most 40 kDa, at most 35 kDa, at most 30 kDa, at most 20 kDa, at most 10 kDa, at most 5 kDa, at most 2 kDa, at most 1 kDa, or at most 500 Da. Combinations of the above-reference ranges are also possible (e.g., from 500 Da to 1000 kDa, from 2 kDa to 1000 kDa, from 500 Da to 2 kDa, from 30 kDa to 50 kDa, from 35 kDa to 45 kDa).

A variety of PFIs or perfluorinated ionomers may also be used in accordance with certain embodiments. A non-limiting example of a PFI is e.g., Nafion®, which is a sulfonated tetrafluoroethylene-based fluoropolymer-copolymer ionomer. However, in other embodiments, other PFIs may be used. Non-limiting examples include Aciplex® or Flemion®. More than one PFI may also be used within in hole transport regionin certain cases. Many such PFIs can be obtained commercially.

The PFI, in some embodiments, has a weight-average molecular weight of at least 500 Da, at least 1 kDa, at least 2 kDa, at least 5 kDa, at least 10 kDa, at least 20 kDa, at least 30 kDa, at least 35 kDa, at least 40 kDa, at least 45 kDa, at least 50 kDa, at least 60 kDa, at least 70 kDa, at least 80 kDa, at least 90 kDa, at least 100 kDa, at least 110 kDa, at least 120 kDa, at least 200 kDa, at least 300 kDa, or at least 500 kDa. The PFI, in some embodiments, has a weight-average molecular weight of at most 1000 kDa, at most 500 kDa, at most 300 kDa, at most 200 kDa, at most 120 kDa, at most 110 kDa, at most 100 kDa, at most 90 kDa, at most 80 kDa, at most 70 kDa, at most 60 kDa, at most 50 kDa, at most 45 kDa, at most 40 kDa, at most 35 kDa, at most 30 kDa, at most 20 kDa, at most 10 kDa, at most 5 kDa, at most 2 kDa, at most 1 kDa, or at most 500 Da. Combinations of the above-reference ranges are also possible (e.g., from 500 Da to 1000 kDa, from 2 kDa to 1000 kDa, from 500 Da to 2 kDa, from 80 kDa to 120 kDa). The PFI, in some embodiments, has a weight-average molecular weight of 100 kDa.

In some cases, the hole transport may also contain one or more materials to facilitate transport of holes across the hole transport layer. Such materials may be interspersed with one or more of the TFB and/or PFI (which may also, be combined together and/or present in different regions), or present as a separate layer or region. For example, in one set of embodiments, the hole transport region may contain PEDOT:PSS, which is poly(3,4-ethylenedioxythiophene) polystyrene sulfonate. PEDOT:PSS can be commercially obtained. As another example, the hole transport region may contain one or more conductive polymers, such as polythiophene. In some embodiments, the hole transport region may include such materials as a sublayer or subregion (for example, as a third sublayer or subregion in addition to one or more sublayers or subregions for TFB and/or PFI). For example, the TFB, PFI, and PEDOT:PSS may be present as 3 separate layers.

The PEDOT, in some embodiments, has a weight-average molecular weight of at least 500 Da, at least 1 kDa, at least 2 kDa, at least 5 kDa, at least 10 kDa, at least 20 kDa, at least 30 kDa, at least 40 kDa, at least 50 kDa, at least 60 kDa, at least 70 kDa, at least 80 kDa, at least 90 kDa, at least 100 kDa, at least 200 kDa, at least 300 kDa, or at least 500 kDa. The PEDOT, in some embodiments, has a weight-average molecular weight of at most 1000 kDa, at most 500 kDa, at most 300 kDa, at most 200 kDa, at most 100 kDa, at most 90 kDa, at most 80 kDa, at most 70 kDa, at most 60 kDa, at most 50 kDa, at most 40 kDa, at most 30 kDa, at most 20 kDa, at most 10 kDa, at most 5 kDa, at most 2 kDa, at most 1 kDa, or at most 500 Da. Combinations of the above-reference ranges are also possible (e.g., from 500 Da to 1000 kDa, from 2 kDa to 1000 kDa, from 500 Da to 2 kDa).

The PSS, in some embodiments, has a weight-average molecular weight of at least 500 Da, at least 1 kDa, at least 2 kDa, at least 5 kDa, at least 10 kDa, at least 20 kDa, at least 30 kDa, at least 40 kDa, at least 50 kDa, at least 60 kDa, at least 70 kDa, at least 80 kDa, at least 90 kDa, at least 100 kDa, at least 200 kDa, at least 300 kDa, or at least 500 kDa. The PSS, in some embodiments, has a weight-average molecular weight of at most 1000 kDa, at most 500 kDa, at most 300 kDa, at most 200 kDa, at most 100 kDa, at most 90 kDa, at most 80 kDa, at most 70 kDa, at most 60 kDa, at most 50 kDa, at most 40 kDa, at most 30 kDa, at most 20 kDa, at most 10 kDa, at most 5 kDa, at most 2 kDa, at most 1 kDa, or at most 500 Da. Combinations of the above-reference ranges are also possible (e.g., from 500 Da to 1000 kDa, from 2 kDa to 1000 kDa, from 500 Da to 2 kDa).

In some embodiments, a sublayer has a minimum cross-sectional thickness of at least 1 nm, at least 2 nm, at least 5 nm, at least 10 nm, at least 20 nm, at least 30 nm, at least 35 nm, at least 40 nm, at least 45 nm, at least 50 nm, at least 55 nm, at least 60 nm, at least 65 nm, at least 70 nm, at least 75 nm, at least 80 nm, at least 85 nm, at least 90 nm, at least 95 nm, at least 100 nm, at least 200 nm, at least 300 nm, at least 500 nm, or at least 900 nm. In some embodiments, the sublayer has a minimum cross-sectional thickness of at most 1000 nm, at most 900 nm, at most 500 nm, at most 300 nm, at most 200 nm, at most 100 nm, at most 95 nm, at most 90 nm, at most 85 nm, at most 80 nm, at most 75 nm, at most 70 nm, at most 65 nm, at most 60 nm, at most 55 nm, at most 50 nm, at most 45 nm, at most 40 nm, at most 35 nm, at most 30 nm, at most 20 nm, at most 10 nm, at most 5 nm, or at most 2 nm. Combinations of the above-referenced ranges are also possible (e.g., from 1 nm to 1000 nm, from 20 nm to 80 nm, from 35 nm to 45 nm, from 40 nm to 60 nm). The sublayer in some embodiments has a cross-sectional thickness of 40 nm.

In some embodiments, a ratio of a first cross-sectional thickness of a first layer to a second cross-sectional thickness of a second layer is at least 1:0.01, at least 1:0.02, at least 1:0.05, at least 1:0.08, at least 1:0.1, at least 1:0.15, at least 1:0.2, at least 1:0.3, at least 1:0.4, at least 1:0.5, at least 1:0.6, at least 1:0.7, at least 1:0.8, at least 1:0.9, or at least 1:0.95. In some embodiments, a ratio of the first cross-sectional thickness to the second cross-sectional thickness is at most 1:99, at most 1:90, at most 1:80, at most 1:70, at most 1:60, at most 1:50, at most 1:40, at most 1:30, at most 1:20, at most 1:10, at most 1:5, at most 1:2, at most 1:1, at most 1:0.99, at most 1:0.15, at most 1:0.1, or at most 1:0.08. Combinations of the above-referenced ranges are also possible (e.g., from 1:0.01 to 1:99, from 1:0.01 to 1:0.99, from 1:0.05 to 1:0.15, from 1:0.02 to 1:0.08). The ratio of the first cross-sectional thickness to the second cross-sectional thickness in some embodiments is 1:0.05.

In some embodiments, the hole transport region comprises a crystalline grain or a plurality of crystalline grains. For example, the TFB, PFI, and/or PEDOT:PSS may have a crystalline grain or a plurality of crystalline grains. However, in some embodiments, one or more of these may be free of crystalline grains. In some embodiments, the presence or absence of a crystalline grain or a plurality of crystalline grains can be determined by methods known to those of skill in the art, including but not limited to x-ray diffraction and transmission electron microscopy.

As mentioned, the device can also include an electron transport region, which may be present as a layer in some cases. In some embodiments, the electron transport region comprises 2,2',2"-(1,3,5-benzinetriyl)-tris(1-phenyl-1-H-benzimidazole) (TPBi) and/or lithium fluoride (LiF). As mentioned, the electron transport region may facilitate the transport of electrons to the light-emitting region, where they can combine with "holes" from the hole transport region.

The electron transport region or layer may have any of the dimensions described above with respect to the hole transport region. For example, in some embodiments, the electron transport region may have a minimum cross-sectional dimension of at least 1 nm, at least 5 nm, at least 10 nm, at least 20 nm, at least 30 nm, at least 40 nm, at least 50 nm, at least 100 nm, at least 500 nm, or at least 900 nm. In some embodiments, the electron transport region has a minimum cross-sectional dimension of at most 1000 nm, at most 900 nm, at most 500 nm, at most 100 nm, at most 50 nm, at most 40 nm, at most 30 nm, at most 20 nm, at most 10 nm, or at most 5 nm. Combinations of the above-referenced ranges are also possible (e.g., from 1 nm to 1000 nm, from 30 nm to 50 nm).

The TPBi may be present as a region, e.g., as a layer in some cases. The TPBi region or layer may have any of the dimensions described above with respect to the electron transport region. For example, in some embodiments, the TPBi region may have a minimum cross-sectional dimension of at least 1 nm, at least 5 nm, at least 10 nm, at least 20 nm, at least 30 nm, at least 40 nm, at least 50 nm, at least 100 nm, at least 500 nm, or at least 900 nm. In some embodiments, the TPBi region has a minimum cross-sectional dimension of at most 1000 nm, at most 900 nm, at most 500 nm, at most 100 nm, at most 50 nm, at most 40 nm, at most 30 nm, at most 20 nm, at most 10 nm, or at most 5 nm. Combinations of the above-referenced ranges are also possible (e.g., from 1 nm to 1000 nm, from 10 nm to 100 nm, from 20 nm to 50 nm).

The LiF may be present as a region, e.g., as a layer in some cases. The LiF region or layer may have any of the dimensions described above with respect to the electron transport region. In some embodiments, the LiF region may have a minimum cross-sectional dimension of at least 0.1 nm, at least 0.2 nm, at least 0.3 nm, at least 0.4 nm, at least 0.5 nm, at least 0.6 nm, at least 0.7 nm, at least 0.8 nm, at least 0.9 nm, at least 1 nm, at least 2 nm, at least 3 nm, at least 4 nm, at least 5 nm, at least 10 nm, at least 20 nm, at least 30 nm, at least 40 nm, at least 50 nm, at least 100 nm, at least 500 nm, or at least 900 nm. In some embodiments, the LiF region has a minimum cross-sectional dimension of at most 1000 nm, at most 900 nm, at most 500 nm, at most 100 nm, at most 50 nm, at most 40 nm, at most 30 nm, at most 20 nm, at most 10 nm, at

most 5 nm, at most 4 nm, at most 3 nm, at most 2 nm, at most 1 nm, at most 0.9 nm, at most 0.8 nm, at most 0.7 nm, at most 0.6 nm, at most 0.5 nm, at most 0.4 nm, at most 0.3 nm, or at most 0.2 nm. Combinations of the above-referenced ranges are also possible (e.g., from 0.1 nm to 1000 nm, from 0.1 nm to 5 nm, from 0.5 nm to 2 nm).

The device may also include a light-emitting region or layer, which is able to emit light through the combination of holes with electrons. The light-emitting region or layer may have any of the dimensions described above with respect to the hole transport region.

In some embodiments, the light-emitting region comprises particles, such as a nanoparticles. The nanoparticle, in certain embodiments, comprises a nanocrystal.

In some embodiments, the light-emitting region comprises perovskite-type materials, e.g., materials having a perovskite structure, of which perovskite itself ($CaTiO_3$) is the prototypical example, as discussed above. However, as is understood by those of ordinary skill in the art, perovskite-type materials (or sometimes, just "perovskite"), such as those discussed herein, are not to be construed as being limited to only $CaTiO_3$, but may include any material having the same crystal structure as the prototypical perovskite crystal structure.

In some embodiments, the light-emitting region has a maximum cross-sectional dimension of at least at least 1 nm, at least 3 nm, at least 5 nm, at least 10 nm, at least 15 nm, at least 18 nm, at least 20 nm, at least 22 nm, at least 25 nm, at least 30 nm, at least 35 nm, at least 40 nm, at least 45 nm, at least 50 nm, at least 60 nm, at least 70 nm, at least 80 nm, at least 90 nm, at least 100 nm, or at least 500 nm. In some embodiments, the perovskite nanocrystal has a maximum cross-sectional dimension of at most 900 nm, at most 500 nm, at most 100 nm, at most 90 nm, at most 80 nm, at most 70 nm, at most 60 nm, at most 50 nm, at most 45 nm, at most 40 nm, at most 35 nm, at most 30 nm, at most 25 nm, at most 22 nm, at most 20 nm, at most 18 nm, at most 15 nm, at most 10 nm, at most 5 nm, or at most 3 nm. Combinations of the above-reference ranges are also possible (e.g., from 1 nm to 900 nm, from 3 nm to 100 nm, from 5 nm from 30 nm, from 5 nm to 20 nm, from 10 nm to 30 nm, from 15 nm to 25 nm, from 18 nm to 22 nm). The perovskite nanocrystal in some embodiments has a maximum cross-sectional dimension of 20 nm.

In some embodiments, the light-emitting region has a minimum cross-sectional thickness of at least 1 nm, at least 2 nm, at least 3 nm, at least 4 nm, at least 5 nm, at least 6 nm, at least 7 nm, at least 8 nm, at least 9 nm, at least 10 nm, at least 20 nm, at least 30 nm, at least 50 nm, at least 80 nm, at least 90 nm, at least 100 nm, or at least 500 nm. In some embodiments, the

perovskite nanocrystal has a cross-sectional thickness of at most 900 nm, at most 500 nm, at most 100 nm, at most 90 nm, at most 80 nm, at most 50 nm, at most 30 nm, at most 20 nm, at most 10 nm, at most 9 nm, at most 8 nm, at most 7 nm, at most 6 nm, at most 5 nm, at most 4 nm, at most 3 nm, or at most 2 nm. Combinations of the above-reference ranges are also possible (e.g., from 1 nm to 900 nm, from 1 nm to 10 nm, from 2 nm to 8 nm, from 4 nm to 6 nm). The perovskite nanocrystal in some embodiments has a cross-sectional thickness of 5 nm.

In some embodiments, the light-emitting region may comprise one or more layers of perovskite nanocrystals. In some cases, the perovskite nanocrystals in a light-emitting region have an average concentration in a layer of from 25 nanometers squared per nanocrystal to 400 nanometers squared per nanocrystal, as can be measured by, for example, atomic force microscopy or transmission electron microscopy.

In some embodiments, the light-emitting device may further comprise an electrode. In some embodiments, the light-emitting device may comprise a first electrode and a second electrode. The electrode in some embodiments may be optically transparent (e.g. to wavelengths of from 300 nm to 700 nm). The first electrode in some embodiments may comprise indium tin oxide. The electrode, in some embodiments, may comprise (as non-limiting examples) a metal, an alloy, a transition metal, copper, graphite, gold, titanium, brass, silver, aluminum, or platinum, or a combination thereof. The second electrode, in some embodiments, comprises aluminum.

In some embodiments, the light-emitting device has a surprisingly large external quantum efficiency. External quantum efficiency generally refers to a ratio of the number of photons emitted from the light-emitting device, to the number of electrons passing through the light-emitting device, e.g., during an application of a voltage between the electron transport region and the hole transport region. The external quantum efficiency can be calculated from the measured intensity, wavelength, and current of the light-emitting device. The intensity and wavelength of the light-emitting device may be measured by photoluminescence spectroscopy, and current can be measured by e.g. an ammeter.

The light-emitting device in some embodiments has an external quantum efficiency of at least 0.01%, at least 0.05%, at least 0.1%, at least 0.2%, at least 0.3%, at least 0.4%, at least 0.5%, at least 0.6%, at least 0.7%, at least 0.8%, at least 0.9%, at least 1%, at least 2%, at least 3%, at least 5%, at least 7%, at least 10%, at least 15%, at least 20%, or at least 25%, etc., at a peak emission wavelength of from 400 nm to 800 nm. The light-emitting device in some

embodiments has an external quantum efficiency of at most 25%, at most 20%, at most 15%, at most 10%, at most 5%, or at most 3%, at a peak emission wavelength of from 400 nm to 800 nm. The light-emitting device in some embodiments has an external quantum efficiency of at most 1%, at most 0.9%, at most 0.8%, at most 0.7%, at most 0.6%, at most 0.5%, at most 0.4%, at most 0.3%, at most 0.2%, at most 0.1%, or at most 0.05%, at a peak emission wavelength of from 400 nm to 800 nm. Combinations of the above-reference ranges are also possible (e.g., from 0.01% to 0.1%, from 0.1% to 1%, from 0.1% to 0.5%). Other combinations of the above-reference ranges are also possible (e.g., from 0.2% to 25%, from 0.2% to 20%). The light-emitting device in some embodiments has an external quantum efficiency of 0.5% at a peak emission wavelength of 469 nm.

In some embodiments, the light-emitting device has a photoluminescence quantum yield, which may refer to a ratio of the number of photons emitted by photoluminescence by the light-emitting device to the number of photons absorbed by the light-emitting device. The number of photons emitted can be measured by photoluminescence spectroscopy.

The light-emitting device in some embodiments has a photoluminescence quantum yield of at least 1%, at least 2%, at least 3%, at least 4%, at least 5%, at least 6%, at least 7%, at least 8%, at least 9%, at least 10%, at least 20%, at least 25%, at least 30%, at least 40%, at least 50%, at least 60%, at least 70%, at least 80%, at least 90%, at least 95%, etc. The light-emitting device in some embodiments has a photoluminescence quantum yield of at most 100%, at most 99%, at most 80%, at most 70%, at most 60%, at most 50%, at most 40%, at most 30%, at most 27%, or at most 20%. The light-emitting device in some embodiments has a photoluminescence quantum yield of at most 10%, at most 9%, at most 8%, at most 7%, at most 6%, at most 5%, at most 5%, at most 3%, or at most 2%. Combinations of the above-reference ranges are also possible (e.g., from 1% to 10%, from 0.1% to 0.5%, etc.). Other combinations of the above-reference ranges are also possible (e.g., from 1% to 100%, from 0.1% to 80%, etc.).

The light-emitting device in some embodiments has a maximum brightness of at least 1 cd/m^2, at least 5 cd/m^2, at least 10 cd/m^2, at least 20 cd/m^2, at least 30 cd/m^2, at least 50 cd/m^2, at least 80 cd/m^2, at least 100 cd/m^2, at least 120 cd/m^2, at least 140 cd/m^2, at least 160 cd/m^2, at least 200 cd/m^2, at least 500 cd/m^2, at least 1000 cd/m^2, or at least 1500 cd/m^2, at least 2000 cd/m^2, at least 3000 cd/m^2, at least 5000 cd/m^2, at least 10,000 cd/m^2, at least 20,000 cd/m^2, etc. at a peak emission wavelength of from 400 nm to 800 nm. In some cases, higher brightnesses are possible, e.g., for a green light-emitting device. For instance, the maximum brightness for

green light may be at least 30,000 cd/m^2, at least 50,000 cd/m^2, at least 100,000 cd/m^2, at least 200,000 cd/m^2, at least 300,000 cd/m^2, at least 500,000 cd/m^2, at least 1,000,000 cd/m^2, etc.

The light-emitting device in some embodiments has a maximum brightness of at most 1,000,000 cd/m^2 (e.g., for a green light-emitting device), at most 100,000 cd/m^2, at most 50,000 cd/m^2, at most 20,000 cd/m^2 (e.g., for a blue light-emitting device), at most 10,000 cd/m^2, at most 5,000 cd/m^2, or at most 4,000 cd/m^2, at a peak emission wavelength of from 400 nm to 800 nm. The light-emitting device in some embodiments has a maximum brightness of at most 3000 cd/m^2, at most 1500 cd/m^2, at most 1000 cd/m^2, at most 500 cd/m^2, at most 200 cd/m^2, at most 160 cd/m^2, at most 140 cd/m^2, at most 120 cd/m^2, at most 100 cd/m^2, at most 80 cd/m^2, at most 50 cd/m^2, at most 30 cd/m^2, at most 20 cd/m^2, at most 10 cd/m^2, or at most 5 cd/m^2, at a peak emission wavelength of from 400 nm to 800 nm. Combinations of the above-reference ranges are also possible (e.g., from 1 cd/m^2 to 3000 cd/m^2, from 100 cd/m^2 to 200 cd/m^2). Other combinations of the above-reference ranges are also possible (e.g., from 1 cd/m^2 to 1,000,000 cd/m^2, from 100 cd/m^2 to 50,000 cd/m^2). The light-emitting device in some embodiments has a maximum brightness of 111 cd/m^2 at a peak emission wavelength of 469 nm.

In some embodiments, methods for fabricating the light-emitting device (e.g., the light-emitting device of any of the embodiments herein) are provided. A method of fabricating the light-emitting device may comprise depositing a hole transport region, a light-emitting region, and an electron transport, e.g., on a substrate. A variety of deposition techniques may be used, such as spin coating, dip coating, lithography, chemical vapor deposition, physical vapor deposition, or the like. In addition, in some embodiments, one or more electrodes may be deposited on the device.

The hole transport region, in some embodiments, is deposited onto a first electrode, and/or onto a substrate comprising a first electrode. The light-emitting region may be deposited after (e.g., directly onto) the hole transport region. In some embodiments, the electron transport region is deposited after (e.g., directly onto) the light-emitting region and/or the hole transport region. In some embodiments, the method may comprise depositing a second electrode after (e.g., directly onto) the electron transport region.

In some embodiments, the electron transport region is deposited onto the second electrode, and/or onto a substrate comprising the second electrode. In some embodiments, the light-emitting region is deposited after (e.g., directly onto) the electron transport region. In some embodiments, the hole transport region is deposited after (e.g., directly onto) the light-emitting

region and/or the electron transport region. In some embodiments, the method may comprise depositing the first electrode after (e.g., directly onto) the hole transport region.

In some embodiments, depositing (e.g., depositing a region, e.g., a hole transport region or a light-emitting region) comprises spin coating. The process of spin coating will may comprise adding a fluid (e.g., a solution or suspension comprising the composition of the electron transport region, a solution or suspension comprising the composition of the hole transport region, a solution or suspension comprising the composition of the light-emitting region) onto a substrate that is rotated before, during, and/or after the fluid is added onto the substrate, such that a composition from the fluid (e.g., a molecule and/or a particle dissolved and/or suspended in the fluid, or a plurality of the molecules and/or the particles) remains on the substrate.

In some embodiments, depositing (e.g., depositing a region) comprises inkjet printing or dip coating a composition from a fluid onto the substrate. The fluid may include, for instance, e.g., a solution or suspension comprising a precursor composition of the electron transport region, a solution or suspension comprising a precursor composition of the hole transport region, a solution or suspension comprising a precursor composition of the light-emitting region, etc.

In some embodiments, one or more regions of the device may be annealed. In some embodiments, annealing comprises heating an article (e.g., comprising a substrate and/or any added material) to a maximum temperature of at least 50 degrees Celsius, at least 100 degrees Celsius, at least 110 degrees Celsius, at least 120 degrees Celsius, at least 125 degrees Celsius, at least 130 degrees Celsius, at least 135 degrees Celsius, at least 140 degrees Celsius, at least 145 degrees Celsius, at least 160 degrees Celsius, at least 180 degrees Celsius, at least 200 degrees Celsius, at least 300 degrees Celsius, at least 400 degrees Celsius, at least 500 degrees Celsius, at least 600 degrees Celsius, at least 700 degrees Celsius, at least 800 degrees Celsius, or at least 900 degrees Celsius. In some embodiments, annealing comprises heating an article to a maximum temperature of at most 1000 degrees Celsius, at most 900 degrees Celsius, at most 800 degrees Celsius, at most 700 degrees Celsius, at most 600 degrees Celsius, at most 500 degrees Celsius, at most 400 degrees Celsius, at most 300 degrees Celsius, at most 200 degrees Celsius, at most 180 degrees Celsius, at most 160 degrees Celsius, at most 145 degrees Celsius, at most 140 degrees Celsius, at most 135 degrees Celsius, at most 130 degrees Celsius, at most 125 degrees Celsius, at most 120 degrees Celsius, or at most 110 degrees Celsius, or at most 110 degrees Celsius. Combinations of the above-reference ranges are also possible (e.g., from 50

degrees Celsius to 1000 degrees Celsius, from 100 degrees Celsius to 200 degrees Celsius, from 140 degrees Celsius to 150 degrees Celsius).

In some embodiments, depositing (e.g., depositing a region such as an electron transport region, depositing an electrode) comprises physical vapor deposition or chemical vapor deposition. In certain cases, physical vapor deposition comprises thermal evaporation (e.g., using an evaporation chamber). The process of thermal evaporation may comprise positioning a substrate above a material to be evaporated (e.g., at a distance of from 200 mm to 1 m), and then evaporating the material to be deposited by reducing the external pressure and increasing the temperature to which the material is exposed. At least some of the evaporated material then coats the substrate.

In some embodiments, methods of operating a light-emitting device (e.g., a light-emitting device of any of the embodiments of this disclosure) are provided. A method of operating a light-emitting device according to certain embodiments comprises applying a voltage across the light-emitting device. The voltage may be applied between the electron transport region and the hole transport region. For example, applying the voltage across the light-emitting device may comprise applying the voltage to a first electrode and a second electrode, wherein the first electrode is electrically connected to the hole transport region and the second electrode is electrically connected to the electron transport region of the light-emitting device. In some embodiments, the light-emitting region is in physical contact with both the electron transport region and the hole transport region.

In some embodiments, the voltage applied across the light-emitting device is at least 0.1 V, at least 0.2 V, at least 0.3 V, at least 0.4 V, at least 0.5 V, at least 0.6 V, at least 0.7 V, at least 0.8 V, at least 0.9 V, at least 1 V, at least 2 V, at least 3 V, at least 4 V, at least 5 V, at least 6 V, at least 6.5 V, at least 7 V, at least 7.5 V, at least 8 V, at least 9 V, at least 10 V, at least 12 V, at least 14 V, at least 16 V, or at least 18 V. In some embodiments, the voltage applied across the light-emitting device is at most 20 V, at most 18 V, at most 16 V, at most 14 V, at most 12 V, at most 10 V, at most 9 V, at most 8 V, at most 7.5 V, at most 7 V, at most 6.5 V, at most 6 V, at most 5 V, at most 4 V, at most 3 V, at most 2 V, at most 1 V, at most 0.9 V, at most 0.8 V, at most 0.7 V, at most 0.6 V, at most 0.5 V, at most 0.4 V, at most 0.3 V, or at most 0.2 V. Combinations of the above-reference ranges are also possible (e.g., from 0.1 V to 20 V, from 0.1 V to 7.5 V).

U.S. Provisional Application No. 62/586,846, filed November 15, 2017 and entitled "MANGANESE-DOPED PEROVSKITE STRUCTURES FOR LIGHT-EMITTING DEVICES AND OTHER APPLICATIONS," is incorporated herein by reference in its entirety for all purposes.

U.S. Provisional Application No. 62/586,837, filed November 15, 2017 and entitled "LIGHT-EMITTING DEVICE STRUCTURES FOR BLUE LIGHT AND OTHER APPLICATIONS," is incorporated herein by reference in its entirety for all purposes.

A PCT application filed on the same day as the instant application, entitled "Light-Emitting Device Structures For Blue Light And Other Applications," by Congreve, *et al.*, is incorporated herein by reference in its entirety for all purposes.

The following examples are intended to illustrate certain embodiments of the present invention, but do not exemplify the full scope of the invention.

EXAMPLE 1

In this example, $CsPbBr_xCl_{3-x}$ perovskite nanocrystals were synthesized with moderate exciton confinement and improved charge injection properties. It was then demonstrated that the emission efficiency and lifetime of the $CsPbBr_xCl_{3-x}$ perovskite nanocrystals were significantly impaired when the perovskite nanocrystals were used with traditional hole transport layers (HTLs) such as NiO_x. A device architecture was then developed that did not affect the emission from the perovskite nanocrystals. Light-emitting device performance with increased to a maximum external quantum efficiency (EQE) of 0.50% and a brightness of 111 cd/m^2 at an emission wavelength of 469 nm. Finally, it was demonstrated that these device improvements were beneficial across the visible spectrum, with high brightness and efficiency devices spanning from 511 nm to 469 nm.

$CsPbBr_xCl_{3-x}$ perovskite nanocrystals were synthesized (see, e.g., Example 2) at low temperature to favor an asymmetric crystal growth. The yielded nanocrystals were approximately 20 nm in the lateral dimension and 5 nm thick.

Absorption and emission properties of the nanocrystals demonstrated a slight excitonic peak and a narrow emission of 23 nm FWHM. These nanocrystals were robust to purification process by polar solvent (e.g., ethyl acetate) washing, and the washing preserved balanced properties of the nanocrystals, such as exciton confinement/emission and charge injection.

The transient decay of a thin film of nanocrystals was monitored as a function of the composition of an underlying layer. All data was measured in air with 379 nm excitation using a Hamamatsu streak camera integrated across the emission wavelength of the nanocrystals.

To improve the emission from a light-emitting device, an HTL constructed of a trilayer made of PEDOT:PSS/TFB/PFI was used. The TFB is an electron-blocking, hole-transport polymer with a strong hole mobility of 0.01 cm^2/Vs. PFI can be used as part of a buffer electron blocking layer leading to high brightness devices. Without wishing to be bound by theory, it may be that strong surface dipole induced by PFI led to a band bending of the HTL to a higher work function, favorable for hole injection, while the isolation of the perovskite layers helped to reduce their exciton quenching process.

In order to better understand the dynamics of the luminescence of the nanocrystals, due to the luminescence of TFB overlapping with that of the nanocrystals, the TFB-only emission was first subtracted from the data taken for samples. The transient decay with PEDOT:PSS/TFB/PFI was virtually identical to the emission behavior from glass, demonstrating that the nanocrystals were not significantly perturbed by the presence of the HTL, and thus this HTL could substantially improve the emission from the nanocrystals relative to current HTLs.

To more clearly quantify the benefits of this HTL switch, devices were fabricated utilizing both NiO_x and PEDOT:PSS/TFB/PFI as the HTL. ITO coated glass was cleaned via solvent washing and plasma cleaning immediately before sequential spin coating of the HTL layers, either PEDOT:PSS, TFB, and PFI, or the NiO_x precursor (followed by heating to form NiO_x). Without wishing to be bound by theory, the presence and/or relative position of the PFI layer helped to maintain nanocrystal emission. Without PFI, electroluminescence from primarily TFB was observed. The nanocrystals were then spuncast from octane, and the partial device was then transferred to a thermal evaporator, where 40 nm of TPBi was evaporated, followed by evaporation of LiF/Al to form the top contact and the device was patterned with a diameter of 2 mm. All device fabrication was performed inside a glovebox in an inert gas atmosphere (e.g., nitrogen, argon). All device testing was done on unpackaged devices in air.

After device fabrication, clear electroluminescence was observed from the perovskite nanocrystal layer in both structures of NiO_x and PEDOT:PSS/TFB/PFI. The electroluminescence spectra from both devices were nearly identical to each other, with a peak

of 469 nm and a FWHM of 24 nm for the NiO_x and 25 nm for the PEDOT:PSS/TFB/PFI. The emission was unchanged as a function of applied voltage.

The NiO_x device, relatively a more conductive structure than PEDOT:PSS/TFB/PFI, demonstrated a low turn-on voltage and high brightness, but was limited by high dark current and the non-radiative recombination of the nanocrystals discussed previously, leading to a maximum EQE of 0.03%. The PEDOT:PSS/TFB/PFI device, in contrast, demonstrated a higher turn-on voltage but a much lower dark current, indicating strong film formation and reduced pinholes. The EQE for PEDOT:PSS/TFB/PFI devices reached a value as high as 0.50% before rolling off at higher current densities. This high quantum efficiency demonstrated the value of PEDOT:PSS/TFB/PFI as an HTL and showed significant efficiency for blue perovskite nanocrystals.

Finally, to demonstrate the versatility of the PEDOT:PSS/TFB/PFI device structure, the bromide to chloride ratio was tuned to adjust the emission wavelength, while keeping the device structure constant. The fabricated devices had emission wavelengths at 469 nm, 481 nm, 488 nm, and 511 nm, with narrow FWHM. The J-V-L characteristics were similar for all devices with low dark currents and turn-on voltages that increased with increased bandgap. There was a substantial increase in efficiency as the emission wavelength redshifted; indeed, a small 7 nm emission wavelength difference between the 481 nm and 488 nm device resulted in a threefold difference in maximum EQE.

As the energetics were shifted towards green, a small gain in quantum efficiency resulted. While the 469 nm device showed a strong efficiency enhancement with the HTL change, the bromide device peaked at 2.3% EQE and 3423 cd/m^2. Without wishing to be bound by theory, it was hypothesized that the energetic requirements for lower bandgap nanocrystals were much less restrictive than those for higher bandgap nanocrystals, and thus the benefits of the PEDOT:PSS/TFB/PFI structure faded as the emission peak redshifted and other structures provided an equally favorable environment. The full set of device parameters are shown in Table 1.

Table 1. Device parameters of blue-green light-emitting devices

Peak Emission Wavelength (nm)	Maximum EQE (%)	Maximum Brightness (cd/m^2)

469	0.50%	111
481	0.44%	212
488	1.41%	830
511	2.37%	3423

As another comparison test, LEDs using different materials as the HTL were excited in a standard setup by sourcing 1 mA to a given device and measuring the spectrum with a spectrometer. Competing HTLs either had significantly reduced luminescence or impure spectra relative to the PEDOT:PSS/TFB/PFI device.

This example demonstrated high efficiency blue perovskite LEDs. In this example, one of the efficiency barriers in blue perovskite nanocrystal LEDs, the architecture itself, was both demonstrated and overcome. The HTL comprising NiO_x was shown to induce non-radiative recombination of the emissive state, fundamentally limiting device performance. A new HTL, PEDOT:PSS/TFB/PFI, that did not significantly influence the nanocrystals, was introduced and provided a strong overall boost in efficiency, with values reaching as high as 0.50% EQE for 469 nm emitting devices. It was further demonstrated that this structure provided strong benefits across the blue-green portion of the spectrum.

EXAMPLE 2

This example demonstrates the synthesis of perovskite nanocrystals used in Example 1.

For synthesis of the perovskite nanocrystals, all synthetic materials were purchased from Sigma Aldrich and used as received unless otherwise noted. 0.814 g of Cs_2CO_3 (purity 99.9%), 40 mL of octadecene (purity 90%) and 2.5 mL of oleic acid (purity 90%) were loaded into 100 mL flask, dried under vacuum at 120 degrees Celsius for 1 h, and then heated to 150 degrees Celsius under N_2 protection, yielding a clear solution. The solution was cooled to room temperature for storage, and re-heated up to 100 degrees Celsius under vacuum before use.

179 mg $PbBr_2$ (0.488 mmol, purity 98%), 73.2 mg $PbCl_2$ (0.2632 mmol, purity 98%), 20 mL of octadecene, 2 mL of oleylamine (purity 98%), 2 mL of oleic acid, and 2 mL of trioctylphosphine (purity 97%) were loaded into a 100 mL three-neck flask, dried under vacuum at 130 degrees Celsius for 45 min., and then heated to 150 degrees Celsius. A resulting clear solution was heated to 165 degrees Celsius under N_2 protection. 1.75 mL of pre-heated Cs-oleate precursors was swiftly injected into the aforementioned solution, and the solution turned to a yellow color immediately. After having reacted for 10 s, a crude product was cooled to room

temperature in an ice/water bath. For the 511 nm emission device, only $PbBr_2$ precursors were used to synthesize $CsPbBr_3$. To tune emission wavelength of the perovskite nanocrystals, a Br^- post-exchanging method was used.

To purify the nanocrystals, an equal volume of anhydrous ethyl acetate (purity 99.8%) was added to the aforementioned crude product to precipitate the nanocrystals. After centrifuging at 4000 rpm) for 5 min., the pellet was dissolved in 10 mL of anhydrous hexane (purity 95%). The nanocrystals were washed again by anhydrous ethyl acetate (volume ratio of ethyl acetate:hexane 3:1), centrifuged at 7000 rpm for 5 min., and re-dispersed in 8 mL of octane or hexane. The solution was filtered by a polytetrafluoroethylene (PTFE) filter (0.2 um) before use.

For light-emitting device fabrication, $Ni(NO_3)_2*6H_2O$, Nafion® perfluorinated resin solution 5 wt. % in lower aliphatic alcohols and water, PFI, LiF (evaporation grade), and Aluminum were purchased from Sigma-Aldrich and used as received. Indium tin oxide (ITO) substrates, TPBi and TFB were purchased from Luminescence Technology, Inc. and used as received. PEDOT:PSS was purchased from Heraeus (Clevios P VP AI 4083) and used as received.

To make the NiO_x precursor, 1.5 M of each $Ni(NO_3)_2*6H_2O$ and ethylene diamine were dissolved in ethylene glycol to obtain a blue colored complex. After stirring for 10 min, the solution was filtered by a 0.4 micrometer PVDF filter.

15 Ohm ITO patterned glass was cleaned by sequential sonicating once in Micron-90 detergent, 2 times in water, 2 times in acetone, and then soaking in boiling isopropanol, for 10 min. each. The films were dried under blowing air and treated with O_2 plasma at 200 W using 0.5 Torr O_2 gas for 5 min. On these clean ITO substrates, a thin layer of PEDOT:PSS (Clevios PVP AI 4083, filtered using 0.4 micrometer PVDF filter) was spun at 4000 rpm for 45 s (ramp = 2500 rpm/s), and annealed at 140 degrees Celsius for 30 min in a nitrogen glovebox. After cooling, a TFB (4 mg/mL in chlorobenzene) layer was spin coated at 3000 rpm for 45 s (2000 rpm/s ramp), and annealed at 125 degrees Celsius for 15 min. A thin layer of PFI (0.05 wt% in isopropanol) was then coated at 3000 rpm for 45 s and dried at 145 degrees Celsius for 10 min.

For NiO_x thin films, the precursor solution was spun on plasma cleaned ITO at 2000 rpm for 90 s (2000 rpm/s), and annealed at 300 degrees Celsius for 1 h in air.

On top of these layers of either PEDOT:PSS/TFB/PFI or NiO_x, $CsPbX_3$ perovskite quantum dots in octane were coated using different spin conditions to achieve a uniform layer.

These films were then taken in the evaporation chamber, where 40 nm TPBi, 1.1 nm LiF, and 60 nm Al were deposited at 6×10^{-6} mbar at 2 Angstroms/s, 0.2 Angstroms/s, and 3 Angstroms/s respectively. Devices were unpackaged and measured in air.

In use of the streak camera, samples were excited by a 379 nm laser from Hamamatsu (C10196) with an 81 ps pulse width. Optical density (OD) filters were used to reduce the excitation intensity. The excitation was incident at a 45 degree angle to the glass face. The photoluminescence (PL) was collected with a 25.4 mm focal length lens normal to the glass face. The PL was focused through a 400 nm longpass filter into an SP2150i spectrograph coupled to a Hamamatsu C10627 streak unit and C9300 digital camera. Data was integrated across the nanocrystal emission wavelength to.

For device characterization, electroluminescence (EL) spectra were taken with an Ocean Optics QE Pro with 100 ms integration time with 1 mA sourced to the device from a Keithley 2400. Current density-voltage and EQE characteristics were measured with an HP 4145A with a calibrated half inch ThorLabs photodetector physically pressed to the face of the device, removing the need for a geometric correction. The device (2 mm radius) was much smaller than the photodetector (PD) (9.7 mm). The PD was smaller than the glass slide (12.2 mm), which, combined with the black material construction of the EQE holder, blocked the collection of wave-guided light, which prevented overestimation of the EQE. Luminance was calculated from the J-V-L curves and the spectra of the device. Pictures were taken with 1 mA sourced to the device from a Keithley 2400.

EXAMPLE 3

In this example, manganese doping of perovskite nanocrystals was shown to increase a photoluminescence quantum yield of excitons while introducing a decay pathway to a long-lived emissive state on the manganese ion. The extent of manganese doping of perovskite nanocrystals was controlled, which resulted in an unexpectedly large increase in blue photoluminescence while preventing significant manganese emission, allowing for NTSC blue perovskite LEDs with efficiencies over 2%. It was demonstrated in this example that the manganese doping increased the photoluminescence quantum yield and lifetime, reduced trap states, and made the perovskite nanocrystals more monodisperse, reducing the emission bandwidth (e.g., full width half maximum (FWHM)). Finally, perovskite nanocrystal downconverters were utilized at the front (e.g., emission side, display side) of the LEDs to build all-perovskite white LEDs.

In some cases, manganese (Mn) doping sites in perovskite nanocrystals are high efficiency emitters in their own right. Without wishing to be bound by theory, excitons generated in the nanocrystal quickly energy transfer to the Mn ions, where they efficiently emit with orange-red color and high yield, with an extremely long emissive lifetime. Doping perovskite nanocrystals with manganese results in a significant increase in the excitonic PLQY, even with the addition of the energy transfer decay pathway, a surprising effect indicating the benefits of Mn doping.

It was discovered that by adding only a small amount of Mn dopant to the perovskite nanocrystal, the PLQY of the material was unexpectedly increased by over three times while maintaining robust and pure blue emission. The Mn doping increased the photoluminescence lifetime and reduced the Urbach energy relative to those of an undoped perovskite nanocrystal, indicating a reduction in trap states. LEDs were then constructed with these materials and EQE was increased from 0.50% to 2.12%, consistent with the PLQY gains. The devices demonstrated higher brightness and narrower emission bandwidth than the undoped control devices, each with a pure blue spectrum which met the NTSC requirement. Finally, perovskite nanocrystals were used as optical downconverters at the front (e.g., the display side) of an LED to build all-perovskite white LEDs.

Manganese-doped perovskite nanocrystals were synthesized as described in detail in Example 4, which method included an addition of a manganese precursor, manganese (II) chloride (see Example 4 for details).

The benefits of Mn doping can be seen in FIG. 2A – FIG. 2D. The photoluminescence of the nanocrystals in solution was measured, FIG. 2A, normalized to the exciton peak around 470 nm. An increase in Mn precursor resulted in an increase in Mn emission at approximately 600 nm, reaching a maximum of approximately 25% of the excitonic peak for one of the perovskite materials doped to an Mn:Pb precursor mole ratio of 1.250 in the perovskite materials. This Mn peak decreased in thin films such that it was only apparent in the most heavily doped sample (Mn:Pb precursor mole ratio of 1.250). The brightness of spuncast films of these materials varied significantly with Mn doping. In FIG. 2B, the PLQY of the exciton peak of thin films of nanocrystals was measured. The undoped films gave a PLQY of only 9%, but the lightly doped films increased as high as 28% PLQY for the sample doped to an Mn:Pb precursor mole ratio of 0.972. Without wishing to be bound by theory, it was hypothesized that the roll-off for higher doping levels was due to energy transfer to the Mn ions. Significant Mn

luminescence was observed for the most heavily doped thin film sample (Mn:Pb precursor mole ratio of 1.250). Without wishing to be bound by theory, a trade-off in Mn doping level emerged from the results for these blue materials: if too little Mn, then the efficiency gains were limited; if too much Mn, then the Mn ions acted as a significant decay pathway.

FIG. 2A-FIG. 2D show some benefits of Mn doping. FIG. 2A is a plot of photoluminescence spectra of perovskite nanocrystals in solution with different amounts of Mn doping. FIG. 2B is a plot of PLQY and 1/e lifetime of thin films of perovskite nanocrystals with each thin film having nanocrystals with a respective amount of Mn doping. FIG. 2C is a plot of time-resolved photoluminescence of perovskite nanocrystal species with different amount of Mn doping. FIG. 2D is a plot of Urbach energy measurements on the absorption spectra, showing that Mn surprisingly slightly reduces the Urbach energy.

To understand the source of this luminescence gain relative to undoped nanocrystals, time-resolved photoluminescence decay was measured. Samples were excited by a 379 nm 81 ps laser and measured with a streak camera. Traces were integrated across the nanocrystal emission wavelength to give the curves in FIG. 2C. The traces agreed with the PLQY results e.g. in FIG. 2B. Without wishing to be bound by theory, light doping resulted in a significant increase in emissive state lifetime whereas additional Mn introduced a new decay pathway, thereby reducing the lifetime at higher doping. Without wishing to be bound by theory, at the light doping levels, the significant brightness increase combined with the longer lifetime demonstrate a reduction in trap state densities in Mn-doped nanocrystals relative to in undoped nanocrystals.

To investigate further, the Urbach energy of the absorption tail was measured (see, e.g., FIG. 2D) using absorption spectroscopy. Without wishing to be bound by theory, typically, one would expect a larger Urbach energy as dopants are added and contribute to the tail absorption. With these materials, however, surprisingly a constant or even slightly reduced Urbach energy was observed, with the undoped control giving 17.4 meV and the Mn doped samples reaching as low as 14.7 meV. Without wishing to be bound by theory, based on the reduced Urbach energy, higher lifetime, and greater PLQY in the presence of Mn, it was deduced that the addition of a small amount of Mn to these nanocrystals passivated a trap state, reducing the non-radiative decay.

Next, devices were fabricated and tested to identify the engineering benefits of this materials improvement. In Example 1 and Example 2, it was demonstrated that a

PEDOT:PSS/TFB/PFI hole transport layer (HTL) allowed for much higher quantum efficiencies at these blue wavelengths. Devices were fabricated in the same way in the current example, which can be briefly summarized as follows. PEDOT:PSS, TFB, and PFI were sequentially spun onto a cleaned ITO-on-glass slide, with an anneal between each spin step. The synthesized nanocrystals were then spuncast onto the HTL. The slides were transferred to a thermal evaporator where 40 nm of TPBi, 1.1 nm of LiF, and 100 nm of Aluminum were evaporated on top, defining a 2 mm diameter device. The device structure can be found in FIG. 3A; the details of device fabrication can be found in Example 2, with the exception that $CsPbX_3$ perovskite quantum dots (e.g., nanocrystals) in octane were replaced with the perovskite nanocrystals synthesized as in Example 4 for devices with Mn-doped nanocrystals.

FIG. 3A is a schematic diagram of a device structure of a light emitting diode (LED). PFI is represented as bandbending to a deeper work function. FIG. 3B is a plot of electroluminescence of fabricated LEDs with nanocrystals of varying Mn amount. FIG. 3C is a plot of current density-voltage-luminance (J-V-L) characteristics for LEDs containing nanocrystals, showing increased brightness across all Mn doping concentrations relative to devices containing the undoped nanocrystals. An image of a device, containing nanocrystals doped to an Mn:Pb precursor mole ratio of 0.972, is inset. FIG. 3D is a plot of external quantum efficiency (EQE) of fabricated light-emitting devices, showing up to a four-fold (4x) enhancement over control (undoped) nanocrystals.

Electroluminescence spectra of devices are presented in FIG. 3B. All samples showed pure blue emission from a perovskite emitter layer. Emission from the Mn peak was not observed from any samples. Without wishing to be bound by theory, it was hypothesized that the long emissive lifetime saturated the emission in such a thin emitter layer.

Increasing Mn content led to a sharp reduction in the full width half maximum (FWHM) of the emission peak (see, e.g., FIG. 3B). Without wishing to be bound by theory, this may have been due to increased monodispersity of the nanocrystals (see, e.g., FIG. 6). By monitoring the emission spectrum as a function of time with a streak camera, a red-shift in emission peak was observed in the first few nanoseconds in the undoped samples (see, e.g., FIG. 5A); that red-shift all but disappeared in the Mn doped nanocrystals (see, e.g., FIG. 5B – FIG. 5E), correlating with the reduced FWHM. This red-shift in undoped nanocrystals decreased significantly in solution; without wishing to be bound by theory, the red-shift may have been due to inter-nanocrystal energy transfer from polydispersity. See Table 2 for the electroluminescence (EL) FWHM of

synthesized samples, along with Mn content, lifetime, PLQY, maximum EQE (max. EQE), and brightness. The Mn-doping concentrations, as a % of Mn in the B site of ABX_3, quoted in Table 2, were determined by inductively coupled plasma emission spectroscopy analysis.

In FIG. 3C, J-V-L characteristics for light-emitting devices are presented. The Mn dopant provided a number of benefits, including a reduction in the turn-on voltage of almost 1 V and stronger brightness under all tested voltage conditions. The devices demonstrated a maximum brightness of 389 cd/m^2 for the device having perovskite nanocrystals doped to an Mn:Pb precursor mole ratio of 1.111, over three times brighter than the best undoped control. EQE was up to more than fourfold greater with devices containing perovskite nanocrystals doped to an Mn:Pb precursor mole ratio of 0.972 vs. devices containing undoped nanocrystals, with devices containing perovskite nanocrystals doped to an Mn:Pb precursor mole ratio of 0.972 reaching a maximum EQE of 2.12% (see, e.g., FIG. 3D). A device containing perovskite nanocrystals doped to an Mn:Pb precursor mole ratio of 1.111 showed EQE reaching as high as 1.46%. These high external quantum efficiency values agreed with improvements in PLQY and lifetime (see, e.g., Table 2) for these Mn-doped perovskite materials.

Table 2: Material and Device Parameters of Mn doped nanocrystals

Mn:Pb precursor mole ratio	% of Mn in B site (%)	Lifetime (ns)	PLQY* (%)	Max. EQE (%)	Brightness (cd/m^2)	EL FWHM (nm)
0	0	2.08	9	0.50	111	25.1
0.694	0.09	3.03	12	0.73	245	18.4
0.972	0.19	3.23	28	2.12	245	17.9
1.111	0.25	2.50	16	1.46	389	17.1
1.250	1.5	1.77	9	0.61	250	17.7

*of the excitonic peak only

These high performance devices allowed for previously inaccessible technologies such as white perovskite LEDs. White LEDs were constructed (see, e.g., FIG. 4A – FIG. 4E). On top (e.g., on the display side) of an efficient blue perovskite LED (Mn:Pb precursor mole ratio 1.111), red and green downconverters were placed. Without wishing to be bound by theory, these red and green downconverters absorbed a portion of the blue light and re-radiated it at a

longer wavelength, allowing for red, green, and the transmitted blue light to reach the eye. When these were properly calibrated, the eye and/or a camera sees white light.

To build downconverters, red and green cesium lead halide perovskite nanocrystals were synthesized (Example 4). The nanocrystals were then suspended in a 200 mg/mL rubber:toluene mixture and poured on a glass slide. The slide was allowed to dry, yielding a rubber film that downconverted to the appropriate colors (see, e.g., FIG. 4B).

FIG. 4A is a schematic diagram of a white LED design. FIG. 4B is a plot of photoluminescence from downconverter layers (dashed red and green) and electroluminescence from the blue and white LEDs (solid lines). Downconverters under room lights and UV illumination are inset in FIG. 4B. FIG. 4C delineates CIE color coordinates of light-emitting devices containing Mn-doped perovskite nanocrystals. In FIG. 4C, photoluminescence of the downconverters are represented by squares; blue and white electroluminescence are represented by circles. The triangle represents the color space that may be achieved with these three colors (red, green, blue) of nanocrystals. The white LED has a CIE coordinate of 0.311, 0.326. FIG. 4D-FIG. 4E are the J-V-L and EQE curves respectively of the white LED, peaking at a brightness of 102 cd/m^2 (see, e.g., FIG. 4D) and an external quantum efficiency of 0.25% (see. e.g., FIG. 4E).

Once appropriately tuned, the properties of the structure as a single LED were measured, yielding the spectrum shown in FIG. 4B. Transmitted blue electroluminescence was observed at emission peak wavelength 469 nm, consistent with the devices in FIG. 3A – FIG. 3D. In FIG. 4B, downconverted peaks were evident at 511 and 627 nm, corresponding to photoluminescence peaks measured on the downconverters individually (dashed lines). The device gave off white emission by eye and camera (see, e.g., FIG. 4C).

From the spectrum, a color coordinate of the device was calculated. The CIE spectrum represents the colors seen by the human eye, see FIG. 4C. White occupies the center of this plot, e.g., at a value of (0.33, 0.33). The white device was close to this true white value, with a CIE coordinate of (0.311, 0.326). The coordinates of the blue device and were found to be (0.127, 0.077). This exceeded the NTSC standard for blue due to its narrow linewidth (see, e.g., FWHM Table 2) and 469 nm emission. When an efficient blue LED is combined with the downconverters, a large percentage of the CIE plot can be covered, represented by the white triangle in FIG. 4C.

Finally, the efficiency of an overall white LED structure was determined. The J-V-L curves are presented in FIG. 4D, and the EQE curve in FIG. 4E. The device peaked at a luminance of 102 cd/m^2 and an efficiency of 0.25%. When compared with the base blue device, a reduction of approximately 10x in efficiency was observed. This value agreed with the measured PLQY of the downconverters (67% and 77% for green and red, respectively) and the waveguide losses in the rubber films.

In this example, manganese doped blue perovskite nanocrystals were synthesized (see also Example 4 for details). It was demonstrated that the Mn dopant provided strong benefits to the performance of the perovskite material as a light emitter, increasing the emissive lifetime and photoluminescence quantum yield while (without wishing to be bound by theory) reducing the trap states, as reflected in a reduction of Urbach energy. Finally, NTSC blue and white LEDs were fabricated, demonstrating the commercial value of these materials.

EXAMPLE 4

This example demonstrates the synthesis of perovskite nanocrystals used in Example 3. All chemicals were purchased from Sigma Aldrich unless specified.

To prepare cesium-oleate (Cs-oleate) precursors, 0.814 g of cesium carbonate (Cs_2CO_3, purity 99.9%), 40 mL of octadecene (purity 90%), and 2.5 mL of oleic acid (purity 90%) were loaded into a 100 mL flask, dried under vacuum at 120 degrees Celsius for 1 h, and then heated to 150 degrees Celsius under nitrogen (N_2) protection, yielding a clear solution. The solution was cooled to room temperature for storage, and re-heated up to 100 degrees Celsius under vacuum before use.

To synthesize undoped perovskite nanocrystals, 165 mg of $PbBr_2$ (0.450 mmol, purity 98%), 83.6 mg of $PbCl_2$ (0.301 mmol, purity 98%), 20 mL of octadecene, 2 mL of oleylamine (purity 98%), 2 mL of oleic acid, and 2 mL of trioctylphosphine (purity 97%) were loaded into a 100 mL three-neck flask, dried under vacuum at 130 degrees Celsius for 45 min., and then heated to 150 degrees Celsius under stirring. The yielded clear solution was heated to 165 degrees Celsius under N_2 protection. Then, 1.7 mL of pre-heated Cs-oleate precursors was swiftly injected into the above solution. After reacting for 10 s, the product was cooled to room temperature in an ice/water bath.

Synthesis of low Mn^{2+} doped perovskite nanocrystals (e.g., Mn:Pb precursor mole ratios 0 and 0.694) involved loading 210 mg (0.572 mmol) of lead (II) bromide ($PbBr_2$, purity 98%), 50 mg (0.397 mmol) of manganese (II) chloride ($MnCl_2$, purity 99.999%), 20 mL of octadecene,

2 mL of oleylamine (purity 98%), 2 mL of oleic acid, and 2 mL of trioctylphosphine (purity 97%) into a 100 mL three-neck flask. See Table 3 for illustrative values for each material for each doping series. This was dried at 130 degrees Celsius for 45 min., and then heated to 150 degrees Celsius under vacuum. The yielded solution was then heated to 165 degrees Celsius under N_2 protection. 1.7 mL of pre-heated Cs-oleate precursors was rapidly injected into the above solution. After having reacted for 10 s, a crude product was cooled to room temperature in an ice/water bath.

Synthesis of high Mn^{2+}doped perovskite nanocrystals (e.g., Mn:Pb precursor mole ratios 0.972, 1.111, and 1.250) involved loading 210 mg of $PbBr_2$ (0.572 mmol, purity 98%), 70 mg $MnCl_2$ (0.556 mmol, purity 99.999%), 20 mL of octadecene, 2 mL of oleylamine (purity 98%), 2 mL of oleic acid, and 2 mL of trioctylphosphine (purity 97%) into 100 mL three-neck flask. This was dried at 130 degrees Celsius for 45 min., and then heated to 150 degrees Celsius under vacuum. The yielded solution was then heated to 165 degrees Celsius under N_2 protection. 1.7 mL of pre-heated Cs-oleate precursors was rapidly injected into the above solution. After having reacted for 10 s, a crude product was cooled to room temperature in an ice/water bath. More examples of initial quantities in the synthesis are given in Table 3.

Table 3 Precursor amounts for five nanocrystal samples

$PbBr_2$ (mg)	$PbCl_2$ (mg)	$MnCl_2$ (mg)	$PbBr_2$ (mmol)	$PbCl_2$ (mmol)	$MnCl_2$ (mmol)	Molar ratio ($PbCl_2$: $PbBr_2$)	Mole ratio ($MnCl_2$: $PbBr_2$)	Mole ratio Cl/Br	Mole ratio Mn/Pb
165	83.6	0	0.450	0.301		0.669	0	0.669	0
210	0	50	0.572	0	0.397	0	0.694	0.694	0.694
210	0	70	0.572	0	0.556	0	0.972	0.972	0.972
210	0	80	0.572	0	0.636	0	1.111	1.111	1.111
210	0	90	0.572	0	0.715	0	1.250	1.250	1.250

To align emission wavelength for Mn^{2+} doped perovskite nanocrystals, an anion (e.g., bromide (Br^-)) exchanging method was used afterwards. Emission alignment by anion exchanging was carried out as follows. The blue emission shift of nanocrystals was aligned by exchanging the as-synthesized colloidal nanocrystal solution with $PbBr_2$ stock solution.

$PbBr_2$ stock solution was prepared by mixing 2.2 g of $PbBr_2$ (6 mmol), 50 mL of octadecene, 2 mL of oleylamine, and 2 mL of oleic acid in a 100 mL flask at 130 degrees Celsius under vacuum for 40 min, and then this was cooled down to room temperature. The amount of $PbBr_2$ stock solution was carefully adjusted by tracking the fluorescent emission peak with a spectrometer (Ocean Optics QEPro). As an example, 0.7 mL of $PbBr_2$ stock solution was used to align the emission of the nanocrystals prepared with 70 mg $MnCl_2$ at 468 nm.

To purify the perovskite nanocrystals, an equal volume of anhydrous ethyl acetate (purity 99.8%) was added to an above crude product to precipitate the nanocrystals. After centrifuging at 4 krpm (kilorevolutions per minute) for 5 min., the precipitate was dissolved in 10 mL of anhydrous hexane (purity 95%). The nanocrystals were washed again by anhydrous ethyl acetate (volume ratio of ethyl acetate:hexane 2.2:1), centrifuged at 7 krpm for 5 min., and re-dispersed in 8 mL of octane or hexane. The solution was filtered by polytetrafluoroethylene (PTFE) filter (0.2 microns) before use.

To synthesize down-conversion green perovskite nanocrystals, 276 mg $PbBr_2$ (0.752 mmol, purity 98%), 20 mL of octadecene, 2 mL of oleylamine (purity 98%), 2 mL of oleic acid were loaded into 100 mL three-neck flask, dried under vacuum at 130 degrees Celsius for 40 min., and then heated to 150 degrees Celsius under stirring. The yielded clear solution was heated to 184 degrees Celsius under N_2 protection. Then, 1.7 mL of pre-heated Cs-oleate precursors was swiftly injected into the above solution which turned to a yellow color immediately. After reacting for 5 s, the product was cooled to room temperature in an ice/water bath. Before preparing green down-conversion film, the crude nanocrystals products were purified by centrifuging at 7krpm (5752 RCF) for 10min, then dispersed the precipitate in 5 mL of hexane.

To synthesize down-conversion red perovskite nanocrystals, 108.8 mg $PbBr_2$ (0.296 mmol, purity 98%), 208.2 mg PbI_2 (0.452 mmol), 20 mL of octadecene, 2 mL of oleylamine (purity 98%), 2 mL of oleic acid were loaded into a 100 mL three-neck flask, dried under vacuum at 130 degrees Celsius for 40 min., and then heated to 150 degrees Celsius under stirring. The yielded clear solution was heated to 184.5 degrees Celsius under N_2 protection. Then, 1.7 mL of pre-heated Cs-oleate precursors was swiftly injected into the above solution which turned to a yellow color immediately. After reacting for 5 s, the product was cooled to room temperature in an ice/water bath. Before preparing a red and green down-conversion film,

the crude nanocrystal products were purified by centrifuging at 7krpm for 10 min, then the precipitate was dispersed in 5 mL of hexane.

To fabricate the downconverting layers, rubber was mixed at 200 mg/mL in toluene and heated at 90 degrees Celsius overnight until a viscous, uniform solution was obtained. 2 mL of this solution was added to a 7 mL glass vial, where 300 uL of the green nanocrystal solution or 100 uL of the red nanocrystal solution was added. The solution was stirred thoroughly with a spatula until uniformly mixed. The vial was left to sit for 2 hours until the bubbles disappeared and was then poured slowly onto a glass slide. This was then allowed to dry overnight in a nitrogen environment. The rubber films could then be cut and stacked to achieve a specific color goal. For the white LED, three red and seven green films were stacked to achieve the appropriate amount of downconversion.

To make the white LED, the previously mentioned downconverting layers were placed on a 0.7 mm glass slide. The edges were wrapped with black tape to prevent any waveguided light from being collected. The slide was then combined with the blue LED such that the glass slide was in contact with the green downconverters, with the red downconverter on top of the green. The red downconverters were placed directly against the glass face of the blue LED. Measurements of efficiency then proceeded as usual.

To fabricate the blue LEDs, a protocol was carried out as discussed in U.S. Provisional Application Ser. No. 62/586,837, filed November 15, 2017 and entitled "Light-Emitting Device Structures for Blue Light and Other Applications," incorporated herein by reference in its entirety, briefly repeated here. Nafion® perfluorinated resin solution 5 wt. % in lower aliphatic alcohols and water (PFI), LiF (evaporation grade), and Aluminum were purchased from Sigma-Aldrich and used as received. ITO substrates, TPBi and TFB were purchased from Luminescence Technology, Inc and used as received. PEDOT:PSS was purchased from Heraeus (Clevios P VP AI 4083) and used as received.

ITO patterned glass was solvent cleaned by sonication in Micron-90 detergent, 2x water, 2x acetone and soaking in boiling isopropanol for 10 minutes per step. The ITO patterned glass were then dried under blowing air and treated with O_2 plasma at 200 W using 0.5 Torr O_2 gas for 5 minutes. PEDOT:PSS was spuncast through a 0.4 μm PVDF filter at 4000 rpm for 45 s (ramp of 2500 rpm/s) in air, and annealed at 140 degrees Celsius for 30 minutes in a nitrogen environment. After cooling, a TFB (4 mg/mL in chlorobenzene) layer was spuncast at 3000 rpm for 45 s (ramp of 2000 rpm/s), and annealed at 125 degrees Celsius for 15 minutes. A thin layer

of PFI (0.05 wt% in isopropanol) was then spuncast at 3000 rpm for 45 s and dried at 145 degrees Celsius for 10 min. On top of these layers, perovskite nanocrystals in octane were spuncast. These films were then transferred to an evaporation chamber, where 40 nm TPBi, 1.1 nm LiF, and 60 nm Al were deposited at 6×10^{-6} mbar at 2 Angstroms/s, 0.2 Angstroms/s, 3 Angstroms/s respectively. Devices were unpackaged and measured in air.

To take the transient measurements, samples were excited by a 379 nm laser from Hamamatsu (C10196) with an 81 ps pulse width. Optical density (OD) filters were used to reduce the excitation intensity. The excitation was incident at a 45 degree angle to the glass face. The PL was collected with a 25.4 mm focal length lens normal to the glass face. The PL was focused through a 400 nm longpass filter into an SP2150i spectrograph coupled to a Hamamatsu C10627 streak unit and C9300 digital camera. Data was integrated across the nanocrystal emission wavelength from 440 nm to 500 nm.

EXAMPLE 5

This example demonstrates the synthesis and performance of perovskite crystals with a number of different dopants. All chemicals were purchased from Sigma Aldrich unless otherwise specified.

Undoped perovskite (methylammonium (MA) lead tribromide, $MAPbBr_3$) crystals were grown by using an anti-solvent vapor diffusion method. Briefly, 0.1 M precursor salts such as methylammonium bromide (MABr) and lead (II) bromide ($PbBr_2$) were dissolved in dimethylformamide (DMF). 3 mL of this precursor solution was placed in a 20 mL vial, then, the vial was placed in a 100 mL tight seal jar which was previously filled with 20 mL dichloromethane (DCM) (antisolvent); the apparatus is shown in Figure 12 (perovskite crystal growth apparatus). The vial was left uncapped for 3 days in the sealed jar to allow the DCM vapors to diffuse into perovskite solution. This slow diffusion of antisolvent vapor resulted in 100-micron sized perovskite crystallites.

A similar recipe was used to grow doped perovskite crystallites except that the concentration of $PbBr_2$ was varied depending on the dopant concentration. Various dopants M = Cu^{2+}, Mn^{2+}, Ni^{2+}, Yb^{3+}, Bi^{3+}, and Pd^{2+} were studied in this example. Bromide salts of these dopants were added to a respective precursor solution to grow doped perovskite crystallites. Typical concentrations were 0.1 M methylammonium bromide (MABr) and 0.1 M (60% $PbBr_2$ + 40% YBr_a, where Y is the dopant) were prepared in DMF. The remainder of the process was same as for undoped crystals.

Figure 13 shows microscopic images of perovskite crystals synthesized using these methods. Figure 13A is a bright field image of control crystals. Figures 13B-E are images under ultraviolet (UV)-illumination of control, Mn-doped, Ni-doped and Yb-doped perovskite crystals respectively. Scale bars are 100 microns.

Individual crystallites were imaged using a microscope under white light (e.g., Figure 13A) and UV-illumination (e.g., Figures 13B-E) to see the difference in emission. Figure 13A is the image of control crystals under bright field. Upon exciting them with UV light the control crystals emitted green color (e.g., Figure 13B). As shown in e.g., Figure 13B, the control crystals showed a poor emission. Upon doping crystallites, the emission intensity greatly increased, which can be seen from e.g., Figures 13C-13E. Mn, Yb, and Ni ions enhanced the photoluminescence (PL), whereas other dopants completely quenched the emission from perovskite.

EXAMPLE 6

This example demonstrates that doping perovskite structures with manganese results in bright, efficient, and stable light-emitting diodes (LEDs). Upon doping blue, green, and red perovskite films with Mn, a significant improvement in the morphology of the perovskite layers as well as the optical properties of the films resulted. The doped films formed highly crystalline layers that demonstrated a strong brightness and lifetime increase relative to undoped samples. Devices showed significant improvements in efficiency, brightness, and stability as compared to those without Mn. In particular, mixed halide red and blue devices both demonstrated excellent spectral stability on top of their high operational stability.

Perovskite films were fabricated by mixing the precursors in dimethylformamide (DMF) or a DMF/(dimethyl sulfoxide (DMSO)) mixture. 20% of phenylethyl ammonium bromide (PEABr) with respect to the A cation was added in order to passivate grain boundaries. The films were fabricated with a standard anti-solvent dripping during the spinning process. Mn was introduced into bulk-like perovskite crystals by replacing a percentage of $PbBr_2$ with $MnBr_2$, facilitating fine control over the Mn doping percentage. Upon doping, an immediate increase in photoluminescence was observed for all three perovskite colors (e.g., Figure 7B). Further, a strong improvement in macro-scale film quality and brightness was observed as Mn was introduced into the films. For red and blue samples, $MnBr_2$ precursor was still used as the Mn source, and the color was adjusted by partially replacing the remaining $PbBr_2$ with PbI_2 or $PbCl_2$, respectively. This gave a mix of halide ions in the film, tuning the emission peak

wavelength. As with the green samples, Mn incorporation led to large film quality and photoluminescence improvements in red and blue materials.

To confirm that a sample maintained the perovskite crystal structure, X-ray diffraction was used (e.g., Figure 7C). All perovskite films adopted a cubic crystal phase. Samples became significantly more crystalline with the addition of Mn. At the high Mn doping level of 30%, intense peaks of only the (100) and (200) planes were evident, indicating the formation of highly crystalline cubic perovskite crystallites. In contrast, the undoped sample showed additional peaks corresponding to the (110) and (210) planes of the cubic phase, indicating the formation of polycrystalline phases. Similar results were observed for red and blue films.

Figure 7A is a schematic diagram of a Perovskite crystal structure.

Figure 7B shows photographic images of perovskite films ABX or $APb_{(1-y)}Mn_yX$ where A is phenylethyl ammonium (PEA) Cesium (Cs) methylammonium (MA) $PEA_{0.2}Cs_{0.4}MA_{0.6}$, y is 0 or 0.15 or 0.3 from left to right, and X is indicated in Figure 7B. These images in Figure 7B demonstrate improved film uniformity and brightness with increased Mn doping at the B-site.

Figure 7C is a series of x-ray diffraction (XRD) spectra of green films. The films showed vanishing peaks at high Mn content, indicating that the materials became very crystalline.

In addition to XRD, the Mn doping significantly influenced the morphology of the perovskite, which can be seen clearly in the scanning electron microscopy (SEM) images in Figure 8. From elemental mapping using energy dispersive X-ray spectrometer (EDS),the presence of Mn throughout the perovskite layer was confirmed. As shown in e.g., Figure 8, the perovskite transitioned from large grains without Mn (e.g., Figures 8A-C) to uniform thin films with small crystalline grains upon Mn incorporation (e.g., Figures 8D-F). Without doping, the crystallites were randomly distributed with large gaps between them, whereas after doping the layer was uniformly covered with a number of crystallites, an important development for efficient devices which require uniform, pinhole-free films. These trends in morphology after Mn doping were similar for all blue, green, and red perovskites. The bromide perovskite formed a combination of rod shaped and spherical crystallites, whereas the mixed halide red perovskites formed a uniform layer covered with nanosized particles on top. Of particular interest, the blue bromide-chloride perovskites formed an ultra-smooth uniform layer upon doping with Mn, whereas control films showed porous amorphous structure with a large number of mesoscopic pores. Similar morphology changes were observed on pure $MAPbBr_3$ perovskites upon the addition of Mn, indicating that the doping effect occurred for different A and X compositions.

Figure 8 shows SEM of perovskite thin films. The films are from small crystallites (e.g., Figures 8A-C, y = 0) to thin films (e.g., Figures 8D-F, y = 0.30) with nanocrystalline grains with increased Mn doping. Scale bars are 1 μm.

Typically, large crystallites are viewed as problematic for light emission, as the charge confinement is lost and the photoluminescence yield decreases. For these doped materials, quite bright luminescence resulted. Further, as shown in e.g. Figure 9, these lifetime increases strongly correlated with the increased photoluminescence quantum yield (PLQY). Thus, the addition of Mn to these bulk films promoted uniform and crystalline grains with improved photoluminescence lifetime and quantum yield performance.

Figure 9 shows optical properties of perovskite thin films. Figure 9 shows that this radiative lifetime increase was paired with a strong increase in PLQY, which, without wishing to be bound by theory, is indicative of a possible reduction in defect states.

LEDs were fabricated to see how these improvements translated to devices. A fabrication procedure was carried out, which is repeated briefly here. More details can be found in the Methods section of this example. First, ITO on glass was cleaned via solvent cleaning and oxygen plasma. PEDOT:PSS and perfluorinated ionomer (PFI, used for green only) were then spuncast. The perovskite layer was spun followed by transfer to a thermal evaporator, where 40 nm TPBi, 1 nm LiF, and 60 nm Aluminum were deposited. The devices were packaged with UV-cured epoxy and a glass cover slip.

Little change was observed in the electroluminescence spectrum for the green LEDs as Mn was introduced, e.g., Figure 10A. The mixed halide devices were more prone to wavelength shifts, as small differences in local halide content can lead to large changes in emissive wavelength. Indeed, the red devices displayed a significant shift in electroluminescence, which, without being bound by theory, can be attributed to different halide uptake during the *in-situ* formation. The blue devices demonstrated similar emission spectra with a significant reduction in electroluminescence FWHM.

Figure 10B illustrates the powerful effect Mn has on $X = Br_3$ green devices. A significant reduction in leakage current, tied to the uniform coverage observed in Figure 8, was observed. The turn on voltage was reduced, and the 30% Mn device reached a maximum luminance of 96,000 cd/m^2 at 8V, among the highest brightness reached for perovskite LEDs. Moreover, as illustrated in Figure 10C, the Mn addition drove a 3-fold increase in external quantum efficiency, reaching a maximum of 3.2% for the 30% Mn device. Importantly, the device

remained efficient at large current densities, maintaining an EQE over 1% even at current densities over 2000 mA/cm^2, allowing it to reach the high brightness observed in Figure 10B. Even more remarkable improvements were observed for the red (Figure 10D-E) and blue (Figure 10F-G) devices. All doped devices showed the same reduction in leakage currents, and the doped devices reached a maximum of 1,470 cd/m^2 for red devices and 11,800 cd/m^2 for blue devices, both among the highest values for their particular wavelengths in perovskite LEDs. The EQEs made the improvements even more striking. Red doped devices reached a maximum of 5.1%, 40 times higher than control. Further, blue bulk devices have traditionally been extremely difficult to fabricate. This was confirmed by the low EQE values of control films. When Mn doping is introduced, however, a 210x improvement was observed, reaching as high as 0.58%. Similar improvements resulted in $MAPbBr_3$ devices, demonstrating that the improvement from Mn doping occurred with different A or X compositions.

Figure 10 shows data for Mn-doped perovskite LEDs. Figure 10A shows electroluminescence spectra of devices in this example. Figure 10B, D, F show J-V-L curves of the green, red, and blue perovskites, respectively. All colors showed a reduction in leakage current and strong brightness increase with Mn addition. Figure 10C, E, G show EQE curves of the green, red, and blue perovskites, respectively. Mn addition increased the maximum efficiency by 3x, 40x, and 210x for green, red, and blue devices, respectively.

Finally, the operational stability of our materials was examined. Stability is an increasing point of concern in perovskite LEDs, as high efficiencies have not yet been paired with long operative lifetimes. In Figure 11, device luminance was measured in real time at a constant current density of 3 mA/cm^2 and the L_{50} is denoted, the time it takes for the luminance to degrade to half its initial value. All control devices reached this threshold in less than a minute. However, the green $y = 0.30$ device took 23 minutes to reach this threshold, demonstrating a significant stability enhancement over the undoped device. Very similar trends resulted when only using MA for the A cation.

The stability of mixed-halide devices have proven particularly challenging in the past due to field-induced ion segregation red-shifting the emission peak on short timescales. The stability of these devices was measured following the previously discussed procedure, e.g., Figure 11B-C. While the control device decayed in less than a minute, the 15% Mn red device, which showed the best stability, emitted at approximately half the initial luminance value for over five hours. During the five hour period, the device showed only a slight voltage increase,

from 3.1 V to 3.8 V. Importantly, a peak redshift of only 5 nm within this entire five hours occurred, e.g., Figure 11B, inset. The device was returned to the degradation setup after measuring the five hour spectrum and remained bright for an additional two hours.

Blue devices presented an even greater challenge, as they are historically unstable across numerous material systems, confirmed by control devices dying in seconds. Yet by adding 30% Mn, the L_{50} was extended to 24 minutes, e.g., Figure 11C. As shown in the inset, this was accompanied with only a small redshift in the emission. Thus, for both the red and blue mixed halide devices, without being bound by theory, Mn addition seemed to slow ion migration in these materials, an important result for their stability going forward.

Figure 11 illustrates the stability of perovskite LEDs. Figure 11A: For X = Br_3, the addition of Mn greatly increased the lifetime, from an L_{50} of <1 minute for the control to 23 minutes for y = 0.30. Samples were packaged and measured at 3 mA/cm^2. Figure 11B: The red y = 0.15 devices survived for over 5 hours. Of particular importance, the wavelength of emission was stable in time (inset). Figure 11C: Mn addition allowed blue devices to survive for 24 minutes with little spectral shift (inset). The blue control devices were too inefficient to measure a quantitative stability but were dead within seconds.

Without being bound by theory, evidence is mounting that defects play an important role in halide mobility, and thus, stability. A drop in optoelectronic defects as observed in Figure 9 correlated directly with an increase in stability. Therefore, the gain from Mn was two-fold: the defect reduction facilitated high performance devices while also driving stability enhancements.

In this example, a significant amount of Mn was doped into perovskite bulk thin films and effects of that doping were studied. Mn doping resulted in highly crystalline grains on the order of 100 nm. These grains showed an increase in photoluminescence yield and lifetime, translating directly to increased device brightness, efficiency, and both spectral and operational stability. The results demonstrated here indicate more efficient and stable LEDs.

EXAMPLE 7

This example provides various methods and materials used in the above examples.

Perovskite Precursors. 0.3M of each methylammonium bromide (MABr) (Sigma, >98%), lead (II) bromide ($PbBr_2$) (Sigma, >99.99%), manganese (II) bromide ($MnBr_2$) (Sigma, >98%), phenylethyl ammonium bromide (PEABr) (Dyesol >98%)), lead (II) iodide (PbI_2) (Sigma, >99.99%), methylammonium iodide (MAI) (Sigma, >98%) and cesium lead iodide ($CsPbI_3$) were dissolved in dimethylformamide (DMF). 0.3M cesium lead bromide ($CsPbBr_3$) was

dissolved in dimethyl sulfoxide (DMSO) by constantly stirring for 2 h. These were mixed in appropriate ratios to maintain the final composition of $PEA_{0.2}Cs_{0.4}MA_{0.6}Pb_{(1-y)}Mn_yBr_3$ and $PEA_{0.2}Cs_{0.4}MA_{0.6}Pb_{(1-y)}Mn_yBr_{0.9}I_{2.1}$ for green and red respectively, where y = 0, 0.15, or 0.3. The precursor solutions were filtered with 0.2 micrometer PTFE syringe filter before using. For the blue devices, 0.3M ($MACl_2$ + $PbCl_2$), 0.3M ($MACl_2$ + $PbBr_2$) and 0.3M ($MACl_2$ + $MnBr_2$) were dissolved in 1:1 DMF:DMSO and used as precursors. These were mixed in proper ratios to obtain final composition of $PEA_{0.2}Cs_{0.4}MA_{0.6}Pb_{(1-y)}Mn_y(BrCl)_3$, where y = 0, 0.15, or 0.3.

Device fabrication. All indium tin oxide (ITO) substrates were cleaned via sonication in detergent, water, and acetone, before submersion in boiling isopropyl alcohol (IPA). The glass was treated with O_2 plasma at 200 W using 0.5 Torr O_2 gas. On these cleaned substrates, a thin layer of poly(3,4-ethylenedioxythiophene) polystyrene sulfonate (PEDOT:PSS) (Clevios PVP AI 4083, filtered using 0.2 micrometer polyvinylidene fluoride (PVDF) filter) was spin coated at 4000 rotations per minute (rpm) with a ramp of 2000 rpm/sec for 45 sec. Then, the films were annealed at 145 degrees C for 30 mins in a nitrogen glovebox. On these PEDOT layers, a thin layer of PFI (Sigma, Nafion® perfluorinated resin solution in 5 wt. % in lower aliphatic alcohols and water) was coated using 15 microliter/mL PFI stock solution in isopropanol, for the green devices only. The films were annealed at 145 degrees C for 30 mins. After cooling, perovskite precursors were spun at 1000 rpm for 10 sec and ramped up to 2800 rpm for 45 sec. After ~ 20 sec, 90 microliters of chloroform was dripped on the spinning perovskite layer. For the iodide perovskites, no PFI layer was used, and the 30% Mn doping involved a mild heating at 40 degrees C for 5 mins to achieve complete formation of perovskite. All these thin films were taken into a deposition chamber to deposit 40 nm 2,2′,2"-(1,3,5-Benzinetriyl)-tris(1-phenyl-1-H-benzimidazole) (TpBi), 1 nm LiF and 60 nm Al layers respectively.

Device measurements. All devices were packaged before measurement. Electroluminescence spectra were taken with an Ocean Optics QE Pro and 500 microAmps sourced to the device from a Keithley 2400. J-V-L curves were taken using an HP4145A and a calibrated Thorlabs photodiode physically held just above the face of the device. The device (1 mm radius) was much smaller than the detector, which was smaller than the glass substrate. When combined with the black material construction of the holder, this prevented the collection of waveguided light and overestimation of the EQE. Stability curves were determined in the same setup by sourcing a constant current and measuring the electroluminescence over time.

Materials characterization. XRD measurements were performed on Bruker D2 Phase diffractometer using a Cu Kα X-ray source. SEM images were captures on Supra55VP Field Emission Scanning Electron Microscope (FESEM) at 5-10 KeV. This scope was equipped with Energy Dispersive X-ray Spectrometer (EDS), which was used to map the elemental composition.

Streak camera. Transient measurements were made on a Hamamatsu streak camera. Samples were excited by a 379 nm, 81 ps pulsed laser. The emission was collected and focused into an SP2150i spectrograph coupled to a C10627 streak unit and C9300 digital camera. The luminescence was integrated across the emission wavelength to generate the curves in Figure 9.

PLQY. Photoluminescence quantum yields were measured in an integrating sphere. Perovskite films were unpackaged and excited by a 445 nm laser at 260 mW/cm^2. All components were calibrated against a calibrated Newport photodetector.

While several embodiments of the present invention have been described and illustrated herein, those of ordinary skill in the art will readily envision a variety of other means and/or structures for performing the functions and/or obtaining the results and/or one or more of the advantages described herein, and each of such variations and/or modifications is deemed to be within the scope of the present invention. More generally, those skilled in the art will readily appreciate that all parameters, dimensions, materials, and configurations described herein are meant to be exemplary and that the actual parameters, dimensions, materials, and/or configurations will depend upon the specific application or applications for which the teachings of the present invention is/are used. Those skilled in the art will recognize, or be able to ascertain using no more than routine experimentation, many equivalents to the specific embodiments of the invention described herein. It is, therefore, to be understood that the foregoing embodiments are presented by way of example only and that, within the scope of the appended claims and equivalents thereto, the invention may be practiced otherwise than as specifically described and claimed. The present invention is directed to each individual feature, system, article, material, kit, and/or method described herein. In addition, any combination of two or more such features, systems, articles, materials, kits, and/or methods, if such features, systems, articles, materials, kits, and/or methods are not mutually inconsistent, is included within the scope of the present invention.

In cases where the present specification and a document incorporated by reference include conflicting and/or inconsistent disclosure, the present specification shall control. If two or more documents incorporated by reference include conflicting and/or inconsistent disclosure with respect to each other, then the document having the later effective date shall control.

All definitions, as defined and used herein, should be understood to control over dictionary definitions, definitions in documents incorporated by reference, and/or ordinary meanings of the defined terms.

The indefinite articles "a" and "an," as used herein in the specification and in the claims, unless clearly indicated to the contrary, should be understood to mean "at least one."

The phrase "and/or," as used herein in the specification and in the claims, should be understood to mean "either or both" of the elements so conjoined, i.e., elements that are conjunctively present in some cases and disjunctively present in other cases. Multiple elements listed with "and/or" should be construed in the same fashion, i.e., "one or more" of the elements so conjoined. Other elements may optionally be present other than the elements specifically identified by the "and/or" clause, whether related or unrelated to those elements specifically identified. Thus, as a non-limiting example, a reference to "A and/or B", when used in conjunction with open-ended language such as "comprising" can refer, in one embodiment, to A only (optionally including elements other than B); in another embodiment, to B only (optionally including elements other than A); in yet another embodiment, to both A and B (optionally including other elements); etc.

As used herein in the specification and in the claims, "or" should be understood to have the same meaning as "and/or" as defined above. For example, when separating items in a list, "or" or "and/or" shall be interpreted as being inclusive, i.e., the inclusion of at least one, but also including more than one, of a number or list of elements, and, optionally, additional unlisted items. Only terms clearly indicated to the contrary, such as "only one of" or "exactly one of," or, when used in the claims, "consisting of," will refer to the inclusion of exactly one element of a number or list of elements. In general, the term "or" as used herein shall only be interpreted as indicating exclusive alternatives (i.e. "one or the other but not both") when preceded by terms of exclusivity, such as "either," "one of," "only one of," or "exactly one of."

As used herein in the specification and in the claims, the phrase "at least one," in reference to a list of one or more elements, should be understood to mean at least one element selected from any one or more of the elements in the list of elements, but not necessarily

including at least one of each and every element specifically listed within the list of elements and not excluding any combinations of elements in the list of elements. This definition also allows that elements may optionally be present other than the elements specifically identified within the list of elements to which the phrase "at least one" refers, whether related or unrelated to those elements specifically identified. Thus, as a non-limiting example, "at least one of A and B" (or, equivalently, "at least one of A or B," or, equivalently "at least one of A and/or B") can refer, in one embodiment, to at least one, optionally including more than one, A, with no B present (and optionally including elements other than B); in another embodiment, to at least one, optionally including more than one, B, with no A present (and optionally including elements other than A); in yet another embodiment, to at least one, optionally including more than one, A, and at least one, optionally including more than one, B (and optionally including other elements); etc.

When the word "about" is used herein in reference to a number, it should be understood that still another embodiment of the invention includes that number not modified by the presence of the word "about."

It should also be understood that, unless clearly indicated to the contrary, in any methods claimed herein that include more than one step or act, the order of the steps or acts of the method is not necessarily limited to the order in which the steps or acts of the method are recited.

In the claims, as well as in the specification above, all transitional phrases such as "comprising," "including," "carrying," "having," "containing," "involving," "holding," "composed of," and the like are to be understood to be open-ended, i.e., to mean including but not limited to. Only the transitional phrases "consisting of" and "consisting essentially of" shall be closed or semi-closed transitional phrases, respectively, as set forth in the United States Patent Office Manual of Patent Examining Procedures, Section 2111.03.

CLAIMS

What is claimed is:

1. A composition, comprising:

a perovskite structure having a formula ABX_3;

wherein

A comprises methylammonium, formamidinium, and/or cesium;

wherein B comprises lead and a dopant, wherein B has a mole percentage of dopant of between 0.1% and 10%;

wherein X comprises one or more halides; and

wherein the dopant comprises manganese, ytterbium, and/or nickel.

2. The composition of claim 1, wherein B has a percentage of dopant of between 0.1% and 5%.

3. The composition of any one of claims 1 or 2, wherein B has a percentage of dopant of between 0.1% and 1.5%..

4. The composition of any one of claims 1-3, wherein A comprises Cs.

5. The composition of any one of claims 1-4, wherein A consists essentially of Cs.

6. The composition of any one of claims 1-5, wherein B consists essentially of lead and the dopant.

7. The composition of any one of claims 1-5, wherein B further comprises Bi.

8. The composition of any one of claims 1-7, wherein X comprises Cl.

9. The composition of any one of claims 1-8, wherein X comprises Br.

10. The composition of any one of claims 1-9, wherein X comprises I.

11. The composition of any one of claims 1-10, wherein X_3 is Br_xCl_{3-x}, x being between 0 and 3.

12. The composition of any one of claims 1-11, wherein the perovskite structure has an Uhrbach energy of at most 16.7 meV.

13. The composition of any one of claims 1-12 wherein the composition comprises a plurality of the perovskite structures.

14. The composition of claim 13, wherein the structures are nanocrystals.

15. The composition of claim 14, wherein the plurality of nanocrystals is monodisperse.

16. A film comprising the composition of any one of claims 1-15.

17. The film of claim 16, wherein the film has a photoluminescence quantum yield (PLQY) of at least 10%.

18. The film of any one of claims 16 or 17, wherein the film has a photoluminescence quantum yield (PLQY) of at least 15%.

19. The film of any one of claims 16-18, wherein the film has a 1/e photoluminescence lifetime of at least 2 ns.

20. The film of any one of claims 16-18, wherein the film has a 1/e photoluminescence lifetime of at least 3 ns.

21. The composition of any one of claims 1-20, wherein the perovskite structure is a nanocrystal.

22. The composition of any one of claims 1-20, wherein the perovskite structure is a film.

23. The composition of claim 22, wherein the film has a thickness of from 5 nm to 1microns.

24. The composition of claim 22, wherein the film comprises crystalline grains having a size of from 20 nm to 10 microns.

25. The composition of any one of claims 1-20, wherein the perovskite structure is a bulk structure.

26. The composition of claim 25, wherein the bulk structure has a minimum dimension of 50 nm.

27. The composition of any one of claims 1-26, wherein the dopant is manganese.

28. The composition of any one of claims 1-26, wherein the dopant is ytterbium.

29. The composition of any one of claims 1-26, wherein the dopant is nickel.

30. A light-emitting device, comprising:

an electron transport region;

a hole transport region; and

a light-emitting region in electrical contact with each of the electron transport region and the hole transport region,

wherein the light-emitting region comprises a perovskite structure having a formula ABX_3, wherein A comprises methylammonium, formamidinium, and/or cesium; B comprises lead and a dopant, B has a mole percentage of dopant of between 0.1% and 10%; and X comprises one or more halides; and

wherein the dopant comprises manganese, ytterbium, and/or nickel.

31. The light-emitting device of claim 30, wherein the hole transport region comprises poly((9,9-dioctylfluorenyl-2,7-diyl)-co-(4,4'-(N-(4-sec-butylphenyl)diphenylamine))) (TFB), and a perfluorinated ionomer (PFI).

32. The light-emitting device of any one of claims 30 or 31, wherein the hole transport region comprises PEDOT:PSS.

33. The light-emitting device of any one of claims 30-32, wherein the light-emitting device is a blue light-emitting device that has an emission peak wavelength of less than or equal to 470 nm.

34. The light-emitting device of any one of claims 30-33, wherein the light-emitting device has an emission peak having a full width half maximum (FWHM) of at most 20 nm.

35. The light-emitting device of any one of claims 30-34, wherein the external quantum efficiency (EQE) of the light-emitting device is greater than 0.2%.

36. The light-emitting device of any one of claims 30-35, wherein the EQE of the light-emitting device is greater than 2%.

37. The light-emitting device of any one of claims 30-36, wherein the EQE of the light-emitting device is greater than 2.1%.

38. The light-emitting device of any one of claims 30-37, wherein the light-emitting device has a turn-on voltage of at most 4 V.

39. The light-emitting device of any one of claims 30-38, wherein the light-emitting device has a maximum brightness of at least 100 cd/m^2.

40. The light-emitting device of any one of claims 30-39, wherein the light-emitting device has a maximum brightness of at least 200 cd/m^2.

41. The light-emitting device of any one of claims 30-40, further comprising at least one perovskite downconverter structure.

42. The light-emitting device of claim 41, wherein the at least one perovskite downconverter structure is on a display side of the light-emitting device.

43. The light-emitting device of any one of claims 41 or 42, wherein the at least one perovskite downconverter structure comprises a red downconverter.

44. The light-emitting device of claim 43, wherein the red downconverter has a PLQY of at least 70%.

45. The light-emitting device of any one of claims 43 or 44, wherein the red downconverter is a perovskite nanocrystal.

46. The light-emitting device of any one of claims 41-45, wherein the at least one perovskite downconverter structure comprises a green downconverter.

47. The light-emitting device of claim 46, wherein the green downconverter has a PLQY of at least 60%.

48. The light-emitting device of any one of claims 46 or 47, wherein the green downconverter is a perovskite nanocrystal.

49. The light-emitting device of any one of claims 41-48, wherein the at least one downconverter structure is suspended in a suspending medium.

50. The light-emitting device of claim 49, wherein the suspending medium comprises rubber.

51. The light-emitting device of any one of claims 30-50, wherein the perovskite downconverter structure is a perovskite nanocrystal downconverter.

52. The light-emitting device of any one of claims 30-51, wherein the light-emitting device has an International Commission on Illumination (CIE) 1931 color space coordinate

within the triangular area defined by vertices (0.661, 0.318), (0.071, 0.660), and (0.127, 0.077).

53. The light-emitting device of any one of claims 30-52, wherein B has a percentage of dopant of between 0.1% and 5%..

54. The light-emitting device of any one of claims 30-53, wherein B has a percentage of dopant of between 0.1% and 1.5%.

55. The light-emitting device of any one of claims 30-54, wherein A comprises Cs.

56. The light-emitting device of any one of claims 30-55, wherein A consists essentially of Cs.

57. The light-emitting device of any one of claims 30-56, wherein B consists essentially of lead and the dopant.

58. The light-emitting device of any one of claims 30-57, wherein B further comprises Bi.

59. The light-emitting device of any one of claims 30-58, wherein X comprises Cl.

60. The light-emitting device of any one of claims 30-59, wherein X comprises Br.

61. The light-emitting device of any one of claims 30-60, wherein X comprises I.

62. The light-emitting device of any one of claims 30-61, wherein X_3 is Br_xCl_{3-x}, x being between 0 and 3.

63. The light-emitting device of any one of claims 30-62, wherein the perovskite structure is a nanocrystal.

64. The light-emitting device of any one of claims 30-62, wherein the perovskite structure is a film.

65. The light-emitting device of any one of claims 30-62, wherein the perovskite structure is a bulk structure.

66. The light-emitting device of any one of claims 30-65, wherein the dopant is manganese.

67. The light-emitting device of any one of claims 30-65, wherein the dopant is ytterbium.

68. The light-emitting device of any one of claims 30-65, wherein the dopant is nickel.

69. A method of fabricating a light-emitting device, comprising:

depositing a first layer on a substrate;

depositing a second layer on the first layer, the second layer comprising a perovskite structure having a formula ABX_3, wherein A comprises methylammonium, formamidinium, and/or cesium; B comprises lead and a dopant, wherein B has a mole percentage of dopant of between 0.1% and 10%; and X comprises one or more halides; and

depositing a third layer on the second layer;

wherein the dopant comprises manganese, ytterbium, and/or nickel.

70. The method of claim 69, wherein the first layer comprises an electron transport region and the third layer comprises a hole transport region.

71. The method of claim 69, wherein the first layer comprises a hole transport region and the third layer comprises an electron transport region.

72. The method of any one of claims 69-71, wherein depositing comprises spin coating.

73. The method of any one of claims 69-72, wherein depositing comprises annealing.

74. The method of any one of claims 69-73, wherein depositing comprises thermal evaporation.

75. The method of any one of claims 69-74, wherein B has a percentage of dopant of between 0.1% and 5%.

76. The method of any one of claims 69-75, wherein B has a percentage of dopant of between 0.1% and 1.5%.

77. The method of any one of claims 69-76, wherein A comprises Cs.

78. The method of any one of claims 69-77, wherein B consists essentially of lead and the dopant.

79. The method of any one of claims 69-78, wherein X_3 is Br_xCl_{3-x}, x being between 0 and 3.

80. The method of any one of claims 69-79, wherein the perovskite structure is a nanocrystal.

81. The method of any one of claims 69-79, wherein the perovskite structure is a film.

82. The method of any one of claims 69-79, wherein the perovskite structure is a bulk structure.

83. The method of any one of claims 69-82, wherein the dopant is manganese.

84. The method of any one of claims 69-82, wherein the dopant is ytterbium.

85. The method of any one of claims 69-82, wherein the dopant is nickel.

86. A method of operating a light-emitting device, comprising:

applying a voltage between an electron transport region and a hole transport region of a light-emitting device, the light-emitting device further comprising a light-emitting region in electrical contact with each of the electron transport region and the hole transport region, the light-emitting region comprising a perovskite structure having a formula ABX_3, wherein A comprises methylammonium, formamidinium, and/or cesium; B comprises lead and a dopant, wherein B has a mole percentage of dopant of between 0.1% and 10%; and X comprises one or more halides;

wherein the dopant comprises manganese, ytterbium, and/or nickel.

87. The method of claim 86, wherein applying the voltage across the light-emitting device comprises applying the voltage to a first electrode and a second electrode, wherein the first electrode is electrically connected to the hole transport region and the second electrode is electrically connected to the electron transport region.

88. The method of any one of claims 86or 87, wherein the voltage applied across the light-emitting device is from 0.1 V to 20 V.

89. The method of any one of claims 86-88, wherein the voltage applied across the light-emitting device is from 0.1 V to 8 V.

90. The method of any one of claims 86-89, wherein the perovskite structure is a nanocrystal.

91. The method of any one of claims 86-89, wherein the perovskite structure is a film.

92. The method of any one of claims 86-89, wherein the perovskite structure is a bulk structure.

93. The method of any one of claims 86-92, wherein the dopant is manganese.

94. The method of any one of claims 86-92, wherein the dopant is ytterbium.

95. The method of any one of claims 86-92, wherein the dopant is nickel.

96. A composition, comprising:

a perovskite structure having a formula ABX_3, wherein

A comprises methylammonium, formamidinium, and/or cesium;

B comprises lead and a dopant; and

X comprises one or more halides, and

wherein the perovskite structure is formed from a source of A, a lead halide, and a halide of the dopant, wherein the dopant halide and the lead halide have a mole ratio of between 0.65 and 1.15;

wherein the dopant comprises manganese, ytterbium, and/or nickel.

97. The composition of claim 96, wherein B has a mole percentage of dopant of between 0.1% and 10%.

98. The composition of any one of claims 96 or 97, wherein B has a percentage of dopant of between 0.1% and 5%.

99. The composition of any one of claims 96-98, wherein A comprises Cs.

100. The composition of any one of claims 96-99, wherein A consists essentially of Cs.

101. The composition of any one of claims 96-100, wherein B consists essentially of lead and the dopant.

102. The composition of any one of claims 96-100, wherein B further comprises Bi.

103. The composition of any one of claims 96-102, wherein X comprises Cl.

104. The composition of any one of claims 96-103, wherein X comprises Br.

105. The composition of any one of claims 96-104, wherein X comprises I.

106. The composition of any one of claims 96-105, wherein X_3 is Br_xCl_{3-x}, x being between 0 and 3.

107. The composition of any one of claims 96-106, wherein the perovskite structure is a nanocrystal.

108. The composition of any one of claims 96-106, wherein the perovskite structure is a film.

109. The composition of any one of claims 96-106, wherein the perovskite structure is a bulk structure.

110. The composition of any one of claims 96-109, wherein the dopant is manganese.

111. The composition of any one of claims 96-109, wherein the dopant is ytterbium.

112. The composition of any one of claims 96-109, wherein the dopant is nickel.

113. A light-emitting device, comprising:

an electron transport region;

a hole transport region; and

a light-emitting region in electrical contact with each of the electron transport region and the hole transport region,

wherein the light-emitting region comprises a perovskite structure having a formula ABX_3, wherein A comprises methylammonium, formamidinium, and/or cesium; B comprises lead and a dopant; and X comprises one or more halides, and wherein the perovskite structure is formed from a source of A, a lead halide, and a halide of the dopant, wherein the dopant halide and the lead halide have a mole ratio of between 0.65 and 1.15;

wherein the dopant comprises manganese, ytterbium, and/or nickel.

114. The light-emitting device of claim 113, wherein B has a mole percentage of dopant of between 0.1% and 10%.

115. The light-emitting device of any one of claims 113 or 114, wherein B has a percentage of dopant of between 0.1% and 1.5%.

116. The light-emitting device of any one of claims 113-115, wherein A comprises Cs.

117. The light-emitting device of any one of claims 113-116, wherein A consists essentially of Cs.

118. The light-emitting device of any one of claims 113-117, wherein B consists essentially of lead and the dopant.

119. The light-emitting device of any one of claims 113-117, wherein B further comprises Bi.

120. The light-emitting device of any one of claims 113-119, wherein X comprises Cl.

121. The light-emitting device of any one of claims 113-120, wherein X comprises Br.

122. The light-emitting device of any one of claims 113-121, wherein X comprises I.

123. The light-emitting device of any one of claims 113-122, wherein X_3 is Br_xCl_{3-x}, x being between 0 and 3.

124. The light-emitting device of any one of claims 113-123, wherein the perovskite structure is a nanocrystal.

125. The light-emitting device of any one of claims 113-123, wherein the perovskite structure is a film.

126. The light-emitting device of any one of claims 113-123, wherein the perovskite structure is a bulk structure.

127. The light-emitting device of any one of claims 113-126, wherein the dopant is manganese.

128. The light-emitting device of any one of claims 113-126, wherein the dopant is ytterbium.

129. The light-emitting device of any one of claims 113-126, wherein the dopant is nickel.

130. A composition, comprising a perovskite structure having a formula $Cs(Pb_zY_{1-z})X_3$, wherein X comprises one or more halides, and z is at least 0.9;
wherein Y comprises manganese, ytterbium, and/or nickel.

131. The composition of claim 130, wherein z is at least 0.95.

132. The composition of any one of claims 130 or 131, wherein z is at least 0.985.

133. The composition of any one of claims 130-132, wherein z is at least 0.99.

134. The composition of any one of claims 130-133, wherein X comprises Cl.

135. The composition of any one of claims 130-134, wherein X comprises Br.

136. The composition of any one of claims 130-135, wherein X comprises I.

137. The composition of any one of claims 130-136, wherein X_3 is Br_xCl_{3-x}, x being between 0 and 3.

138. The composition of any one of claims 130-137, wherein the perovskite structure is a nanocrystal.

139. The composition of any one of claims 130-137, wherein the perovskite structure is a film.

140. The composition of any one of claims 130-137, wherein the perovskite structure is a bulk structure.

141. The composition of any one of claims 130-140, wherein Y is manganese.

142. The composition of any one of claims 130-140, wherein Y is ytterbium.

143. The composition of any one of claims 130-140, wherein Y is nickel.

144. A light-emitting device, comprising:

an electron transport region;

a hole transport region; and

a light-emitting region in electrical contact with each of the electron transport region and the hole transport region,

wherein the light-emitting region comprises a perovskite structure having a formula $Cs(Pb_zY_{1-z})X_3$, wherein X comprises one or more halides, and z is at least 0.9;

wherein Y comprises manganese, ytterbium, and/or nickel.

145. The light-emitting device of claim 144, wherein z is at least 0.95.

146. The light-emitting device of any one of claims 144 or 145, wherein z is at least 0.985.

147. The light-emitting device of any one of claims 144-146, wherein z is at least 0.99.

148. The light-emitting device of any one of claims 144-147, wherein X comprises Cl.

149. The light-emitting device of any one of claims 144-148, wherein X comprises Br.

150. The light-emitting device of any one of claims 144-149, wherein X comprises I.

151. The light-emitting device of any one of claims 144-150, wherein X_3 is Br_xCl_{3-x}, x being between 0 and 3.

152. The light-emitting device of any one of claims 144-151, wherein the perovskite structure is a nanocrystal.

153. The light-emitting device of any one of claims 144-151, wherein the perovskite structure is a film.

154. The light-emitting device of any one of claims 144-151, wherein the perovskite structure is a bulk structure.

155. The light-emitting device of any one of claims 144-154, wherein Y is manganese.

156. The light-emitting device of any one of claims 144-154, wherein Y is ytterbium.

157. The light-emitting device of any one of claims 144-154, wherein Y is nickel.

158. A light-emitting device, comprising:

a blue light-emitting region comprising a first perovskite having a formula ABX_3, wherein A comprises methylammonium, formamidinium, and/or cesium, B comprises lead and a dopant, and X comprises one or more halides;

a red light-emitting region positioned to downconvert blue light from the blue light-emitting region and emit red light, the red light-emitting region comprising a second perovskite; and

a green light-emitting region positioned to downconvert blue light from the blue light-emitting region and emit green light, the green light-emitting region comprising a third perovskite;

wherein the dopant comprises manganese, ytterbium, and/or nickel.

159. The light-emitting device of claim 158, wherein the dopant and lead have a mole ratio of between 0.65 and 1.15.

160. The light-emitting device of any one of claims 158 or 159, wherein B has a percentage of dopant of between 0.1% and 5%.

161. The light-emitting device of any one of claims 158-160, wherein B has a percentage of dopant of between 0.1% and 1.5%.

162. The light-emitting device of any one of claims 158-161, wherein the first perovskite is formed from a source of A, a lead halide, and a halide of the dopant, wherein the dopant halide and the lead halide have a mole ratio of between 0.65 and 1.15.

163. The light-emitting device of any one of claims 158-162, wherein A comprises Cs.

164. The light-emitting device of any one of claims 158-163, wherein A consists essentially of Cs.

165. The light-emitting device of any one of claims 158-164, wherein B consists essentially of lead and the dopant.

166. The light-emitting device of any one of claims 158-164, wherein B further comprises Bi.

167. The light-emitting device of any one of claims 158-166, wherein X comprises Cl.

168. The light-emitting device of any one of claims 158-167, wherein X comprises Br.

169. The light-emitting device of any one of claims 158-168, wherein X comprises I.

170. The light-emitting device of any one of claims 158-169, wherein X_3 is Br_xCl_{3-x}, x being between 0 and 3.

171. The light-emitting device of any one of claims 158-170, wherein the dopant is manganese.

172. The light-emitting device of any one of claims 158-170, wherein the dopant is ytterbium.

173. The light-emitting device of any one of claims 158-170, wherein the dopant is nickel.

174. A light-emitting device, comprising:

a blue light-emitting region comprising a first perovskite having a formula $Cs(Pb_zY_{1-z})X_3$, wherein X comprises one or more halides, z is at least 0.9, and Y comprises manganese, ytterbium, and/or nickel;

a red light-emitting region positioned to downconvert blue light from the blue light-emitting region and emit red light, the red light-emitting region comprising a second perovskite; and

a green light-emitting region positioned to downconvert blue light from the blue light-emitting region and emit green light, the green light-emitting region comprising a third perovskite.

175. The light-emitting device of claim 174, wherein z is at least 0.95.

176. The light-emitting device of any one of claims 174 or 175, wherein z is at least 0.985.

177. The light-emitting device of any one of claims 174-176, wherein z is at least 0.99.

178. The light-emitting device of any one of claims 174-177, wherein X comprises Cl.

179. The light-emitting device of any one of claims 174-178, wherein X comprises Br.

180. The light-emitting device of any one of claims 174-179, wherein X comprises I.

181. The light-emitting device of any one of claims 174-180, wherein X_3 is Br_xCl_{3-x}, x being between 0 and 3.

182. The light-emitting device of any one of claims 174-181, wherein Y is manganese.

183. The light-emitting device of any one of claims 174-181, wherein Y is ytterbium.

184. The light-emitting device of any one of claims 174-181, wherein Y is nickel.

185. A composition, comprising a perovskite structure having a formula $Cs(Pb_zY_{1-z})X_3$, wherein X comprises one or more halides, z is at least 0.9, and Y comprises manganese, ytterbium, and/or nickel.

186. The composition of claim 185, wherein z is at least 0.95.

187. The composition of any one of claims 185or 186, wherein z is at least 0.985.

188. The composition of any one of claims 185-187, wherein z is at least 0.99.

189. The composition of any one of claims 185-188, wherein X comprises Cl.

190. The composition of any one of claims 185-189, wherein X comprises Br.

191. The composition of any one of claims 185-190, wherein X comprises I.

192. The composition of any one of claims 185-191, wherein X_3 is Br_xCl_{3-x}, x being between 0 and 3.

193. The light-emitting device of any one of claims 185-192, wherein the perovskite structure is a nanocrystal.

194. The light-emitting device of any one of claims 185-192, wherein the perovskite structure is a film.

195. The light-emitting device of any one of claims 185-192, wherein the perovskite structure is a bulk structure.

196. The light-emitting device of any one of claims 185-195, wherein Y is manganese.

197. The light-emitting device of any one of claims 185-195, wherein Y is ytterbium.

198. The light-emitting device of any one of claims 185-195, wherein Y is nickel.

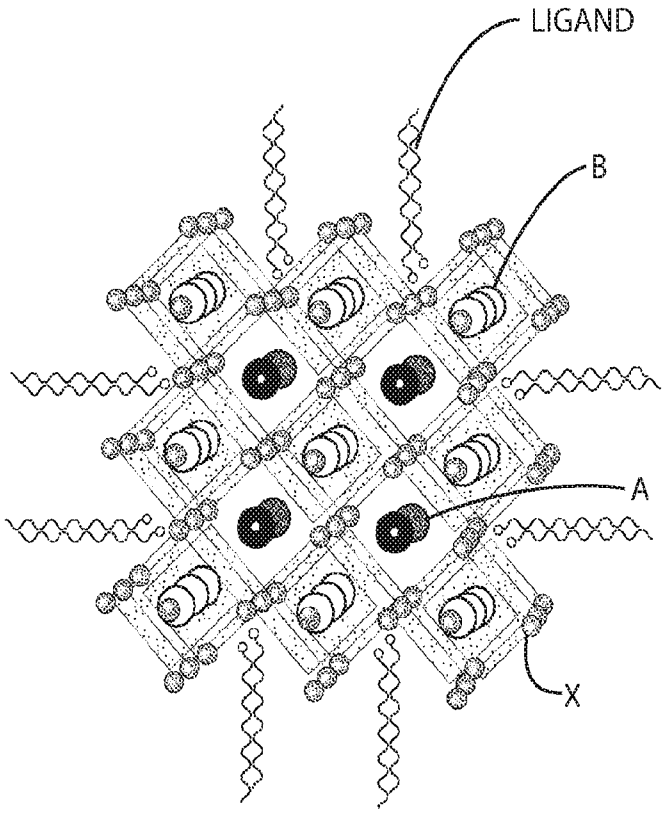

FIG. 1

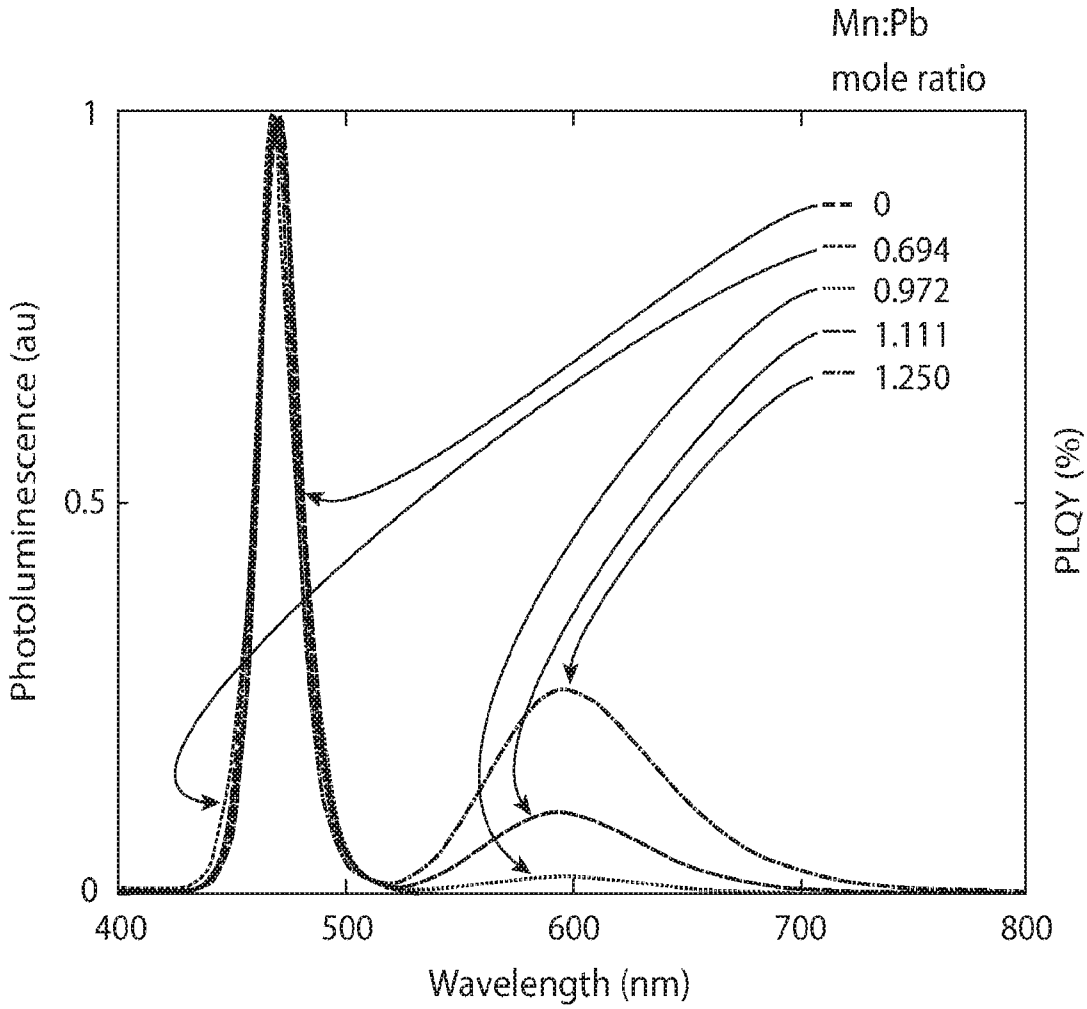
Mn:Pb
mole ratio
0
0.694
0.972
1.111
1.250
Photoluminescence (au)
PLQY (%)
Wavelength (nm)
1
0.5
0
400
500
600
700
800

FIG. 2A

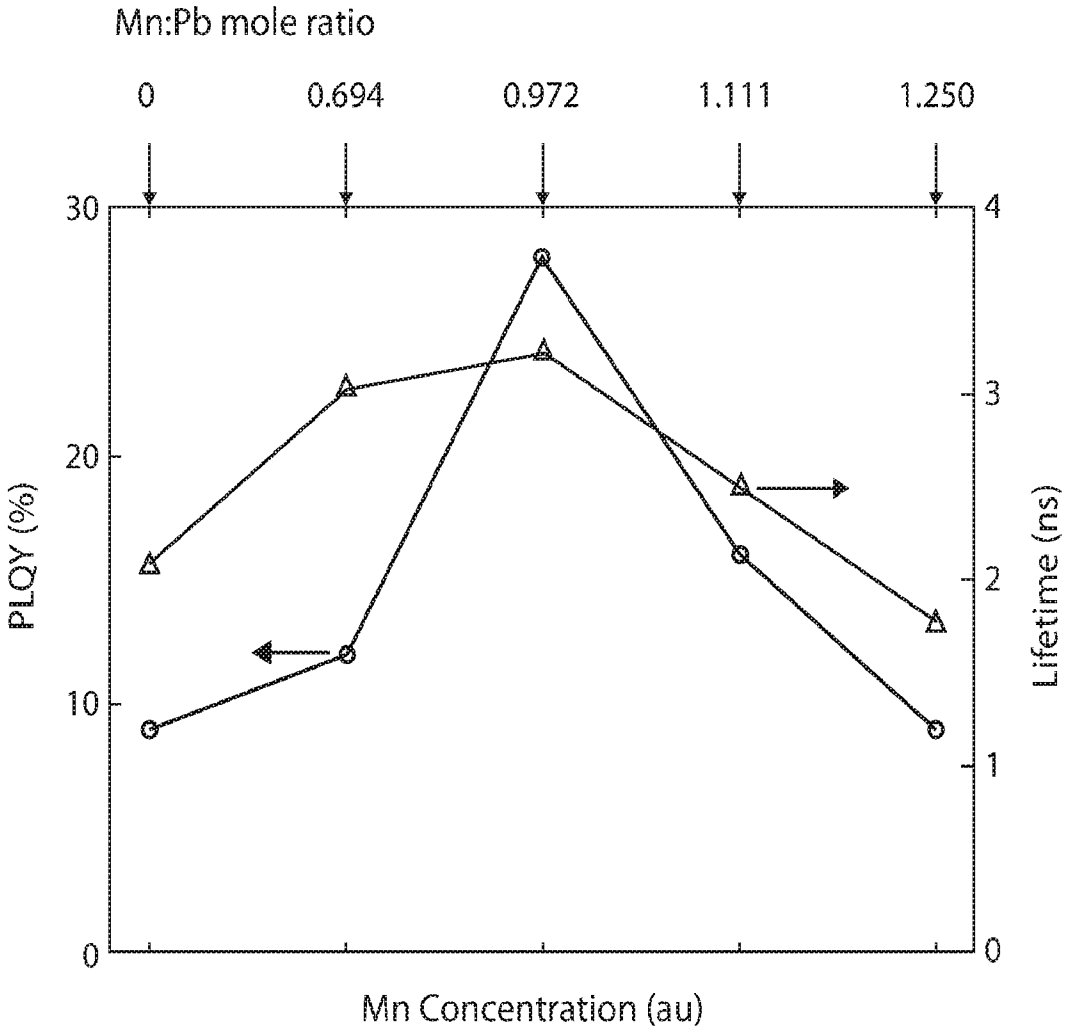
Mn:Pb mole ratio
0
0.694
0.972
1.111
1.250
30
20
10
0
PLQY (%)
4
3
2
1
0
Lifetime (ns)
Mn Concentration (au)

FIG. 2B

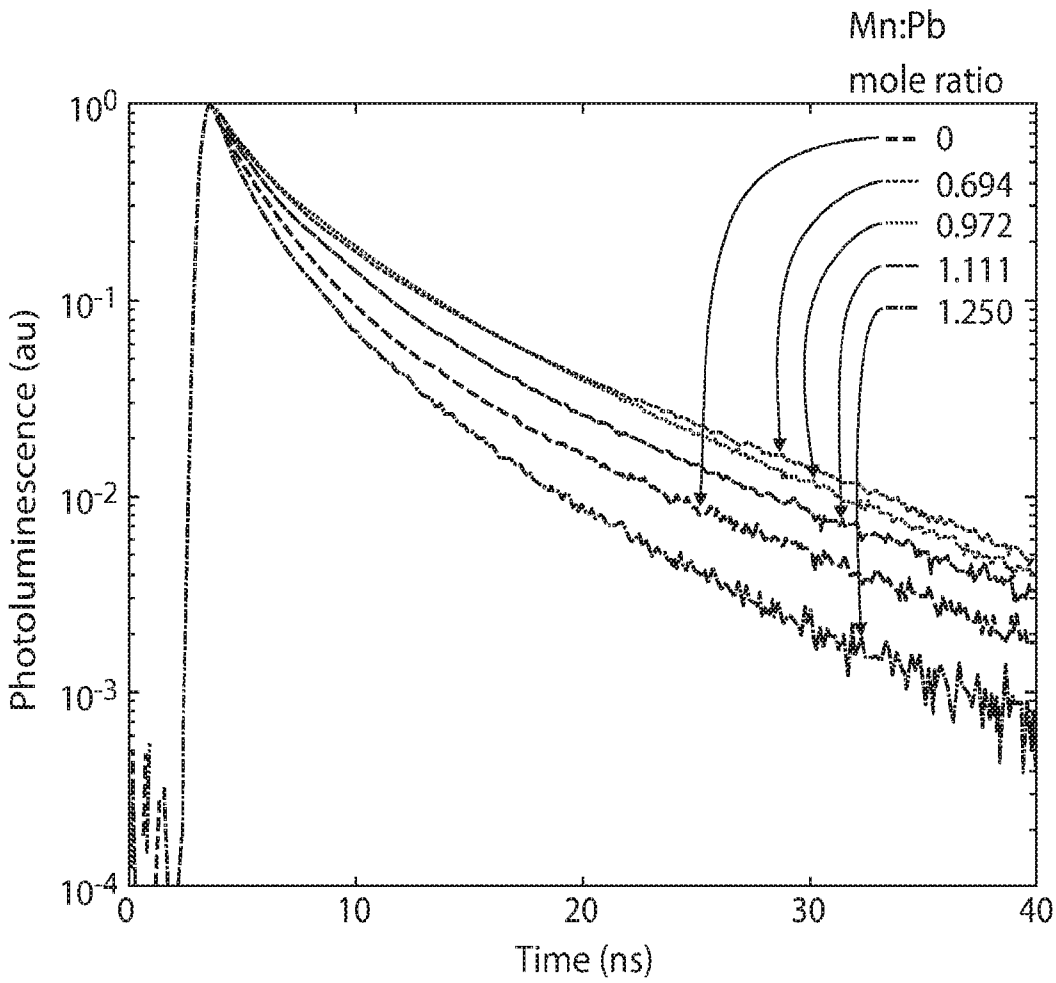
Mn:Pb
mole ratio
0
0.694
0.972
1.111
1.250
Photoluminescence (au)
10^{0}
10^{-1}
10^{-2}
10^{-3}
10^{-4}
0
10
20
30
40
Time (ns)

FIG. 2C

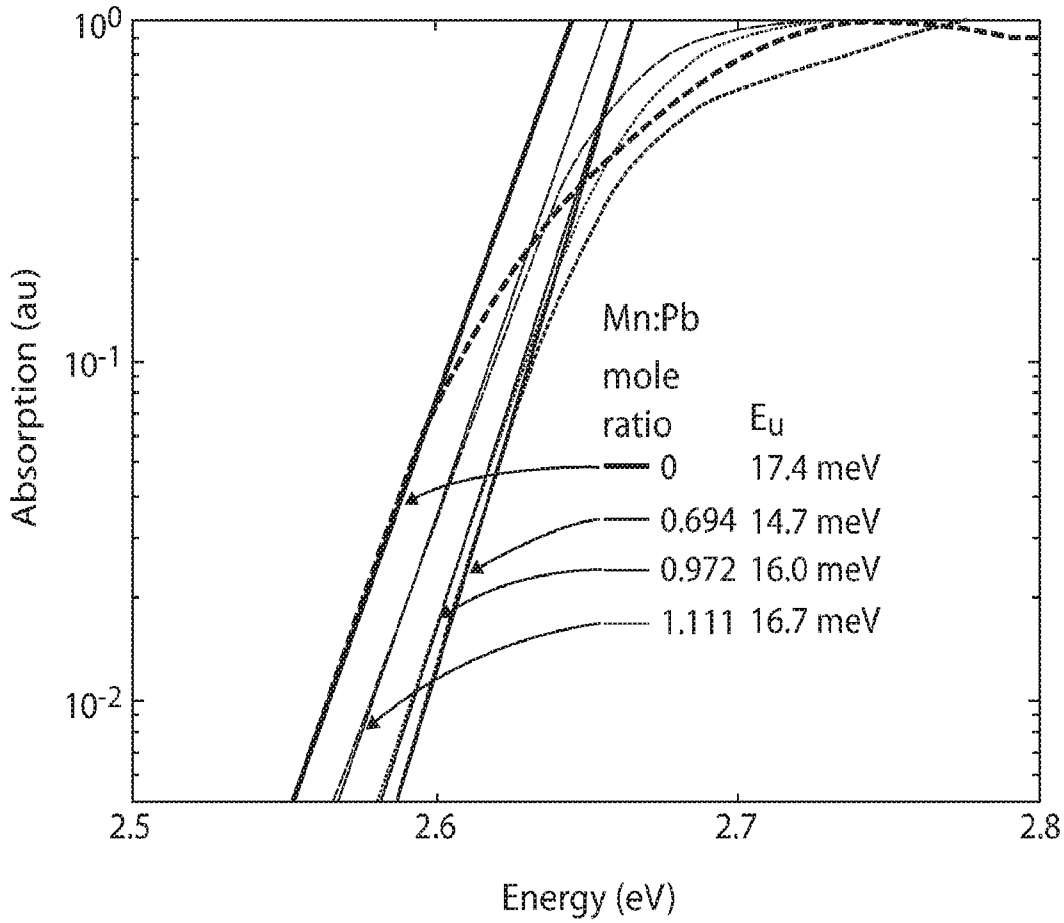
Absorption (au)
10^0
10^{-1}
10^{-2}
2.5
2.6
2.7
2.8
Energy (eV)
Mn:Pb
mole
ratio
Eu
0
17.4 meV
0.694
14.7 meV
0.972
16.0 meV
1.111
16.7 meV

FIG. 2D

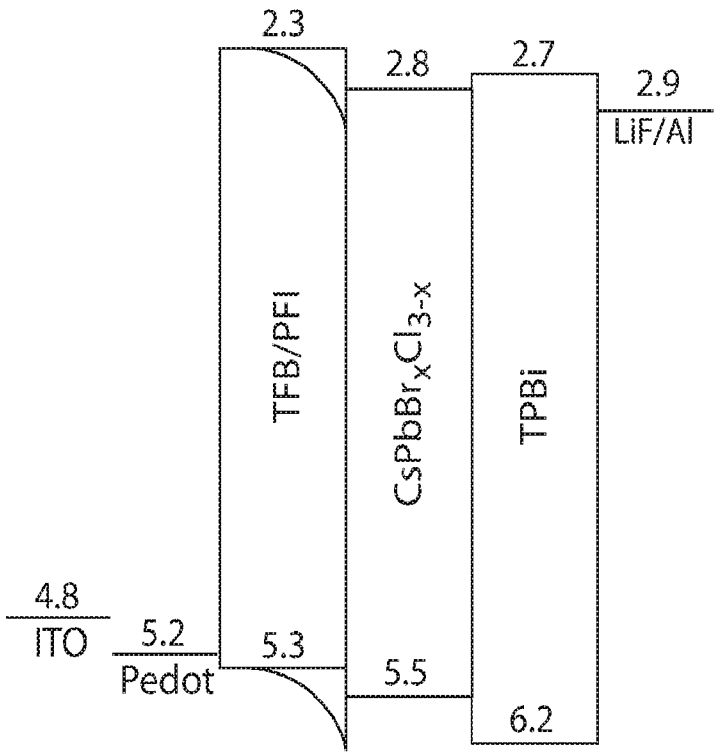
2.3
2.8
2.7
2.9
LiF/Al
TFB/PFI
$CsPbBr_xCl_{3-x}$
TPBi
4.8
ITO
5.2
Pedot
5.3
5.5
6.2

FIG. 3A

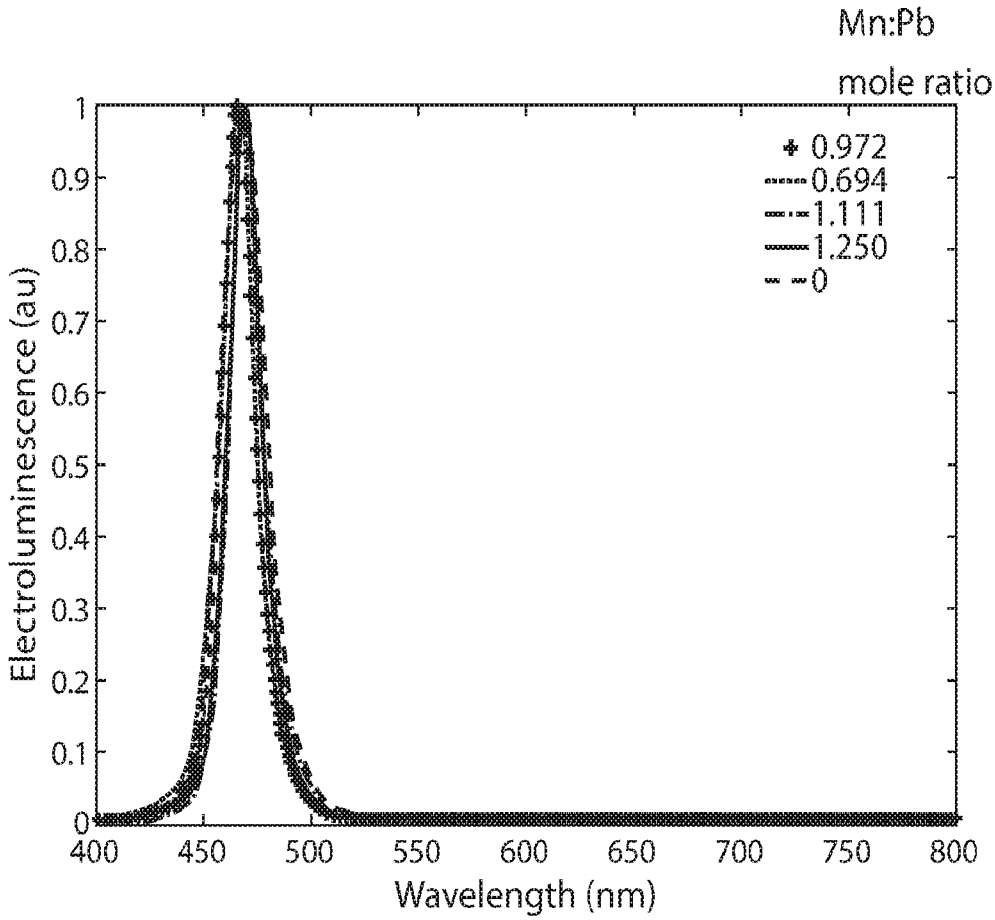
Mn:Pb
mole ratio
0.972
0.694
1.111
1.250
0
Electroluminescence (au)
Wavelength (nm)
0
0.1
0.2
0.3
0.4
0.5
0.6
0.7
0.8
0.9
1
400
450
500
550
600
650
700
750
800

FIG. 3B

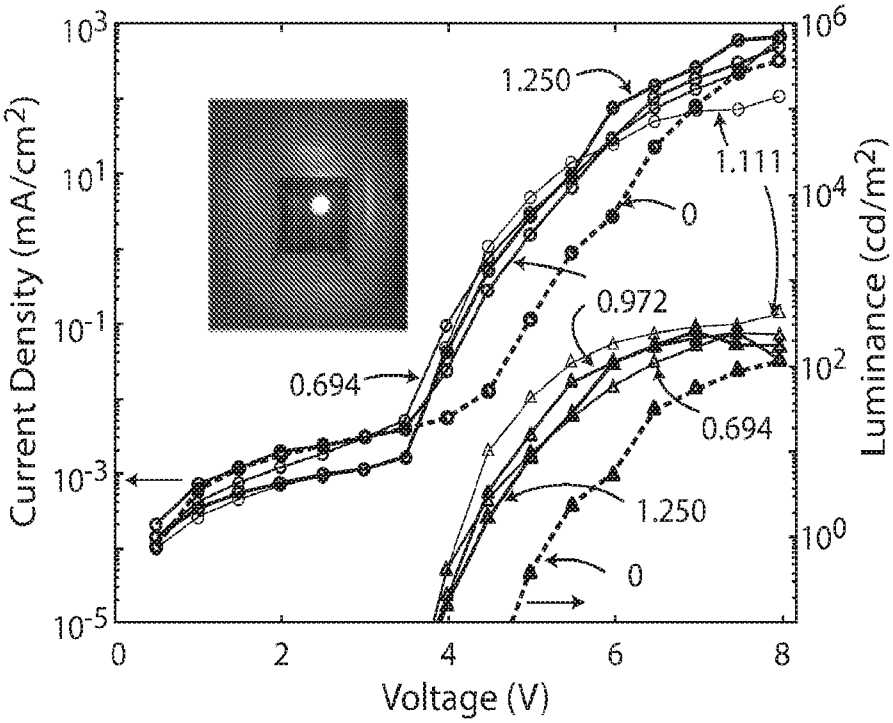
Current Density (mA/cm^2)
Luminance (cd/m^2)
Voltage (V)
1.250
1.111
0
0.972
0.694
0.694
1.250
0

FIG. 3C

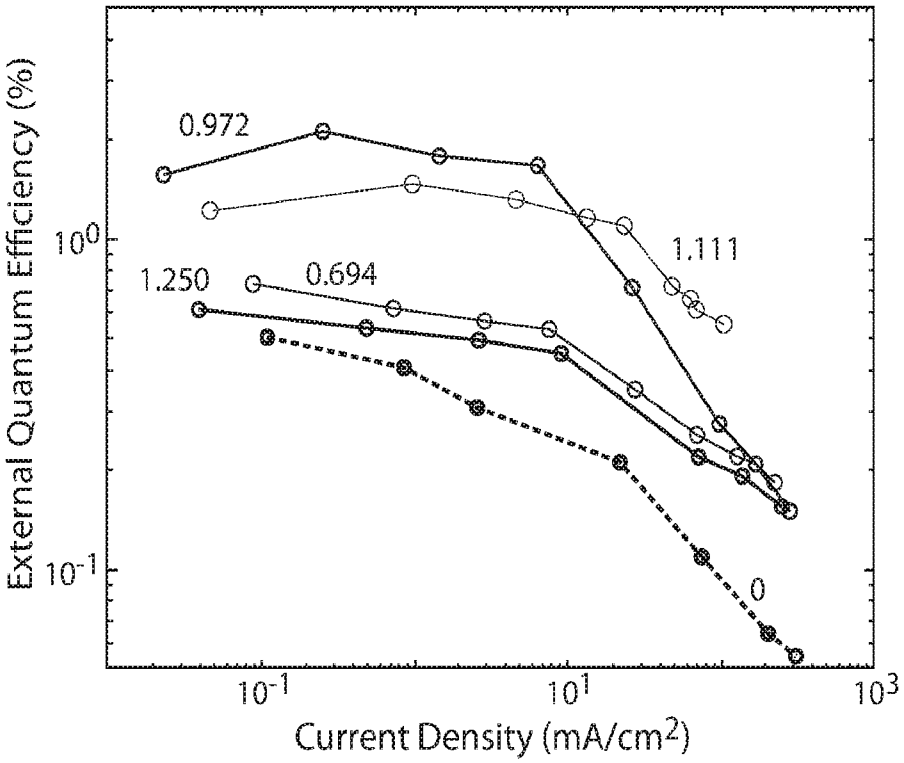
External Quantum Efficiency (%)
10^0
10^{-1}
0.972
1.111
1.250
0.694
0
10^{-1}
10^1
10^3
Current Density (mA/cm^2)

FIG. 3D

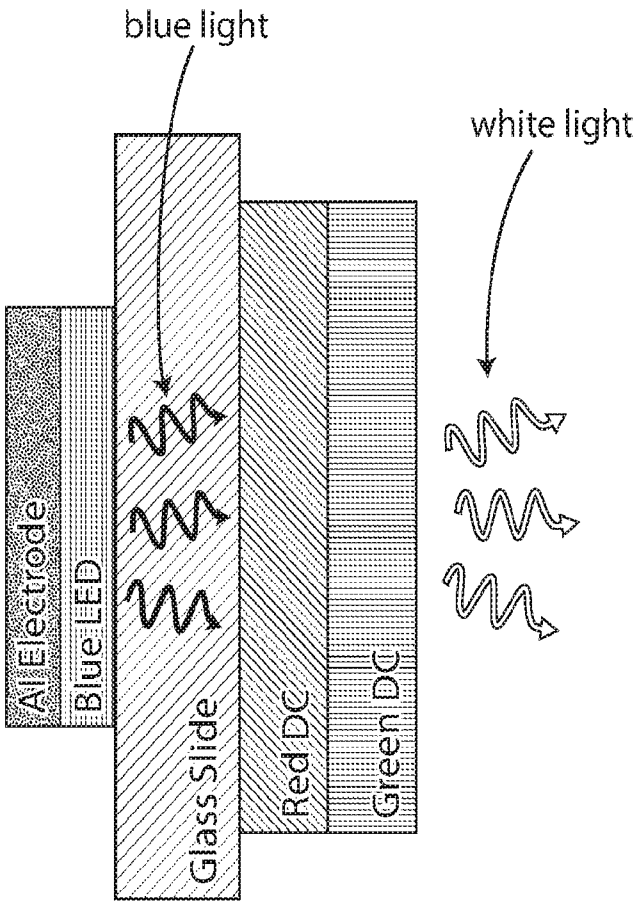
blue light
white light
Al Electrode
Blue LED
Glass Slide
Red DC
Green DC

FIG. 4A

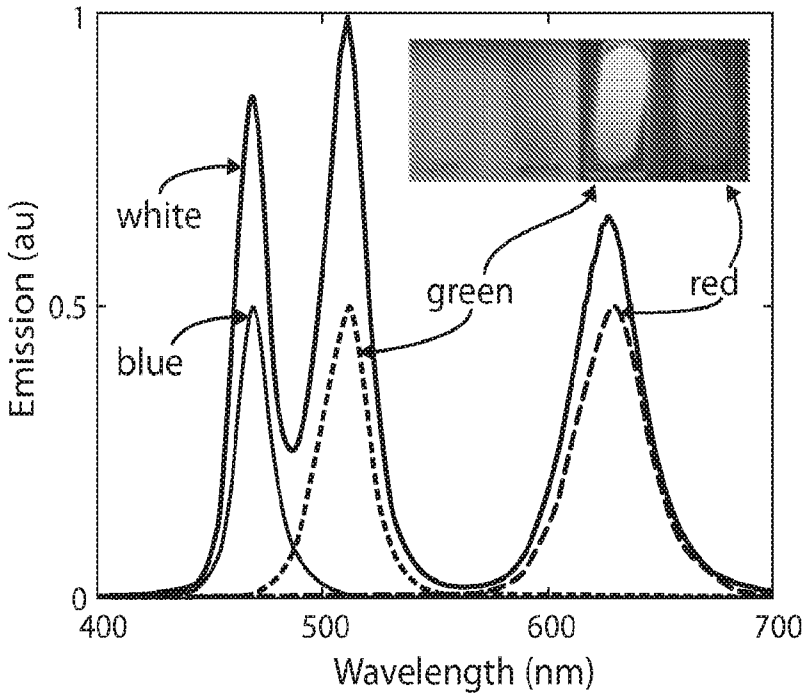
1
0.5
0
Emission (au)
white
blue
green
red
400
500
600
700
Wavelength (nm)

FIG. 4B

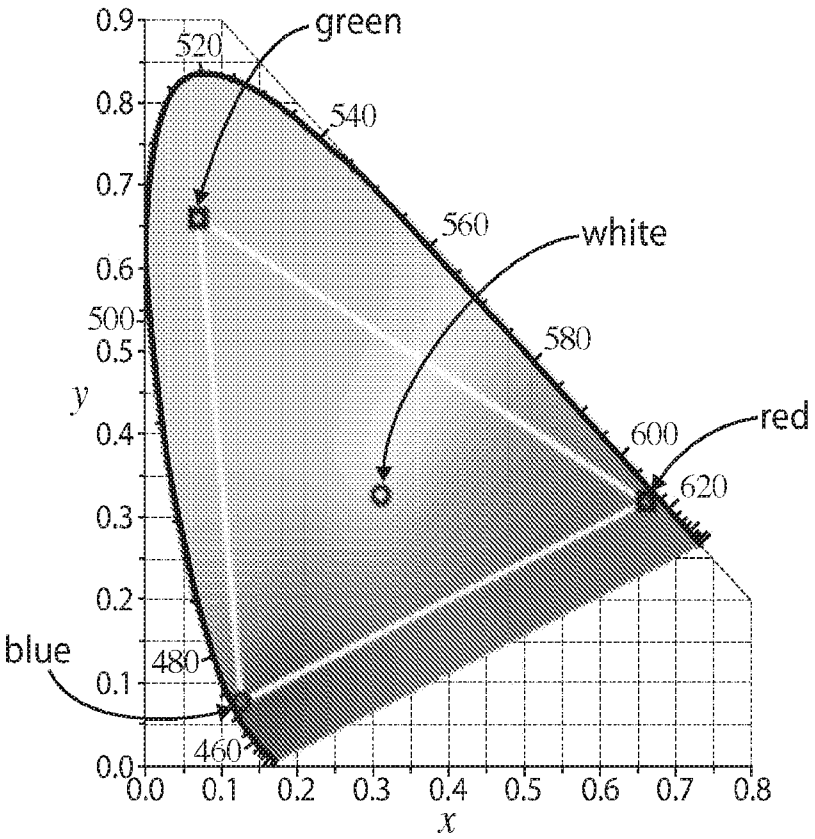
green
520
540
560
white
580
600
red
620
500
480
blue
460
0.9
0.8
0.7
0.6
0.5
0.4
0.3
0.2
0.1
0.0
y
0.0
0.1
0.2
0.3
0.4
0.5
0.6
0.7
0.8
x

FIG. 4C

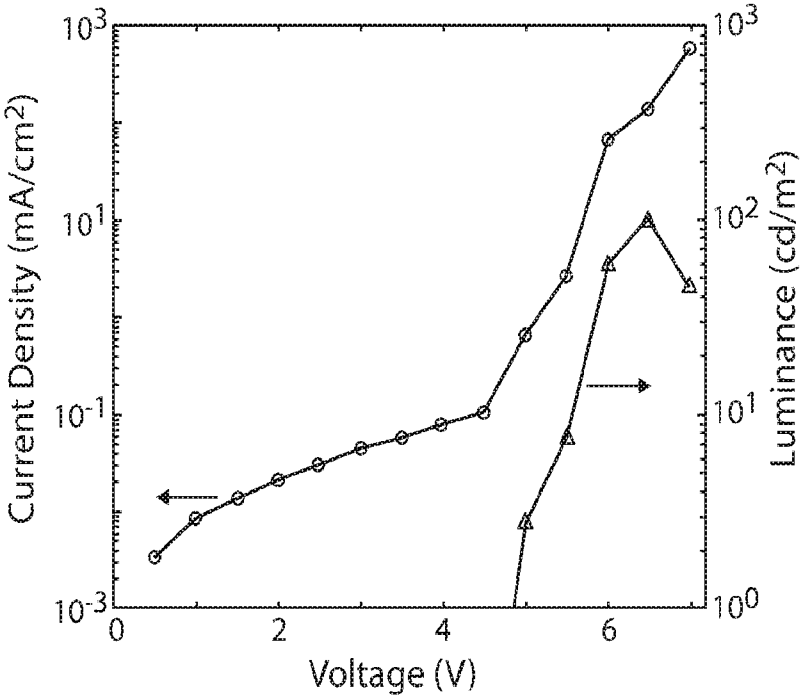
Current Density (mA/cm2)
Luminance (cd/m2)
Voltage (V)
10^3
10^1
10^-1
10^-3
10^2
10^0
0
2
4
6

FIG. 4D

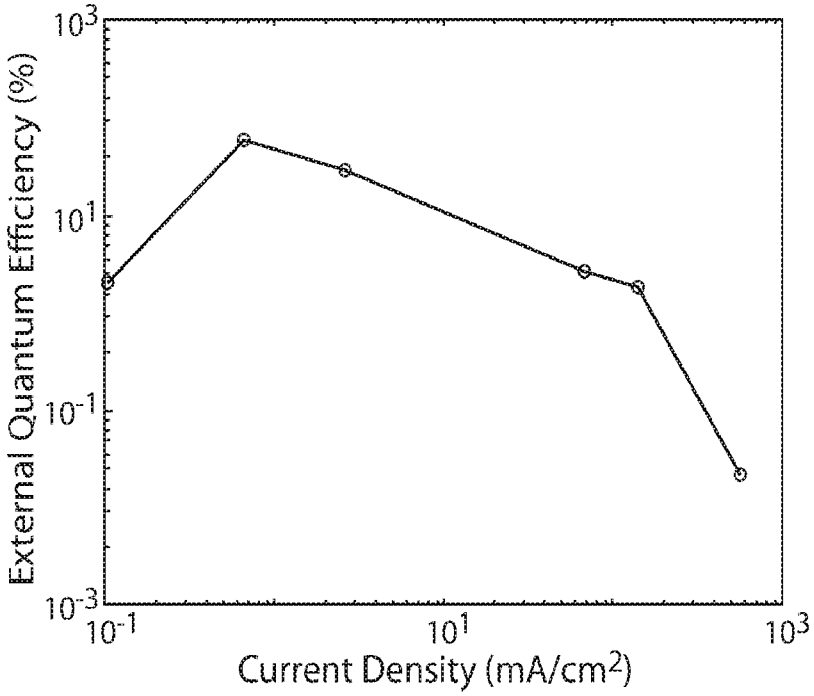
External Quantum Efficiency (%)
10^3
10^1
10^{-1}
10^{-3}
10^{-1}
10^1
10^3
Current Density (mA/cm^2)

FIG. 4E

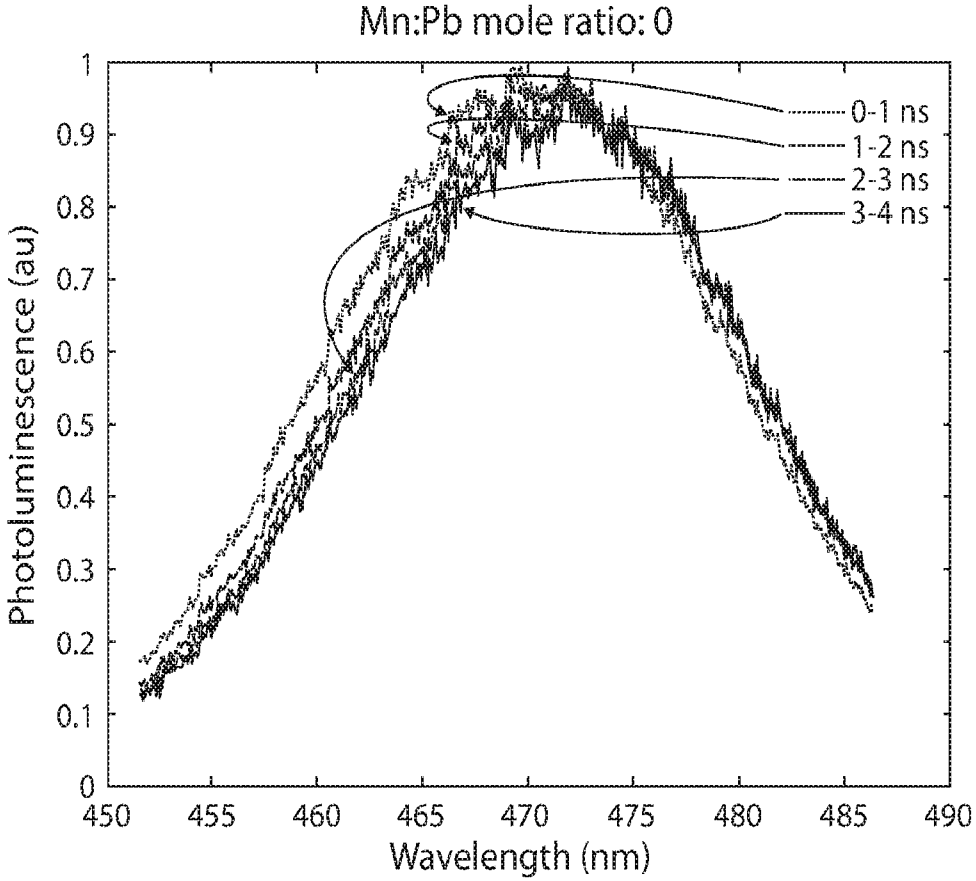
Mn:Pb mole ratio: 0
Photoluminescence (au)
Wavelength (nm)
0-1 ns
1-2 ns
2-3 ns
3-4 ns
0
0.1
0.2
0.3
0.4
0.5
0.6
0.7
0.8
0.9
1
450
455
460
465
470
475
480
485
490

FIG. 5A

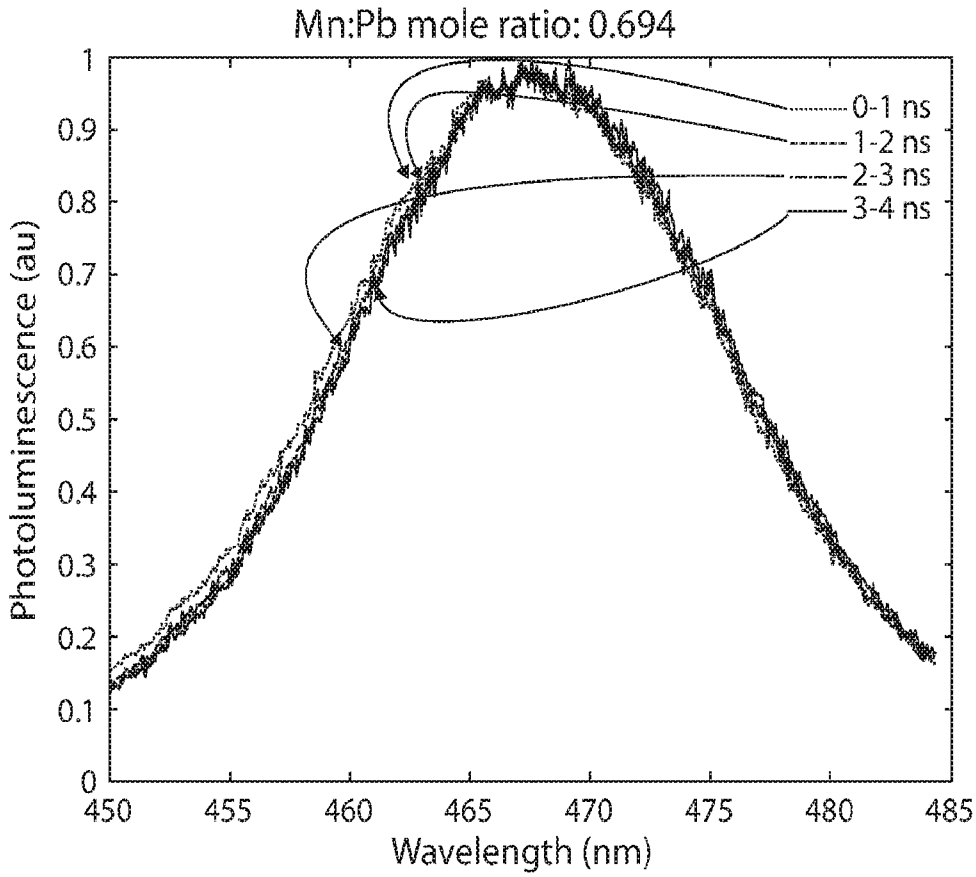
Mn:Pb mole ratio: 0.694
Photoluminescence (au)
Wavelength (nm)
0-1 ns
1-2 ns
2-3 ns
3-4 ns
0
0.1
0.2
0.3
0.4
0.5
0.6
0.7
0.8
0.9
1
450
455
460
465
470
475
480
485

FIG. 5B

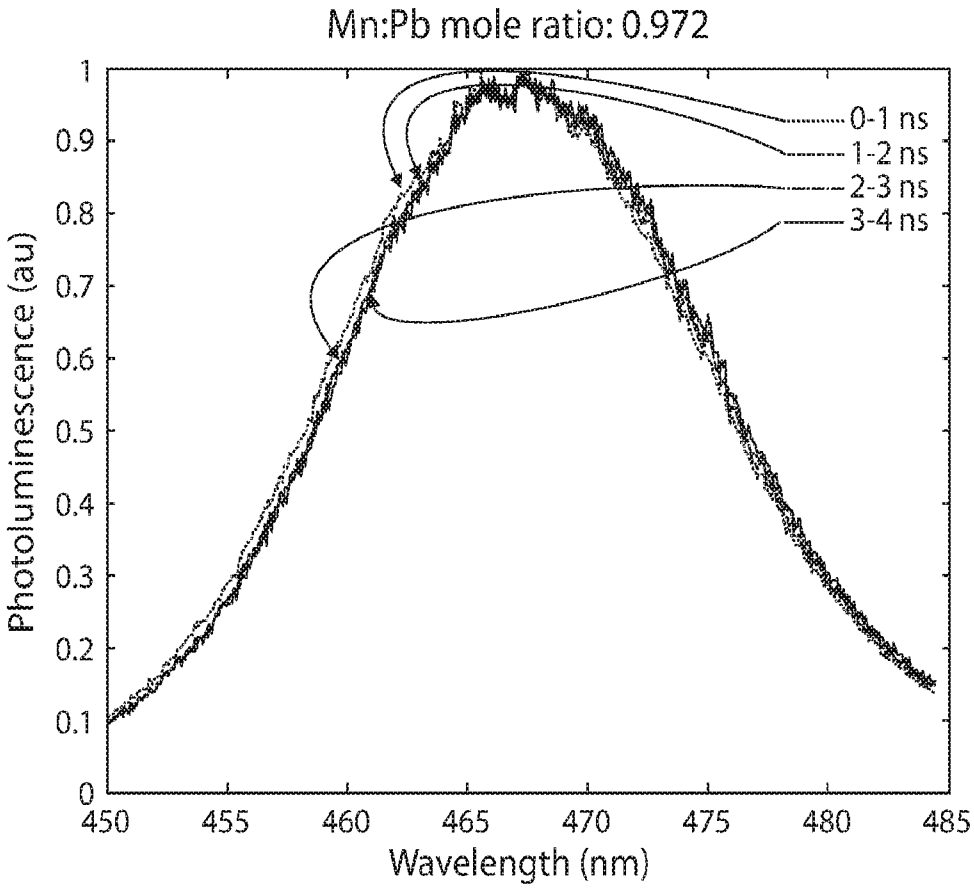
Mn:Pb mole ratio: 0.972
Photoluminescence (au)
Wavelength (nm)
0-1 ns
1-2 ns
2-3 ns
3-4 ns
0
0.1
0.2
0.3
0.4
0.5
0.6
0.7
0.8
0.9
1
450
455
460
465
470
475
480
485

FIG. 5C

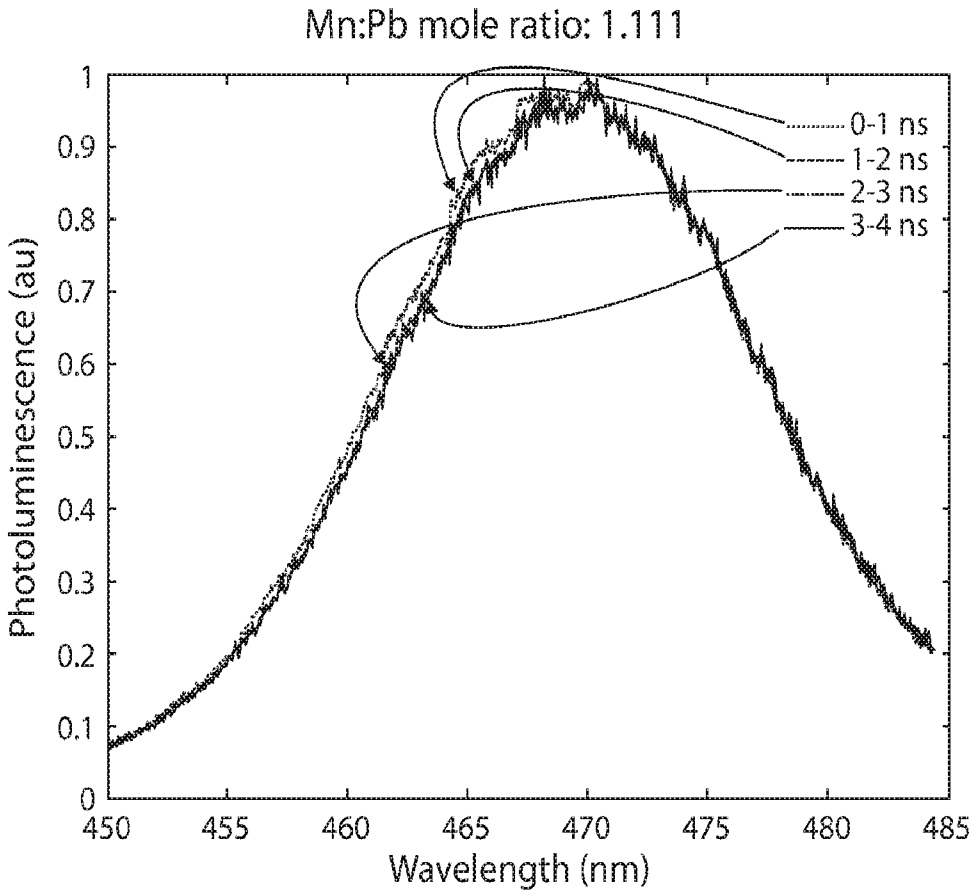
Mn:Pb mole ratio: 1.111
Photoluminescence (au)
Wavelength (nm)
0-1 ns
1-2 ns
2-3 ns
3-4 ns
0
0.1
0.2
0.3
0.4
0.5
0.6
0.7
0.8
0.9
1
450
455
460
465
470
475
480
485

FIG. 5D

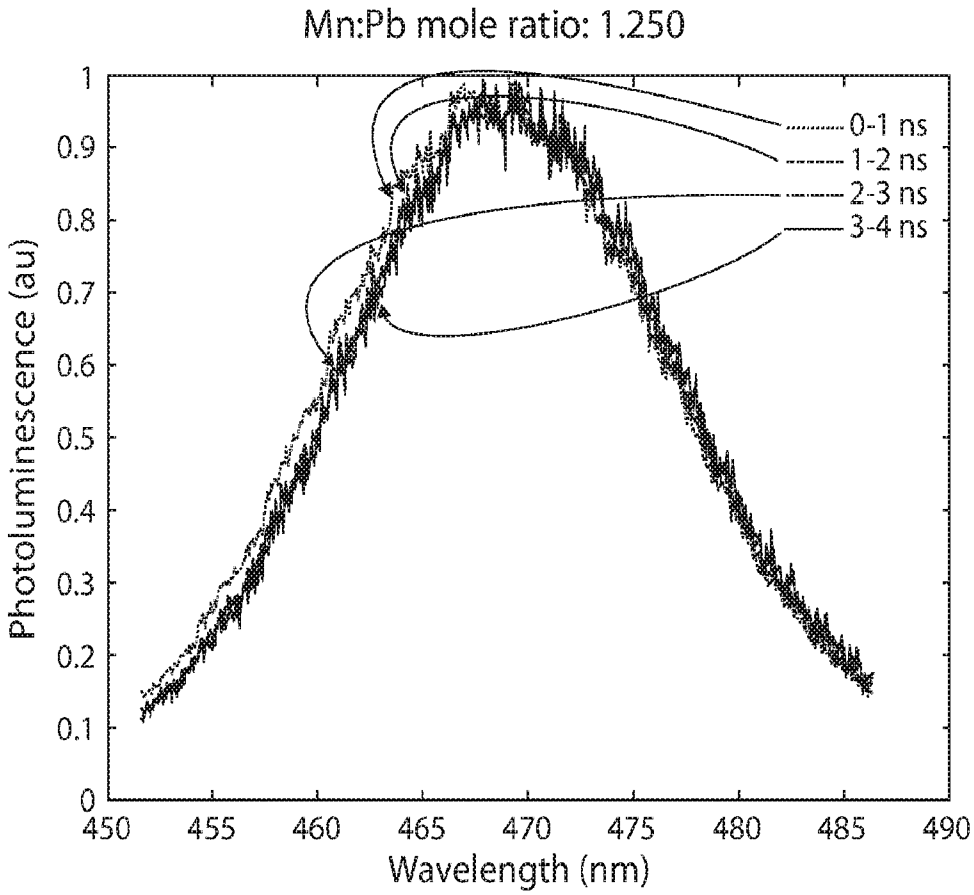
Mn:Pb mole ratio: 1.250
Photoluminescence (au)
Wavelength (nm)
0-1 ns
1-2 ns
2-3 ns
3-4 ns
0
0.1
0.2
0.3
0.4
0.5
0.6
0.7
0.8
0.9
1
450
455
460
465
470
475
480
485
490

FIG. 5E

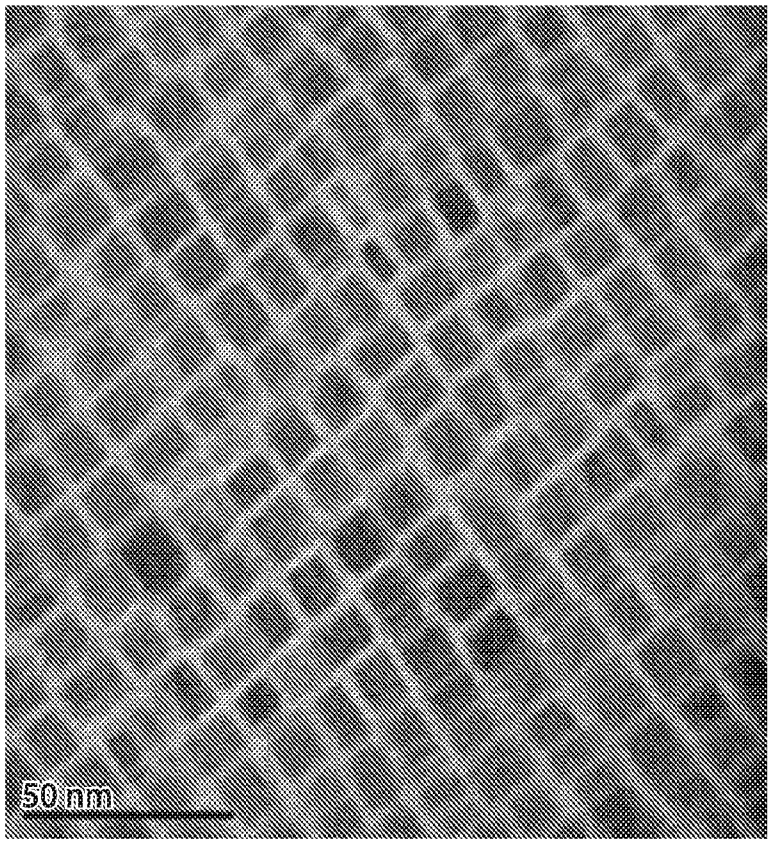

FIG. 6

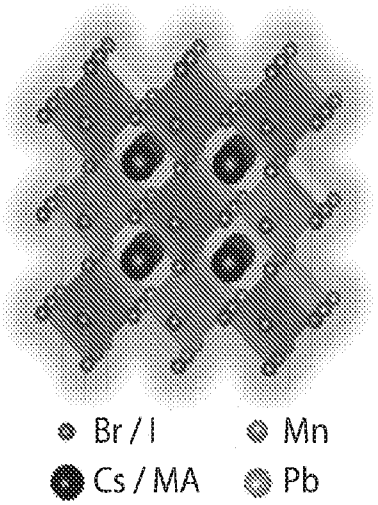

FIG. 7A

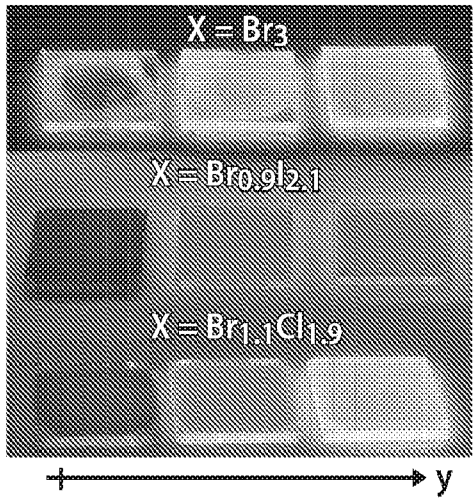

FIG. 7B

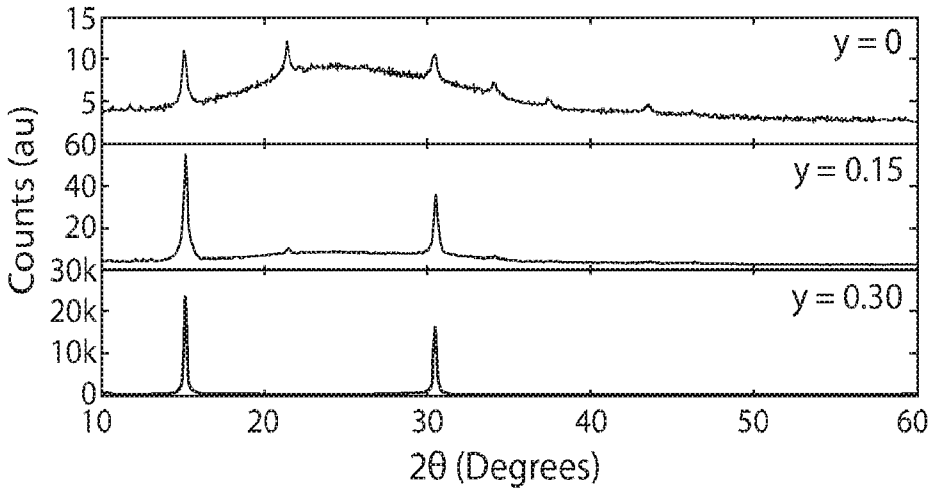

FIG. 7C

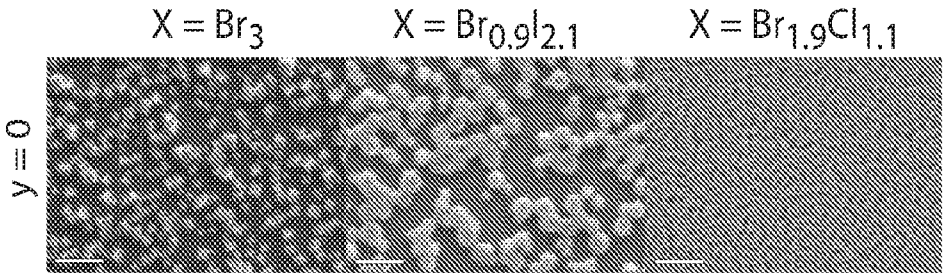

FIG. 8A FIG. 8B FIG. 8C

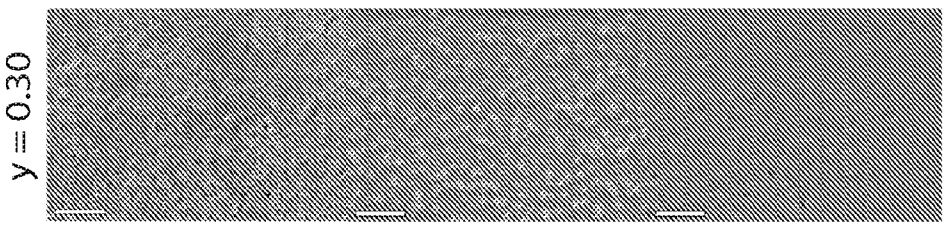

FIG. 8D FIG. 8E FIG. 8F

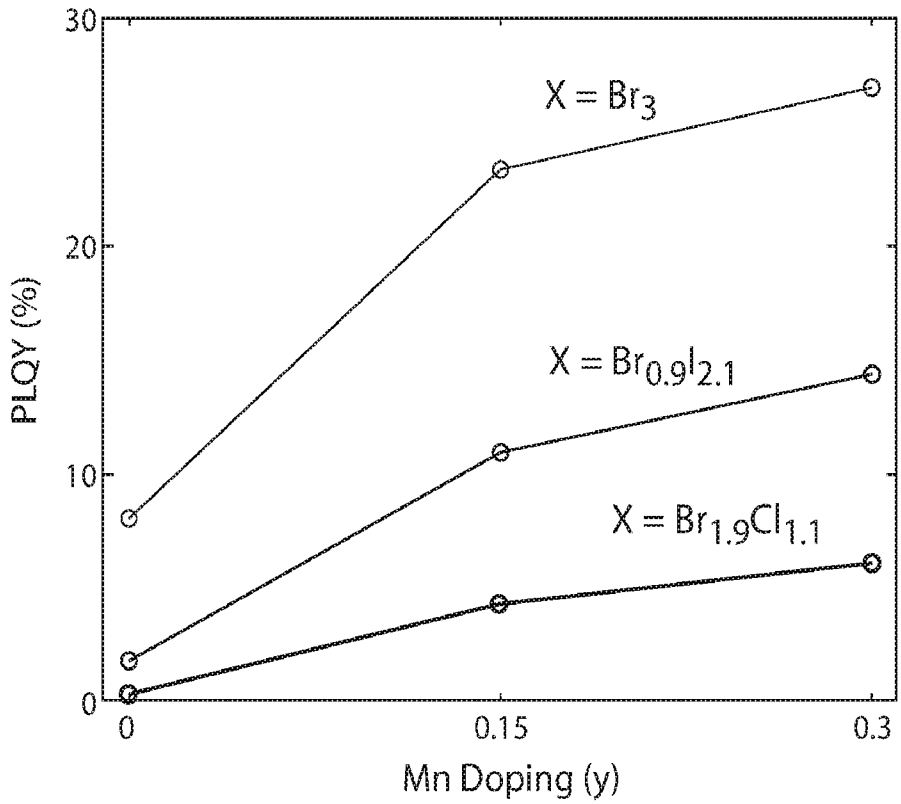

FIG. 9

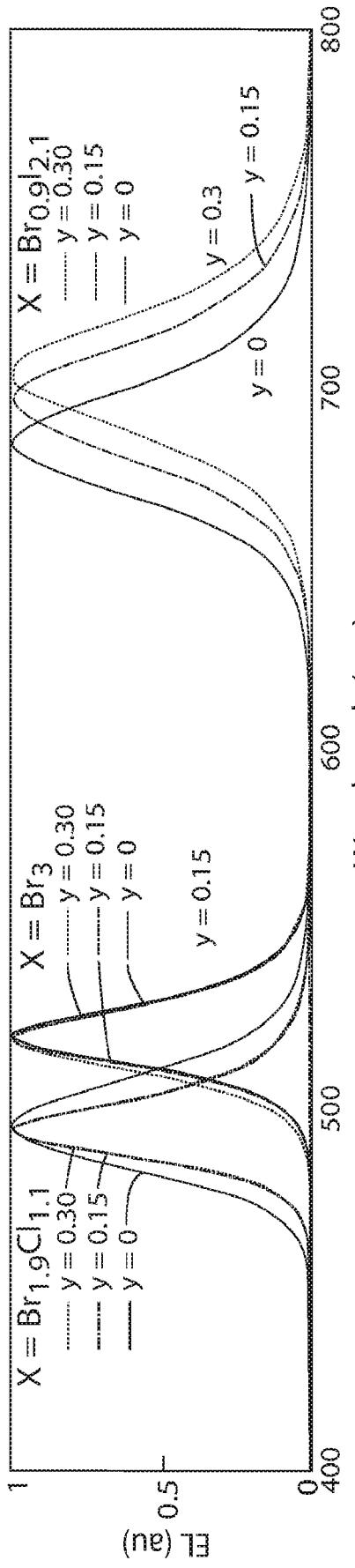
X = Br1.9Cl1.1
y = 0.30
y = 0.15
y = 0
X = Br3
y = 0.30
y = 0.15
y = 0
y = 0.15
X = Br0.9I2.1
y = 0.30
y = 0.15
y = 0
y = 0.3
y = 0.15
y = 0
EL (au)
0
0.5
1
400
500
600
700
800
Wavelength (nm)

FIG. 10A

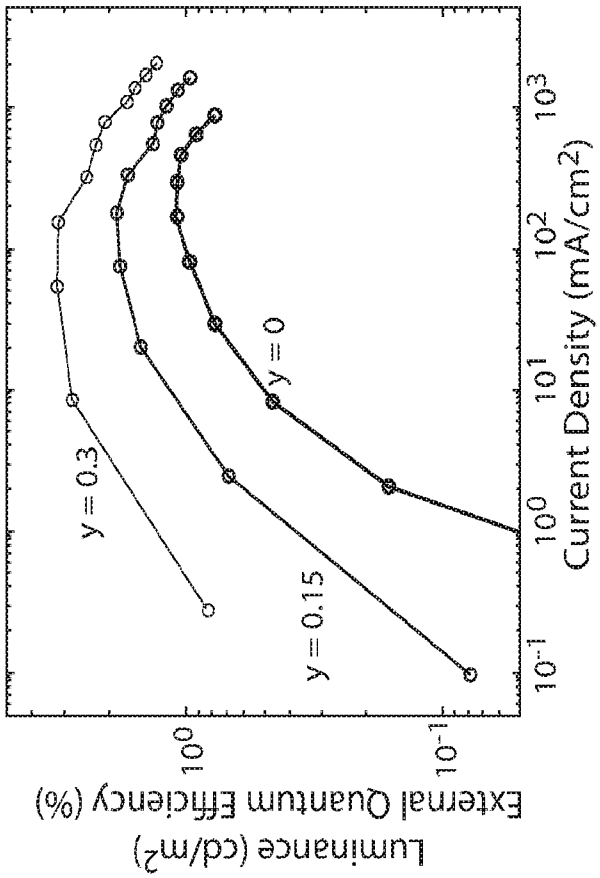

Fig. 10C

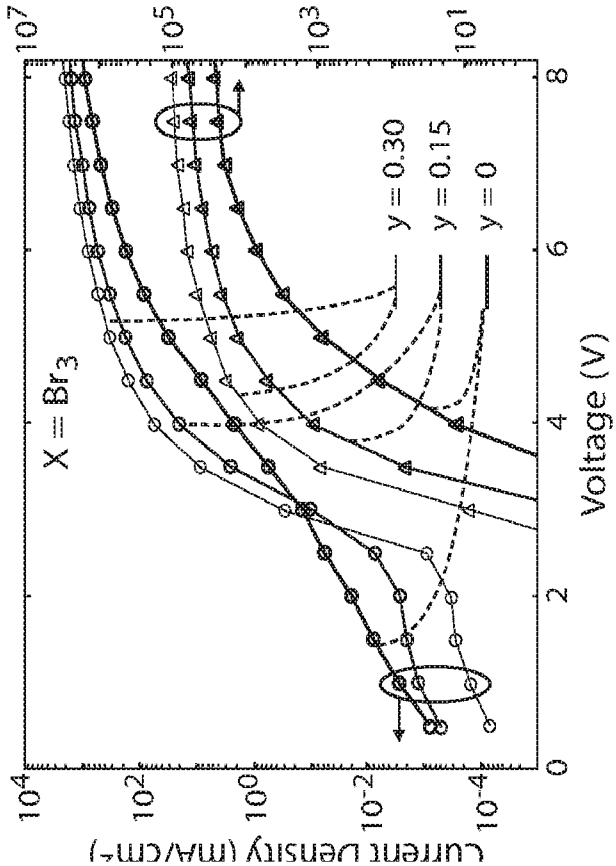

Fig. 10B

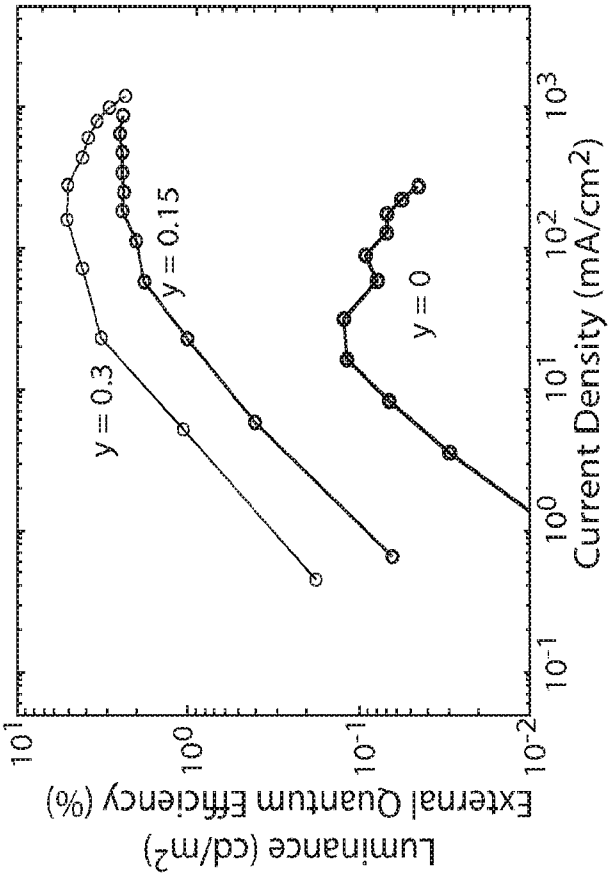

Fig. 10E

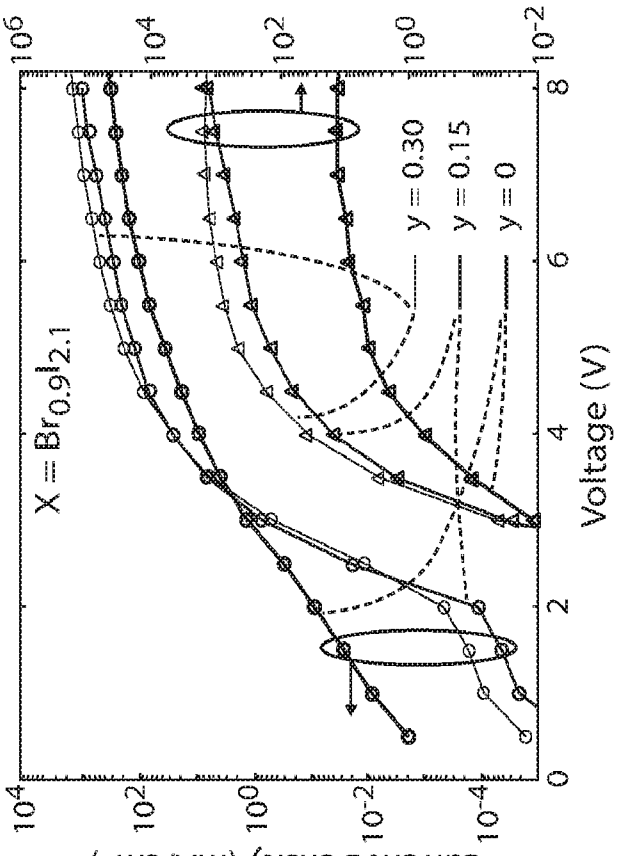

Fig. 10D

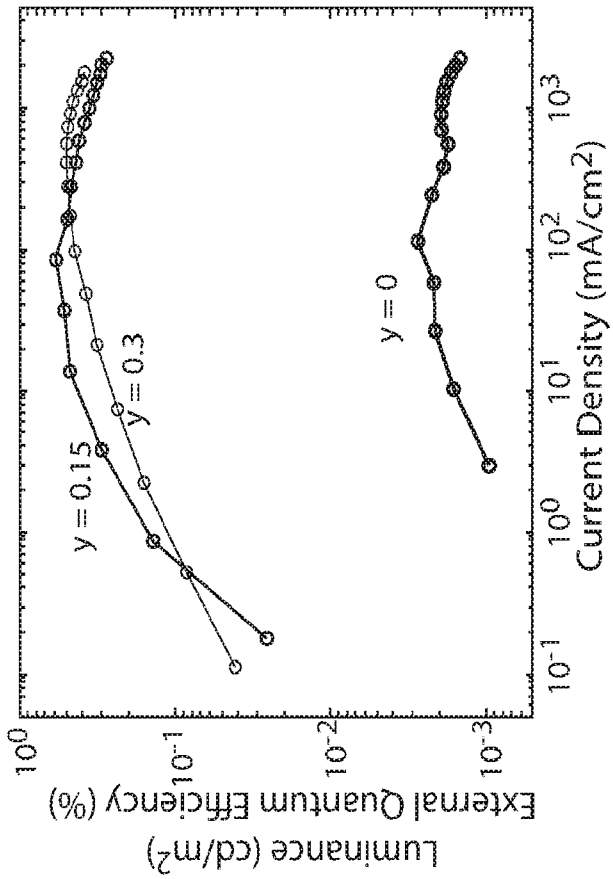

Fig. 10G

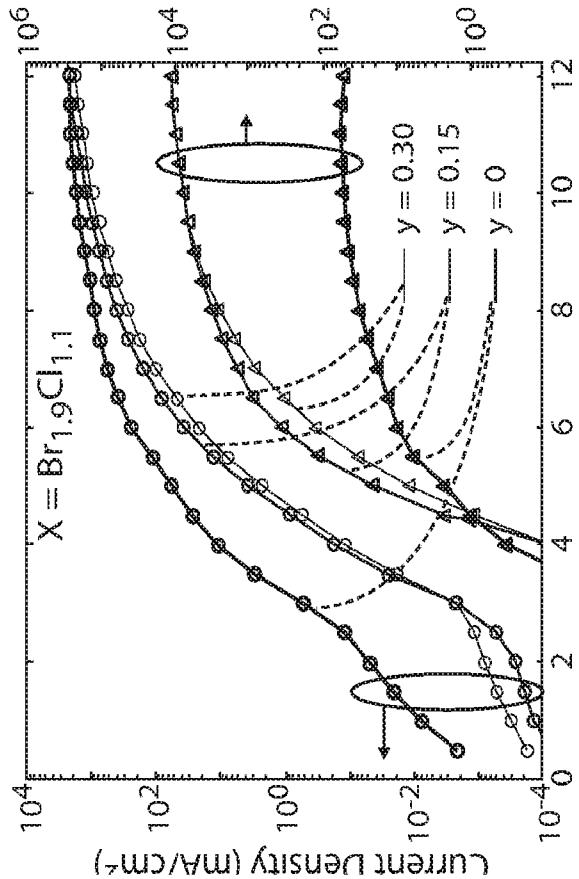

Fig. 10F

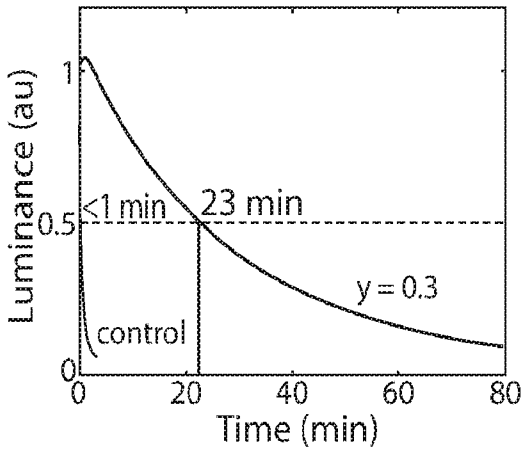

FIG. 11A

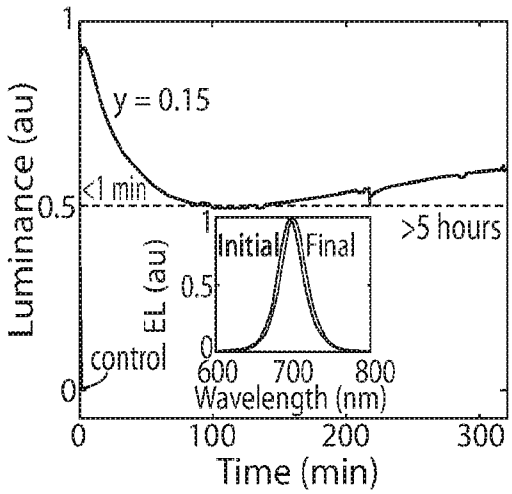

FIG. 11B

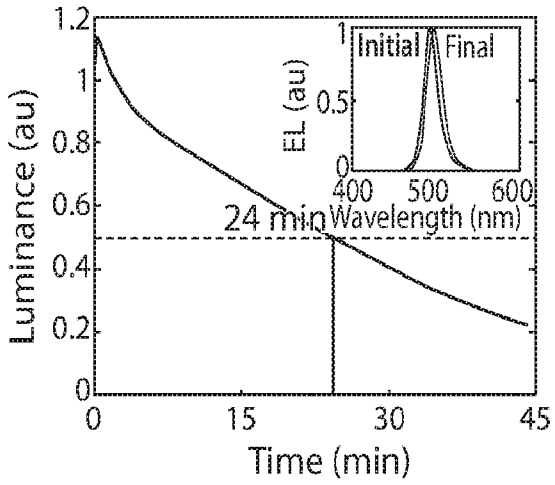

FIG. 11C

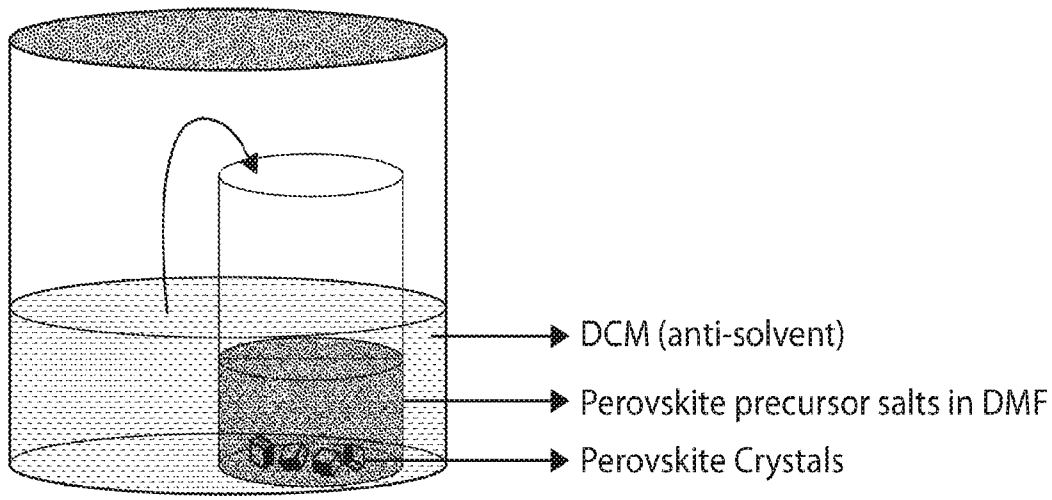
DCM (anti-solvent)
Perovskite precursor salts in DMF
Perovskite Crystals

FIG. 12

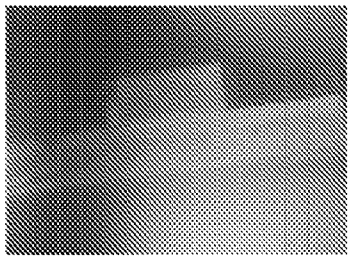

FIG. 13A

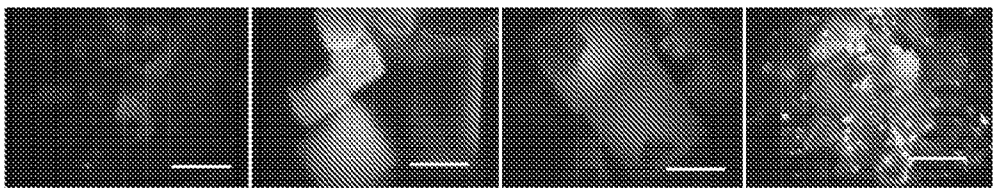

Control Mn doped Ni doped Yb doped

FIG. 13B FIG. 13C FIG. 13D FIG. 13E

INTERNATIONAL SEARCH REPORT

International application No.
PCT/US 18/61261

A. CLASSIFICATION OF SUBJECT MATTER

IPC(8) - C01G 21/16, C09K 11/57, C07F 7/24, H01G 9/20, H01L 51/50, H01L 51/42 (2019.01)
CPC - C09K 11/0833, C09K 11/665, H01L 2251/306, H01L 51/001, H01L 51/0032, H01L 51/502, H01L 51/5024

According to International Patent Classification (IPC) or to both national classification and IPC

B. FIELDS SEARCHED

Minimum documentation searched (classification system followed by classification symbols)

See Search History Document

Documentation searched other than minimum documentation to the extent that such documents are included in the fields searched

See Search History Document

Electronic data base consulted during the international search (name of data base and, where practicable, search terms used)

See Search History Document

C. DOCUMENTS CONSIDERED TO BE RELEVANT

Category*	Citation of document, with indication, where appropriate, of the relevant passages	Relevant to claim No.
X -- Y -- A	LIU et al, 'Mn2+-Doped Lead Halide Perovskite Nanocrystals with Dual Color Emission Controlled by Halide Content', Journal of the American Chemical Society, volume 138, 19 October 2016 (19.10.2016), pg 14954-14961 and associated Supporting Information.	1-3, 96-98, 130-132, 185-187 ---------- 30-32, 69-72, 86-88, 113-115, 144-146, 158, 160/158, 174-176 ---------- 159, 160/159
Y	ZHANG et al, 'Enhancing the Brightness of Cesium Lead Halide Perovskite Nanocrystal Based Green Light-Emitting Devices through the Interface Engineering with Perfluorinated Ionomer', Nano Letters, volume 16, 8 January 2016 (08.01.2016), pg 1415-1420.	30-32, 69, 71, 72/(69, 71), 86-88, 113-115, 144-146
Y	LI et al, 'Highly Efficient Perovskite Nanocrystal Light-Emitting Diodes Enabled by a Universal Crosslinking Method', Advanced Materials, volume 28, 16 March 2016 (16.03.2016), pg 3528-3534.	31, 32/31, 69-70, 72/(69-70)
Y -- A	PALAZON et al, 'Polymer-Free Films of Inorganic Halide Perovskite Nanocrystals as UV-to-White Color-Conversion Layers in LEDs', Chemistry of Materials, volume 28, 19 April 2016 (19.04.2016), pg 2902-2906.	158, 160/158, 174-176 ---------- 159, 160/159
A	US 2016/0268510 A1 (KOREA RESEARCH INSTITUTE OF CHEMICAL TECHNOLOGY), 15 September 2016 (15.09.2016), Table 1, para [0012]-[0013].	159, 160/159

☒ Further documents are listed in the continuation of Box C. ☐ See patent family annex.

* Special categories of cited documents:

"A" document defining the general state of the art which is not considered to be of particular relevance

"E" earlier application or patent but published on or after the international filing date

"L" document which may throw doubts on priority claim(s) or which is cited to establish the publication date of another citation or other special reason (as specified)

"O" document referring to an oral disclosure, use, exhibition or other means

"P" document published prior to the international filing date but later than the priority date claimed

"T" later document published after the international filing date or priority date and not in conflict with the application but cited to understand the principle or theory underlying the invention

"X" document of particular relevance; the claimed invention cannot be considered novel or cannot be considered to involve an inventive step when the document is taken alone

"Y" document of particular relevance; the claimed invention cannot be considered to involve an inventive step when the document is combined with one or more other such documents, such combination being obvious to a person skilled in the art

"&" document member of the same patent family

Date of the actual completion of the international search	Date of mailing of the international search report
17 January 2019	04 FEB 2019
Name and mailing address of the ISA/US Mail Stop PCT, Attn: ISA/US, Commissioner for Patents P.O. Box 1450, Alexandria, Virginia 22313-1450 Facsimile No. 571-273-8300	Authorized officer: Lee W. Young PCT Helpdesk: 571-272-4300 PCT OSP: 571-272-7774

INTERNATIONAL SEARCH REPORT

International application No.
PCT/US 18/61261

C (Continuation). DOCUMENTS CONSIDERED TO BE RELEVANT

Category*	Citation of document, with indication, where appropriate, of the relevant passages	Relevant to claim No.
X	PAROBEK et al, 'Exciton-to-Dopant Energy Transfer in Mn-Doped Cesium Lead Halide Perovskite Nanocrystals', Nano Letters, volume 16, 31 October 2016 (31.10.2016), pg 7376-7380.	1-3, 96-98, 130-132, 185-187
A	KIM et al, 'Metal halide perovskite light emitters', Proceeding of the National Academy of Sciences of the United States of America, volume 113, issue 42, 18 October 2016 (18.10.2016), pg 11694-11702.	1-3, 30-32, 69-72, 86-88, 96-98, 113-115, 130-132, 144-146, 158-160, 174-176, 185-187

INTERNATIONAL SEARCH REPORT

International application No.
PCT/US 18/61261

Box No. II Observations where certain claims were found unsearchable (Continuation of item 2 of first sheet)

This international search report has not been established in respect of certain claims under Article 17(2)(a) for the following reasons:

1. ☐ Claims Nos.:
because they relate to subject matter not required to be searched by this Authority, namely:

2. ☐ Claims Nos.:
because they relate to parts of the international application that do not comply with the prescribed requirements to such an extent that no meaningful international search can be carried out, specifically:

3. ☒ Claims Nos.: 4-29, 33-68, 73-85, 89-95, 99-112, 116-129, 133-143, 147-157, 161-173, 177-184, 188-198
because they are dependent claims and are not drafted in accordance with the second and third sentences of Rule 6.4(a).

Box No. III Observations where unity of invention is lacking (Continuation of item 3 of first sheet)

This International Searching Authority found multiple inventions in this international application, as follows:

1. ☐ As all required additional search fees were timely paid by the applicant, this international search report covers all searchable claims.

2. ☐ As all searchable claims could be searched without effort justifying additional fees, this Authority did not invite payment of additional fees.

3. ☐ As only some of the required additional search fees were timely paid by the applicant, this international search report covers only those claims for which fees were paid, specifically claims Nos.:

4. ☐ No required additional search fees were timely paid by the applicant. Consequently, this international search report is restricted to the invention first mentioned in the claims; it is covered by claims Nos.:

Remark on Protest

☐ The additional search fees were accompanied by the applicant's protest and, where applicable, the payment of a protest fee.

☐ The additional search fees were accompanied by the applicant's protest but the applicable protest fee was not paid within the time limit specified in the invitation.

☐ No protest accompanied the payment of additional search fees.